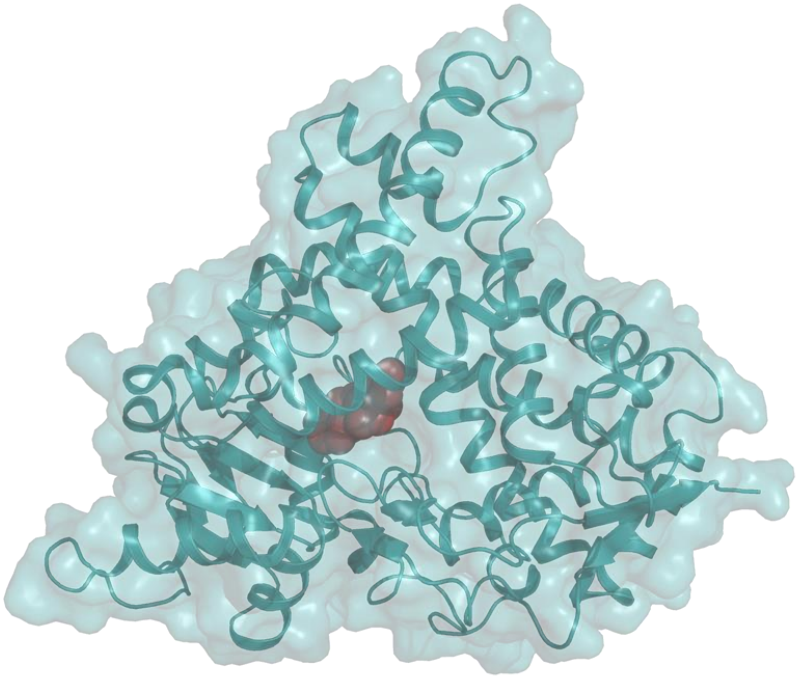

Non-steroidal aromatase inhibitors for hormone-dependent breast cancer: virtual screening and *in vitro* effects

Cristina Maria Ferreira Almeida

Mestrado em Bioquímica

Faculdade de Ciências da Universidade do Porto

Instituto de Ciências Biomédicas Abel Salazar da Universidade do Porto

2019

Orientador

Doutora Cristina Isabel Borges Dias Amaral, PhD, Investigadora do UCIBIO.REQUIMTE/FFUP

Coorientadores

Professora Doutora Natércia Aurora Almeida Teixeira, PhD, Prof. Catedrática, FFUP

Professor Doutor Pedro Manuel Azevedo Alexandrino Fernandes, PhD, Prof. Associado, FCUP

U.PORTO
FACULDADE DE CIÊNCIAS
UNIVERSIDADE DO PORTO

U.PORTO
INSTITUTO DE CIÊNCIAS
BIOMÉDICAS ABEL SALAZAR
UNIVERSIDADE DO PORTO

Todas as correções determinadas pelo júri, e só essas, foram efetuadas.

O Presidente do Júri,

Porto, _____/_____/_____

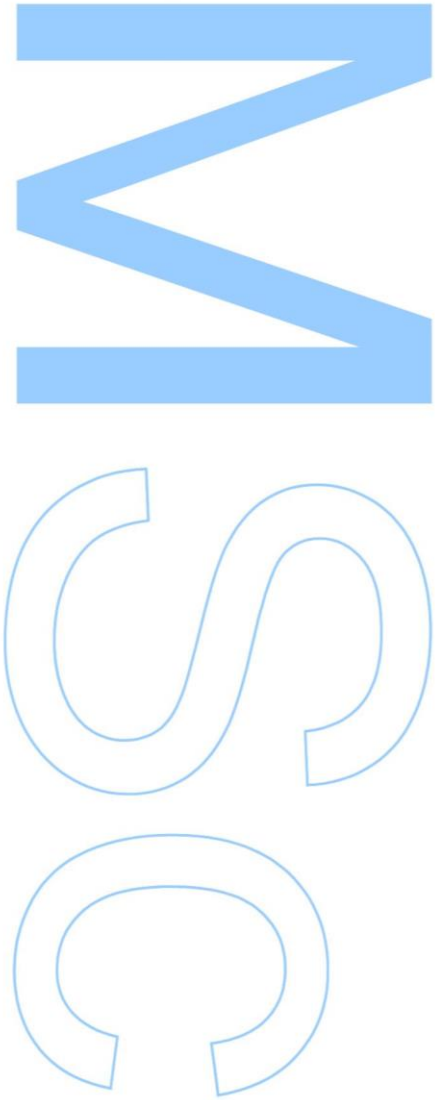

Esta dissertação foi realizada no UCIBIO.REQUIMTE – Departamento de Ciências Biológicas, Laboratório de Bioquímica da Faculdade de Farmácia da Universidade do Porto, sob a orientação da Doutora Cristina Isabel Borges Dias Amaral e da Professora Doutora Natércia Aurora Almeida Teixeira e no UCIBIO.REQUIMTE – Grupo de Química Teórica e Bioquímica Computacional da Faculdade de Ciências da Universidade do Porto, sob a orientação do Professor Doutor Pedro Manuel Azevedo Alexandrino Fernandes. Teve ainda a orientação, como tutor interno do Instituto de Ciências Biomédicas Abel Salazar da Universidade do Porto, o Professor Doutor Paulo Correia de Sá.

Este projeto teve o apoio financeiro da Fundação para a Ciência e Tecnologia (FCT), através da atribuição de um contrato à Doutora Cristina Amaral no âmbito do programa de financiamento (DL 57/2016 – Norma Transitória) e da bolsa de pós-doutoramento (SFRH/BPD/98304/2013). Este trabalho foi também financiado pela Unidade de Ciências Biomoleculares Aplicadas-UCIBIO, financiada por fundos nacionais através da FCT/MCTES (UID/Multi/04378/2019).

Author's Oral/Poster Communications

C. Almeida, A. Oliveira, C. Amaral, M.J. Ramos, G. Correia-da-Silva, N. Teixeira, P.A. Fernandes. "A multi-target approach for hormone-dependent breast cancer: estrogen receptors and aromatase" Encontro de Jovens Investigadores de Biologia Computacional Estrutural, EJIBCE, Porto, Portugal, 21 December, **2018** – Poster communication

C. Almeida, A. Oliveira, C. Amaral, M.J. Ramos, G. Correia-da-Silva, N. Teixeira, P.A. Fernandes. "Non-steroidal aromatase inhibitors for hormone-dependent breast cancer: a virtual screening approach." 12º Encontro de Investigação Jovem da Universidade do Porto, IJUP 2019, Porto, Portugal, 13-15 February, **2019** – Oral Communication

C.F. Almeida, T.V. Augusto, G. Correia-da-Silva, A. Oliveira, P.A. Fernandes, M.J. Ramos, S. Cunha, N. Teixeira, C. Amaral. "Discovery of a multi-target compound for ER^+ breast cancer: characterization of its biological effects" 14th Young European Scientist Meeting, 14th YES Meeting, Porto, Portugal, 12-15 September, **2019** – Poster Communication

Agradecimentos/Acknowledgments

Em primeiro lugar, agradeço à minha orientadora, Doutora Cristina Amaral, por mais uma vez me acompanhar no meu progresso científico e me ajudar a crescer enquanto profissional. Agradeço também toda a dedicação, apoio, em todos os momentos, e persistência ao longo deste ano, procurando sempre garantir o sucesso do meu trabalho, mas também o meu bem-estar. Agradeço também toda a amizade, conselhos e todas as oportunidades que me tem proporcionado. Sem dúvida que o sucesso deste trabalho se deve também a ti. Muito obrigada!

À Prof. Doutora Natércia Teixeira, agradeço por mais uma vez me ter aceite no laboratório e por ter assumido o papel de coorientadora. Agradeço a sua dedicação, disponibilidade, preocupação, persistência, amizade e acompanhamento que me mantiveram sempre confiante, mesmo nos momentos de maior dúvida. Para além disso, agradeço o conhecimento científico tem procurado sempre transmitir-me e as oportunidades que me tem proporcionado de forma a que possa progredir no mundo da ciência. Foi um privilégio trabalhar novamente consigo ao longo deste ano. Muito obrigada!

Ao Prof. Doutor Pedro Alexandrino Fernandes, agradeço por ter aceite fazer parte deste projeto, sendo meu coorientador, e por todo o entusiasmo que sempre demonstrou relativamente ao meu trabalho. Agradeço também a forma como me recebeu no Grupo de Química Teórica e Bioquímica Computacional, procurando fazer-me sentir à vontade desde o primeiro momento.

Um agradecimento muito especial à Doutora Ana Oliveira por ter sido o meu braço direito na Faculdade de Ciências, transmitindo-me todos os conhecimentos necessários sobre Bioquímica Computacional. Agradeço toda a paciência, simpatia e disponibilidade para esclarecer as minhas dúvidas e incertezas. Para além disso, não posso deixar de lhe agradecer pelo facto de me fazer companhia todos os dias ao almoço e por todos os bons momentos. Obrigada!

Não posso deixar de agradecer à Prof. Doutora Georgina Correia da Silva pelo constante acompanhamento ao longo deste ano e por se mostrar sempre disponível para qualquer esclarecimento e ajuda.

Agradeço também à Prof. Doutora Maria João Ramos pela forma acolhedora como me recebeu no laboratório, por toda a simpatia, interesse e acompanhamento durante a minha estadia na Faculdade de Ciências.

Um agradecimento especial ao Tiago por toda a ajuda, companheirismo, disponibilidade e pelos conselhos que me deu ao longo dos últimos tempos.

Não posso deixar de agradecer a todos os investigadores e colaboradores do laboratório de Bioquímica da Faculdade de Farmácia, em especial à Patrícia, ao João, ao Luís, à Marta, à Beatriz, à Daniela, ao Ricardo e à Ana Paula por toda a ajuda, companheirismo e por todos os bons momentos.

De forma semelhante, agradeço a todos os investigadores e colaboradores do Grupo de Química Teórica e Bioquímica Computacional da Faculdade de Ciências. Agradeço especialmente ao Rui, ao João, à Fabiola e ao Óscar pelo companheirismo, pelos conselhos, pelos lanchinhos e por toda a ajuda e paciência quando alguma coisa decidia não funcionar devidamente.

Aos meus amigos, de forma especial à Clara, à Catarina, à Rita e ao Zé, agradeço por todo apoio, acompanhamento, bons momentos e, acima de tudo, pela amizade aos longo destes anos. Foram sem dúvida uma peça fundamental para o meu sucesso!

Por fim, agradeço à minha família, em especial aos meus pais, por estarem sempre comigo. Sem eles, nada disto seria possível.

A todos, o meu mais sincero obrigada!

Abstract

Breast cancer is currently the most frequently diagnosed cancer among women and the second leading cause of cancer-related death worldwide. Around 70% of all breast cancer cases diagnosed are estrogen receptor-positive (ER^+), a subtype of breast tumor that depends on estrogens for growth and proliferation. After the initial use of selective ER modulators (SERMs), like tamoxifen, the aromatase inhibitors (AIs) emerged as a better therapeutic option and, in fact, are nowadays used as first-line therapy for this subtype of cancer. However, besides their clinical success, they are responsible for some side effects, being the development of endocrine resistance the major clinical concern. Because of that, it is crucial to develop new therapeutic options to treat this type of tumors. Considering this, the present work focused on the discovery of multi-target compounds able to simultaneously modulate the activity of aromatase, ERα and ERβ, as well as, on the discovery of new non-steroidal AIs, using computational and biological approaches.

The computational studies have identified a possible multi-target compound, designated as MT1. Our biological studies using an ER^+ breast cancer cell line (MCF-7aro) and a non-cancerous cell line (HFF-1) revealed that MT1 only at the highest concentration had cytotoxic effects on HFF-1 cells and that, in ER^+ breast cancer cells, MT1 presented growth-inhibitory properties. Moreover, besides this compound was not able to inhibit aromatase in human placental microsomes, MT1 may exert its effects on ER^+ breast cancer cells via aromatase, ERα and ERβ, by inducing a reduction in aromatase expression levels and acting as an ERα antagonist and ERβ agonist. Furthermore, MT1 caused MCF-7aro cell cycle arrest and induced apoptotic cell death.

In relation to the discovery of novel non-steroidal AIs, by virtual screening (VS), two compounds, NS8 and NS16, were selected for the biological studies. Unfortunately, neither NS8 nor NS16 were able to inhibit aromatase in human placental microsomes, though, NS16 induced significant effects on MCF-7aro viability, without affecting non-cancerous cells, reason why more studies must be performed in order to understand its mechanism of action.

In conclusion, this study contributed to the discovery of new molecules with growth-inhibitory properties in ER^+ breast cancer cells. For the first time, a multi-target compound capable of simultaneously modulate the key targets responsible for estrogen production/signaling was discovered, using this type of computational approaches. In addition, the overall study provided crucial structural insights related to the inhibition of aromatase, ERα antagonists and ERβ agonists, through the analysis of molecular descriptors, which helped to discover a multi-target compound.

Keywords: estrogen receptor-positive (ER^+) breast cancer, multi-target, aromatase inhibitors (AIs), computational, virtual screening

Resumo

O cancro da mama é o cancro mais frequente nas mulheres e a segunda principal causa de morte relacionada com cancro em todo o mundo. Cerca de 70% de todos os casos de cancro da mama diagnosticados são recetores de estrogénio-positivos (ER^+), um subtipo de tumor que depende dos estrogénios para crescer e proliferar. Depois do uso inicial de moduladores seletivos do ER (SERMs), como o tamoxifeno, os inibidores da aromatase (AIs) surgiram como uma melhor opção terapêutica e são hoje em dia usados como primeira linha de tratamento neste tipo de tumores. Contudo, apesar do seu sucesso clínico, eles são responsáveis por alguns efeitos adversos, sendo o desenvolvimento de resistência endócrina a principal preocupação clínica. Por causa disso, é crucial desenvolver novas opções terapêuticas para tratar este tipo de tumores. Considerando isto, este trabalho teve como foco a descoberta de compostos multi-alvo capazes de simultaneamente modular a atividade da aromatase, do ERα e do ERβ, bem como, a descoberta de novos AIs não esteroides, usando abordagens computacionais e biológicas.

Estudos computacionais indicaram a existência de um possível composto multi-alvo, designado por MT1. Os nossos estudos biológicos usando uma linha celular de cancro da mama ER^+ (MCF-7aro) e uma linha celular não cancerígena (HFF-1), revelaram que o MT1 tinha efeitos tóxicos nas células HFF-1 apenas à concentração mais elevada, e que nas células de cancro da mama ER^+, o composto apresentava propriedades inibidoras do crescimento. Para além disso, apesar do MT1 não ser capaz de inibir a aromatase em microssomas de placenta humana, este composto parece exercer os seus efeitos nas células de cancro da mama ER^+, através da aromatase, do ERα e do ERβ, induzindo uma redução nos níveis de expressão da aromatase e atuando como antagonista do ERα e agonista do ERβ. Além disso, o MT1 provocou uma retenção do ciclo celular nas células MCF-7aro e induziu morte celular por apoptose.

Em relação à descoberta de novos AIs não esteroides, por *virtual screening* (VS), foram selecionados dois compostos, NS8 e NS16, para estudos biológicos. Curiosamente, nem o NS8 nem o NS16 foram capazes de inibir a aromatase em microssomas de placenta humana, contudo, o NS16 reduziu significativamente a viabilidade das células MCF-7aro, não afetando, no entanto, as células não cancerígenas, razão pela qual mais estudos devem ser realizados de forma a perceber o seu mecanismo de ação.

Em conclusão, este estudo contribuiu para a descoberta de novas moléculas com propriedades inibidoras do crescimento em células cancerígenas mamárias ER^+. Pela primeira vez, um composto multi-alvo capaz de simultaneamente modular os alvos

chave responsáveis pela produção/sinalização do estrogénio foi descoberto, usando este tipo de abordagens computacionais. Adicionalmente, o estudo proporcionou conhecimentos estruturais cruciais em relação à inibição da aromatase, aos antagonistas do ERα e aos agonistas do ERβ, através da análise de descritores moleculares, os quais ajudaram a descobrir um composto multi-alvo.

Palavras-chave: cancro da mama recetor de estrogénio-positivo (ER^+), multi-alvo, inibidores da aromatase (AIs), computacional, *virtual screening*

Table of Contents

Index of Figures

Index of Tables

Abbreviations List

AF-1: Transactivation Function 1

AF-2: Transactivation Function 2

AIs: Aromatase Inhibitors

Ana: Anastrozole

AP-1: Activator Protein 1

AR: Androgen Receptor

ASA: Water-Accessible Surface Area

ASD: Androstenedione

cAMP: Cyclic Adenosine Monophosphate

cDNA: Complementary Deoxyribonucleic Acid

CFBS: Charcoal Heat-Inactivated Fetal Bovine Serum

COX-1: Cyclooxygenase 1

COX-2: Cyclooxygenase 2

CPR: NADPH-Cytochrome P450 Redutase

DBD: DNA Binding Domain

DCF: 2', 7'-dichlorofluorescein

$DCFH_2$: 2', 7'-dichlorodihydrofluorescein

$DCFH_2$-DA: 2', 7'-dichlorodihydrofluorescein diacetate

DMEM: Dulbeco's Modified Eagle's Medium

DMSO: Dimethyl Sulfoxide

DNA: Deoxyribonucleic Acid

E1: Estrone

E2: 17β-estradiol

E3: 16α-estriol

ECFP: Extended Connectivity Fingerprints

EDTA: Ethylenediaminetetraacetic acid

EGFR: Epidermal Growth Factor Receptor

ER: Estrogen Receptor

ERE: Estrogen Response Element

Exe: Exemestane

FBS: Fetal Bovine Serum

FGFR1: Fibroblast Growth Factor Receptor 1

GFRs: Growth Factor Receptors

GPR30: G Protein-Coupled Estrogen Receptor

H12: Helix 12

HER2: Human Epidermal Growth Factor Receptor 2

HREs: Hormone Response Element

HSP70: Heat Shock Protein 70

HSP90: Heat Shock Protein 90

HTS: High-Throughput Screening

HTST: 16α-hydroxytestosterone

ICI: ICI 182 780

IGF1R: Insulin-Like Growth Factor Receptor 1

LBD: Ligand Binding Domain

LDH: Lactate Dihydrogenase

Let: Letrozole

LibMCS: Library MCS

MAPK: Mitogen-Activated Protein Kinase Pathway

MEM: Minimum Essential Medium

MFI: Mean Fluorescence Intensity

mRNA: Messenger Ribonucleic Acid

MTT: 3-(4,5-dimethylthiazol-2-yl)-2,5 diphenyltetrazolium bromide

NADPH: Nicotine Adenine Dinucleotide Phosphate

NLS: Nuclear Localization Signal

NO: Nitric Oxide

NR: Nuclear Receptors

PCR: Polymerase Chain Reaction

PDB: Protein Data Bank

PGE_2: Prostaglandin E_2

PHTPP: 4- [2-phenyl – 5,7, bis (trifluoromethyl) pyrazol [1, 5-a] pyrimidin-3-yl] phenol

PI: Propidium Iodide

PR: Progesterone Receptor

qPCR: Quantitative Polymerase Chain Reaction

RLU: Relative Luminescence Units

ROS: Reactive Oxygen Species

SEM: Standard Error of the Mean

SERDs: Selective Estrogen Receptor Down-Regulators

SERMs: Selective Estrogen Receptors Modulators

SP-1: Specificity Protein 1

STS: Staurosporine

T: Testosterone

TCA: Trichloroacetic Acid

TKR: Tyrosine Kinase Receptors

VdW: Van der Waals

VS: Virtual Screening

1. Introduction

1.1. Breast cancer

Breast cancer is the most common type of cancer among women and the second most frequently diagnosed cancer worldwide and, like other malignancies, its incidence rises dramatically with age (1-3). It is estimated that more than two million new cases of this type of tumor were diagnosed in 2018, resulting in more than 620 000 deaths (3). Nevertheless, the mortality rate related to this type of cancer has been decreasing as a result of the improvements in public health and the emergence of new therapeutic options (1).

Breast tumors can be divided in several subtypes, luminal A, luminal B, $HER2^+$ and basal-like, considering the expression pattern of estrogen receptor (ER), progesterone receptor (PR) and human epidermal growth factor 2 (HER2). Luminal A carcinomas present a high expression of ER and PR and are considered low-risk cancers, being linked to a better prognosis. On the other hand, luminal B tumors have a lower expression of ER and PR, but an elevated expression of HER2, being more aggressive carcinomas than luminal A. The $HER2^+$ breast cancers show only an overexpression of HER2, while basal-like tumors, usually the most aggressive subtype, do not exhibit overexpression of ER, PR or even HER2 and, because of this, they are commonly designated as triple-negative breast cancers (1, 4).

About 75% of all breast cancer cases in post-menopausal women and 60% of the cases in pre-menopausal women are hormone-dependent/ER^+ breast cancers (5). In ER^+ breast cancer, the ERs are overexpressed and, consequently, estrogens play a central role in tumor development and survival. The treatment for this type of breast cancer is based on endocrine therapy that is constituted by anti-estrogens, compounds that interfere with estrogen-dependent pathways, or aromatase inhibitors (AIs), which inhibit aromatase, preventing the synthesis of estrogens (6, 7).

1.2. Aromatase

Estrogens are synthesized by the enzyme aromatase, which belongs to the cytochrome P450 family, characterized by the presence of a heme group (8-10). Aromatase is encoded by the *CYP19A1* gene located on chromosome 15 and is generally expressed in several tissues including gonads, brain, adipose tissue, skin, bone, blood vessels, endometrium and breast tissue, being well conserved among vertebrates (8, 9, 11). Despite that, in women, the expression pattern of aromatase varies with age. In pre-menopausal women, aromatase is essentially expressed in the granulosa cells of ovaries, while in post-menopausal women, when ovaries are no longer

functional, aromatase is essentially expressed in other peripheral tissues, like adipose breast tissue. During pregnancy, there is also high expression of this enzyme in placenta (8, 12-14). In humans, the expression of aromatase is tightly regulated. Its gene consists of ten exons, the untranslated exons Is (I.1, I.2. 2a, I.3, I.4, I.5, I.6, I.7, I.f and PII) and the translated exons II-X, which are expressed in a tissue-specific manner and associated with the respective promoter that is regulated by a specific mechanism. In normal breast tissue, the expression of aromatase is ensured by promoter I.4 that is regulated by glucocorticoids. However, in breast cancer cases, where aromatase is overexpressed, there is a transcriptional switch from I.4 promotor to II and I.3 promoters, as a result of the activation of cAMP-mediated pathways induced by prostaglandin E_2 (PGE_2), locally synthetized by cyclooxygenase isoenzymes (COX-1 and COX-2) (8, 15).

Aromatase is responsible for the conversion of androgens into estrogens. In fact, aromatase binds with high specificity to the C19 androgens, androstenedione (ASD), testosterone (T) and 16α-hydroxytestosterone (HTST) and, by catalyzing an aromatization reaction of the A-ring, it converts them into C18 steroids, estrone (E_1), 17β-estradiol (E_2) and 16α-estriol (E_3), respectively (15, 16) **(Fig. 1)**. This reaction involves a second protein, the NADPH-cytochrome P450 reductase (CPR), that is responsible for catalyzing the electron transfer to aromatase. Moreover, it comprises three steps each one requiring one mole of oxygen and one mole of NADPH. The first two steps are hydroxylations of the C19 methyl group, in which the residues Ala306 and Thr310 participate, and the third step involves a dehydration and the delocalization of electrons leading to the aromatization of A-ring (15-18). In this last step, Ala306 and Thr310 along with Asp309 contribute to the aromatization process (17). This makes aromatase a unique enzyme and the only one in vertebrates that performs this type of reaction (16).

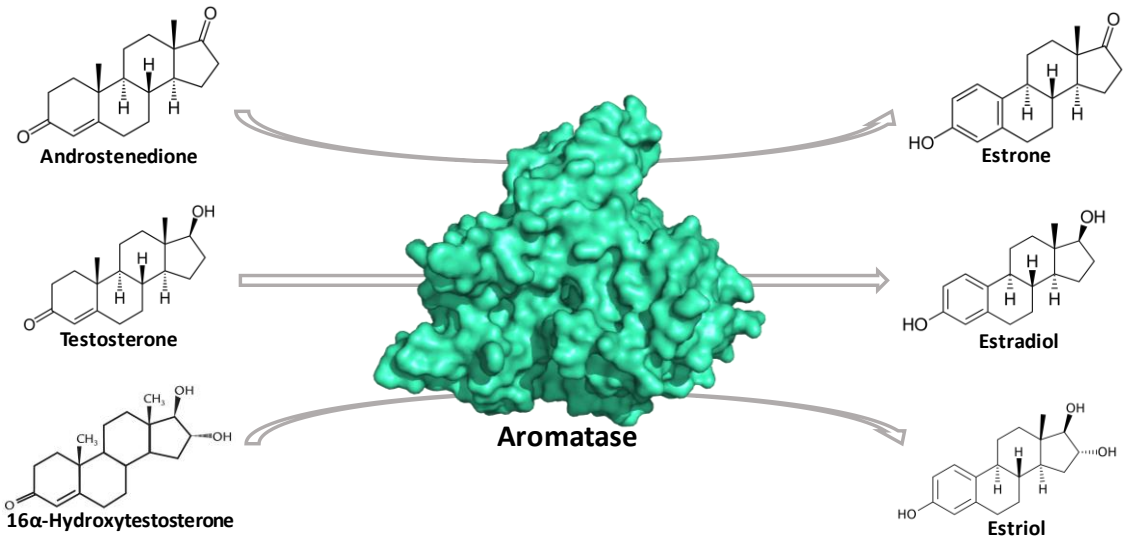

Figure 1: Conversion of androgens, androstenedione (ASD), testosterone (T) and 16α-hydroxytestosterone (HTST), into estrogens, estrone (E1), estradiol (E2) and estriol (E3), respectively, by aromatase.

The aromatase structure was fully elucidated just in 2009 by Ghosh *et al*., using X-ray crystallography (19). This enzyme, anchored to endoplasmic reticulum membrane by an amino terminal domain, is functional as a monomer and consists of 503 amino acids arranged into twelve α-helices and ten β-strands (16, 19, 20) **(Fig. 2)**. Its binding site is small, presenting less than 400 $Å^3$, and comprises the residues Ile305, Ala306, Asp309, Thr310, Phe221, Trp224, Ile133, Phe134, Val370, Leu372, Val373, Met374, Leu477 and Ser478 (21). Some of these residues, namely Phe221, Trp224 and Met374 are especially important for the binding of androgen substrates, since mutation studies regarding these residues indicate that their absence decrease the catalytical activity of aromatase (8, 21). Moreover, these residues are also described to be important for the binding of AIs (8). Additionally, some studies attribute a special role to Asp309, pointing that this residue is directly involved in substrate binding and catalysis (18, 22). More recently, in 2018, the crystal structure of aromatase complexed with T was resolved, showing that this androgen binds to aromatase in a similar manner as observed for ASD (23). In fact, both ASD and T bind to aromatase by interacting specially with the residues Phe221, Trp224, Asp309 and Met374. Despite this, the residues Arg115, Phe134, Thr310 and Val370 are also considered important for their binding (8, 21, 23).

The elucidation of the aromatase structure, of its active site and of the interaction between the substrates T and ASD with the active site of the enzyme (19, 23) was a breakthrough for the future development of potent AIs.

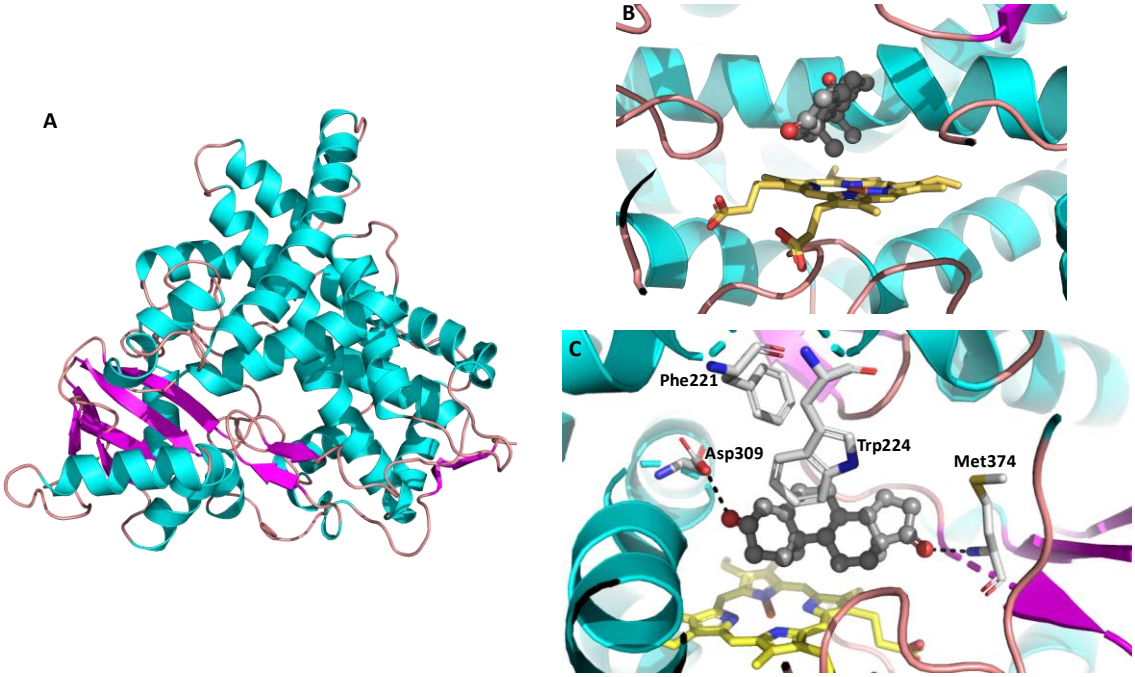

Figure 2: Aromatase structure representation (code 3S79). **(A)** Aromatase is composed by 12 α-helices (blue) and 10 β-strands (magenta). Images **(B)** and **(C)** show the binding site of the enzyme, containing the heme group (yellow) and, in this case, aromatase is complexed with androstenedione (ASD; grey). **(C)** ASD binds to aromatase by interacting with specific residues like Phe221, Trp224, Asp309, and Met 374.

1.3. Estrogen and Estrogen Receptors

1.3.1. Estrogens

Estrogens are steroid hormones involved in crucial female processes. Although reproduction is the main process in which estrogens play a central role, these hormones also display important functions in bone homeostasis, growth, brain function, development of the mammary glands and musculoskeletal and cardiovascular systems. Estrone (E_1), 17β-estradiol (E_2) and 16α-estriol (E_3) are the main estrogens present in women, being E_1 the fundamental form of estrogen in post-menopausal women and E_2 the principal estrogen with key functions in pre-menopausal women. E_3 is the predominant estrogen during pregnancy (13, 24).

E_2 deficiency is associated with several symptoms and pathologies that can induce various adverse effects. Some of the most frequent symptoms are associated with menopause and include hot flashes, mood swings and increased bone reabsorption (25), being the latter directly involved in the development of osteoporosis (25). In order to attenuate these problems, hormone replacement therapy with estrogens is usually prescribed. However, an increase in circulating levels of estrogens may give rise to serious adverse effects like bleeding problems, increased risk for the occurrence of

strokes, as well as, development of endometrial and breast cancers (25). Besides that, the development of breast cancer depends on other factors like age, radiation exposure, body weight and family history. Considering this, a general block of estrogen action should not be favorable. For that reason, over the years, scientists have been trying to develop tissue-selective ER modulators (26, 27).

In relation to ER^+ breast cancer, the first evidence of the role of these hormones in this pathology occurred in 1896, after an oophorectomy, where it was observed the regression of breast cancer (28). Nowadays, the importance of ovarian steroidogenesis and circulating estrogen levels on the development of breast tumors are undoubted. In fact, a long-term exposure to estrogens achieved by early menarche, late menopause, estrogen replacement therapy during menopause, obesity and elevated circulating levels of E_2 is associated with a higher risk of developing this type of malignancy (29, 30).

1.3.2. Estrogen receptors

Estrogens exert their effects by binding to two isoforms of ER (ERα and ERβ). These receptors belong to the steroid receptors family that is included in the nuclear receptors (NR) superfamily of transcription factors (31, 32). NR exert crucial roles in several biological processes such as cell growth and death, development, metabolism, reproduction and immunity, which make them important targets for the treatment of a variety of diseases (33). The analysis of human genome has revealed the existence of 48 NR and some of them are considered “orphan receptors” because, until now, their ligands remain unknown (33).

All members of NR superfamily share a common structure **(Fig. 3)** that comprises six different functional domains (A-F) with several degrees of sequence homology between the different members of the family (34). The A/B domain, the N-terminal region, is the less conserved segment of nuclear receptors. The ERα and ERβ share only 17% of homology in this domain, what may explain the specific actions of each ER isoform on target genes (31, 32, 34). This segment presents a transactivation function domain (AF-1), which when phosphorylated on some specific residues can lead to the activation of the receptor in a ligand-independent manner (35). Furthermore, this domain binds to the transcription machinery when the receptor is within the nucleus and, until now, no secondary structure has been identified for this region (25, 34). C domain is a highly conserved region where DNA-binding domain (DBD) is localized. ERα and ERβ exhibit 94% homology in this domain. DBD is essentially composed by α-helices and contains two zinc finger-like motifs, that allow its binding to DNA, and two distinct subregions

responsible for DNA recognition and dimerization of the receptor (34, 36, 37). D domain is another low conserved segment known as hinge region and responsible for the link between C and E domains. This domain has also a nuclear localization signal (NLS) and ERα and ERβ exhibit 36% homology in this domain (34, 38). E domain is a variable region where ERα and ERβ share 59% homology. This ligand binding domain (LBD) displays important features for the function of the receptors, namely a ligand binding site, a co-activator/co-repressor interaction region, a dimerization interface and a transactivation function domain (AF-2), which is responsible for the transcriptional regulation in a ligand-dependent manner (31, 34). LBD is composed of twelve α-helices sandwiched with two β sheets, however, the LBD of ERα and ERβ has only eleven α-helices because helix 2 (H2) is absent (25, 36). Helix 12 (H12) is a very flexible helix crucial for AF-2 activity that changes its conformation upon binding of different compounds (31, 36, 39). Finally, F domain, where ERα and ERβ share an homology of 18%, is the C-terminal region of NR and seems to present important roles regarding the protection of the receptors against proteolysis (34, 37, 38).

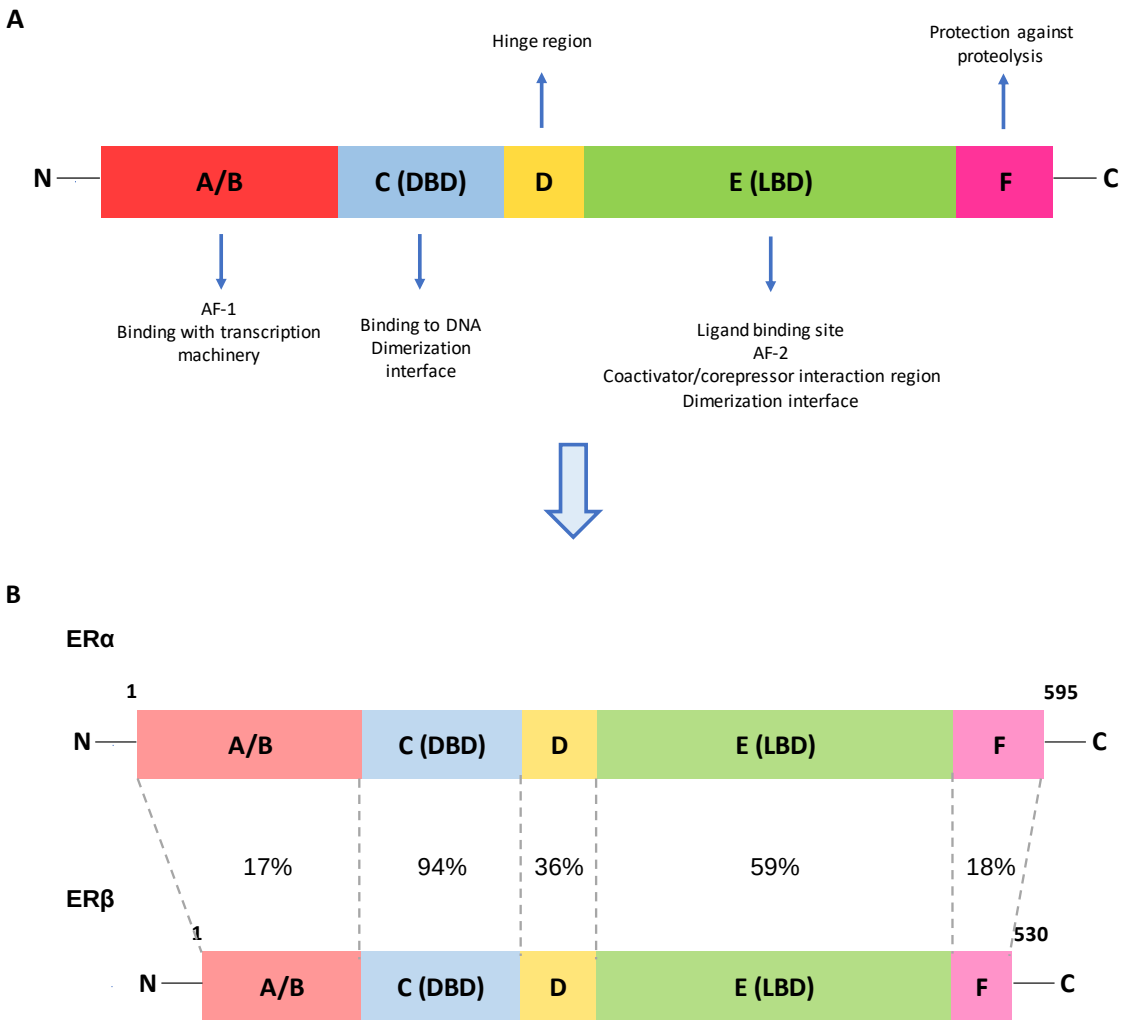

Figure 3: Schematic representation of NR structure **(A)** and comparison of the structures of ERα and ERβ **(B)**.

1.3.3. ERα and ERβ

ERα was cloned for the first time in 1985 from the human breast cancer cell line MCF-7 (40) and in 1996, ERβ was cloned from rat prostate (41). These receptors share an overall sequence homology of 47% (34) and are encoded by different chromosomes. ERα is encoded by the *ESR1* gene on chromosome 6. It has a molecular weight of 66 kDa and presents 595 amino acids, while ERβ, encoded by the *ESR2* gene located on chromosome 14, has a molecular weight of 59 kDa and 530 amino acids (35, 42, 43). As mentioned above, the LBD of these two receptors share a homology of 59%, but the ligand-binding cavities exhibit a huge similarity with only two different amino acid residues. The ERα residues Leu384 and Met421 are replaced, respectively, by Met336 and Ile373 in ERβ (26, 44). These differences together with some different residues outside of the LBD are enough to originate pockets with distinct sizes for ligand binding (38).

ERs exhibit distinct tissue expression patterns and functions. ERα has a fundamental role in the mammary gland, uterus, bone, hypophysis, adipose tissue, skeletal muscle preservation and in the regulation of metabolism. ERα is also expressed in ovaries, prostate, liver, heart and male reproductive organs, such as testes and epididymis. On the other hand, ERβ is critical for the function of immune and nervous systems, but is also found in kidney, mammary gland, bladder, ovaries, brain, bone, heart, lung, prostate, intestinal mucosa and colon (38, 43, 45, 46). Additionally, both receptors have important physiological roles in ovaries development and function, as well as, in the cardiovascular system (46).

ERα and ERβ display key roles on ER^+ breast cancer. In this pathological status, as in normal breast cells, ERα is one of the predominant proteins involved in the regulation of the endocrine function (7), being responsible for growth, survival and proliferation of breast epithelial cells, which in cancer cases leads to the promotion of tumor development (46, 47). In fact, during the diagnosis process, the overexpression of this receptor is an evidence of a hormone-dependent tumor (48). On the other hand, ERβ displays anti-proliferative properties when is co-expressed with ERα in breast cancer epithelial cells, promoting apoptosis and thus, counteracting the ERα effects and acting as a tumor suppressor (27, 46, 49, 50). Considering this, the use of ERα antagonists or ERβ agonists seems to be an attractive therapeutic approach for the treatment of ER^+ breast cancer cases (46, 49). However, in some rare cases where there is no expression of ERα (ERα-negative tumors), ERβ can also promote cell growth and proliferation. Taking into account the possibility of ERβ to act as a inhibitor or as a promoter of breast tumors development, it is also referred as a “bi-faceted” receptor (49).

In addition to the important roles mediated by ERs in hormone-dependent breast cancer, they are also deeply involved in other tumors, as prostate, colon and ovarian cancers, where both ER isoforms display similar functions to the observed for ER^+ breast cancer (46, 47, 49).

1.3.4. Signaling pathways of ER

Estrogens exert their functions through genomic or non-genomic pathways (7) **(Fig. 4)**. In the genomic pathway, ERs are generally activated by the binding of estrogens. Initially, ER is located within the cytosol, where chaperon proteins, like HSP70 and HSP90 are bind to LBD domain. These proteins keep ERs in an inactivated state and prevent them from being degraded. Upon binding of estrogen to LBD, this domain suffers conformational changes that result in the dissociation of the ER from the HSP

and, subsequent, dimerization (homodimers or heterodimers) (35, 42). After that, the estrogen-ER complex is translocated to the nucleus. Although this process remains unclear, it seems that D domain has a crucial role on it. This domain has a NLS that is able to interact with importins and some microtubule-associated molecular proteins, mediating the transport of the complex into the nucleus (38). Once inside the nucleus, the DBD of the ER interact with a 5'-AGGTCAnnnTGACCT-3' DNA palindrome sequence, located in the estrogen response element (ERE) within the promoters of target genes (38, 51). This binding allows the interaction of the AF-1 with the transcriptional machinery and receptor's LBD with co-activators or co-repressors. These interactions modulate the transcription of target genes involved in the regulation of cell proliferation and survival, such as, growth factors, growth factor receptors (GFRs), transcription factors (for example, c-Myc, c-Fos and c-Jun) and cell cycle components, like cyclin D1 and p21 (4, 7). This is considered the classical signaling pathway **(Fig. 4a)**. ERs are also able to modulate the transcription of genes located in alternative EREs in a ligand-dependent manner but without direct DNA binding. This is known as non-classical or ERE-independent genomic pathway. This is possible because of the ability of the ERs to interact with other transcription factors, like activator protein 1 (AP1) and specificity protein 1 (SP1) (4, 51, 52) **(Fig. 4b)**. Besides these two different genomic mechanisms, there is still a third mechanism that involves the ER activation in a ligand-independent manner via phosphorylation of the AF-1 domain by several kinases, such as, Cdk2, p38 MAPK, p44/42 MAPK, JNK and PI3K/Akt (4, 8, 51) **(Fig. 4c)**. This process is often involved in the development of endocrine resistance (8, 35).

Additionally, estrogens are also capable to induce non-genomic and rapid effects. These effects are mediated by GFRs, like fibroblast growth factor receptor-1 (FGFR1), insulin-like growth factor receptor-1 (IGF1R), epidermal growth factor receptor (EGFR), HER2 and G protein-coupled receptors, like G protein-coupled ER (GPR30) (35, 53). These pathways lead to the generation of second messengers such as Ca^{2+}, cAMP and nitric oxide (NO) and to the activation of several kinases, like PLC/PKC, RAS/RAF/MAPK and cAMP/PKA, activating, in that way, several different signaling pathways (35, 54, 55) **(Fig. 4d)**.

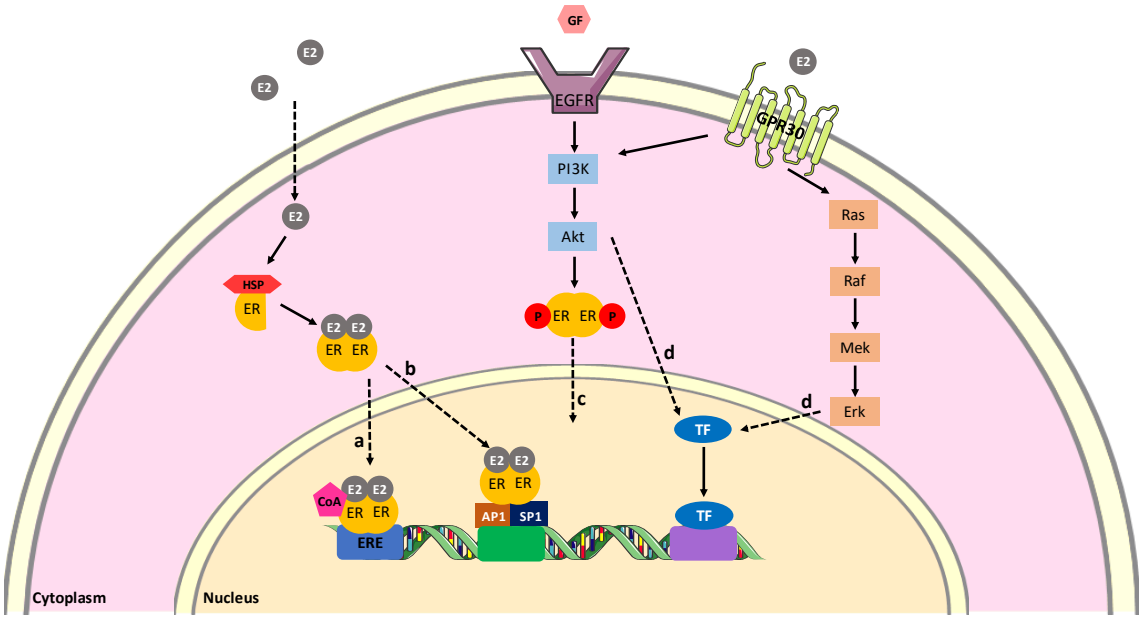

Figure 4: ER signaling pathways. **(a)** In the classical pathway, after the binding of E2, the ERs dimerize and are translocated to the nucleus where the estrogen-ER complex interact with EREs inducing the recruitment of co-activators (CoA), or co-repressors, and the transcription of target genes. **(b)** ERs can also bind to different EREs in a ligand-dependent manner. This genomic pathway is known as non-classical or ERE-independent. **(c)** ERs can be activated by phosphorylation of the AF-1 domain via kinases and, once phosphorylated, they are able to modulate the transcription of genes. **(d)** Finally, estrogens are able to induce rapid effects through non-genomic pathways. In this case, the membrane isoform of the ERs (GPR30) activates several kinases signaling pathways that activate some transcription factors (TF), which then can induce the transcription of target genes.

1.3.5. Agonism vs antagonism

As stated above, LBD is an important region of the ERs constituted by eleven α-helices and harboring the AF-2 transactivation function domain for which H12 is essential (39). AF-2 is composed by the helices H3, H4, H5 and H12 being the latter the main regulator of this transactivation function, as it undergoes huge shifts depending on the type of compound that is bound (31, 56). When an agonist binds to ER, H12 is repositioned, joining to H3, H5, H6 and H11, occluding the ligand binding site (57). This is the active conformation of the ER and in that state, the position of H12 allows LBD to adopt a conformation that favors the binding of co-activators which are critical for transcriptional activation, as they act like intermediaries between the ERs and all the machinery involved in transcription (25, 31, 47) **(Fig. 5A)**. Co-activators that belong to the CBP/p300 and SRC/p160 families harbor a LXXLL motif (L refers to leucine and X to any other residue), also known as NR boxes (36), which is responsible for their binding to ERs through interaction with AF-2 (25, 37, 39, 47, 56). In contrast, when an antagonist binds to LBD, H12 adopts a different position moving towards H3 and H5, what buries some important residues for AF-2 activity, thus, preventing the co-activator recruitment

(57, 58). Furthermore, in this inactive conformation, H12 occupies the co-activator binding site because, like co-activators, this helix also has a NR box-like sequence (LXXML where L refers to leucine, M to methionine and X to any other residue) that is able to perfectly mimic the interactions made by the LXXLL motif of the co-activators (34, 39) **(Fig. 5B)**. Consequently, there are no intermediaries between the receptor and the transcriptional machinery, what impairs the transcription of target genes.

As these two conformations are a consequence of the type of ligands that binds to the ERs, the structure and the bonds that such compounds establish with the LBD of the ER are determinant for H12 position. In general, ER ligands contain two hydroxyl groups, separated by a lipophilic linker scaffold and at least one of these groups should be a phenolic hydroxyl group. These groups are able to interact with some specific residues of the ERs (Glu353/305 and Arg394/346, respectively for ERα/ERβ) and a water molecule, establishing strong H-bonds with them (25, 46). On the other hand, the majority of antagonists are larger than agonists, which is directly associated with the different positions displayed by H12 and, consequently, with the different conformations of the receptors (31, 59). All this information is fundamental for the discovery and development of new ER ligands considering the desired effects.

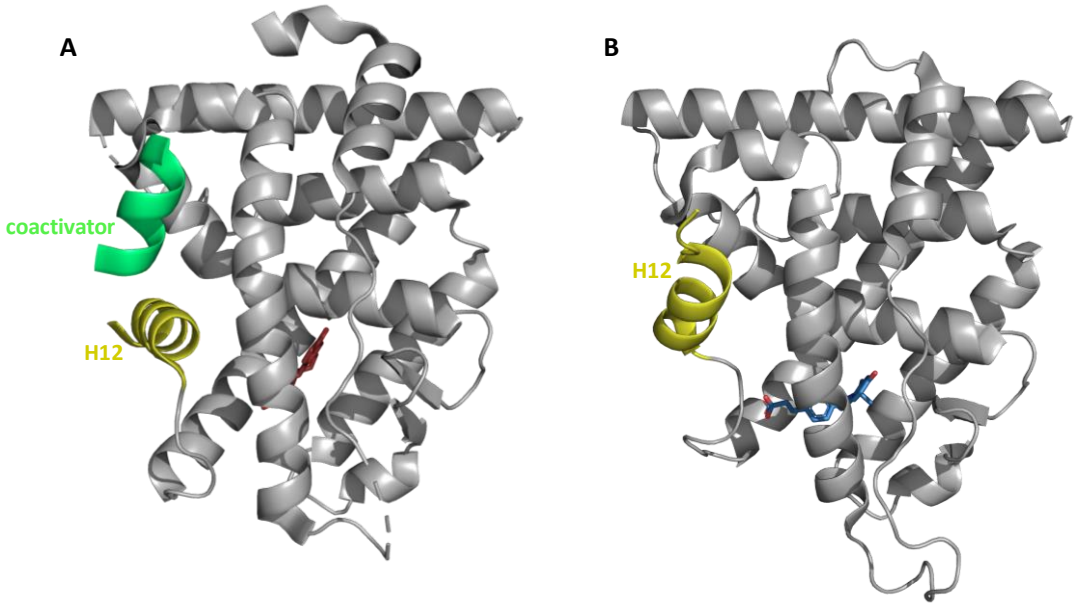

Figure 5: Active and inactive conformations of ERs. Both images represent the LBD domain in a monomeric form. In **A**, it is represented an ERα LBD complexed with the agonist 17β-estradiol (code 1GWR). At this active conformation, H12 adopts a position that allows the binding of coactivators. In **B**, the structure represents an ERα LBD complexed with tetrahydroisoquinoline phenol 1, an antagonist (code 5FQP). This ligand induces a different H12 conformation (inactive conformation), which avoids the binding of coactivators.

1.4. Endocrine therapy

Breast cancer treatment comprises different therapeutic options that are applied depending on several factors like, tumor subtype, stage of the tumor and biological state of the patients. Sometimes, before surgery, an additional treatment can be useful to reduce the size of the tumor and find the best treatments for the cancer. This is known as neoadjuvant therapy. After surgery, it is important to lower the risk of cancer recurrence. This type of treatment is known as adjuvant therapy and can be done using radiation therapy, chemotherapy, target therapy and endocrine/hormonal therapy.

Endocrine therapy is the mainstay treatment for ER^+ breast cancer, since it is responsible for lowering the estrogen levels and, consequently, inhibit the growth and proliferation of the tumor (60). It is constituted by AIs, that inhibit the production of estrogens, and by anti-estrogens like, selective estrogen receptor modulators (SERMs) and selective estrogen receptor down-regulators (SERDs), compounds that interfere with estrogen-dependent pathways (6, 7, 61).

1.4.1. Aromatase Inhibitors

AIs are specific drugs that, by inhibiting the aromatase action, are able to reduce the estrogen levels in more than 90% without interfering with the production of other steroids (62, 63). According to their chemical structure, these compounds are classified into two subtypes, steroidal (type I) and non-steroidal (type II). Steroidal AIs are analogs of ASD, the natural substrate of aromatase. Because of this, type I AIs directly compete with androgens to the active site of the enzyme, binding in a covalent manner and causing its irreversible inactivation. During this process, these compounds are converted by aromatase into reactive intermediates, which in turn bind permanently to the enzyme, inactivating it and leading to its degradation by the proteasome. Because of this, steroidal AIs are also known as “suicidal inhibitors”. On the other hand, the non-steroidal AIs interact reversely and non-covalently with the heme moiety of aromatase, saturating the enzyme binding site and preventing the binding of androgens to aromatase (35, 64-66).

In addition, AIs are also grouped in three generations according to their chronological order of appearance and evolutional modifications **(Fig. 6)**. The first-generation of AIs includes aminoglutethimide and testolactone, which were marketed in the late 1970s. Aminoglutethimide was the first non-steroidal AI that was applied in clinical studies for hormone-dependent breast cancer treatment (15). However, this compound showed high toxicity and lack of specificity, since it interfered with other cytochrome P450 enzymes, and because of that it was withdrawn (20, 65). Testolactone

was a steroidal AI structurally related to T but with lower potency than aminoglutethimide (65). The second-generation AIs comprises the steroidal formestane (4-hydroxyandrostenedione) and the non-steroidal fadrozole that were developed during the 1980s and 1990s. Although these compounds were about 700 times more potent than aminoglutethimide, their clinical use showed some disadvantages, since formestane exhibited poor oral bioactivity, being administrated by intramuscular injection, while fadrozole showed a short half-life and affected the biosynthesis of aldosterone, progesterone and corticosterone (20, 35, 65). Finally, the third-generation of AIs includes the non-steroidal triazole derivatives, anastrozole (Ana) and letrozole (Let), and the steroidal exemestane (Exe), (15, 20). These compounds are more selective than the compounds from the previous generations and are, nowadays, used as first-line therapeutic options for post-menopausal women in adjuvant treatment for early and metastatic stages (67, 68). Furthermore, recent guidelines also point the use of these AIs in pre-menopausal women after ovaries ablation (60, 69).

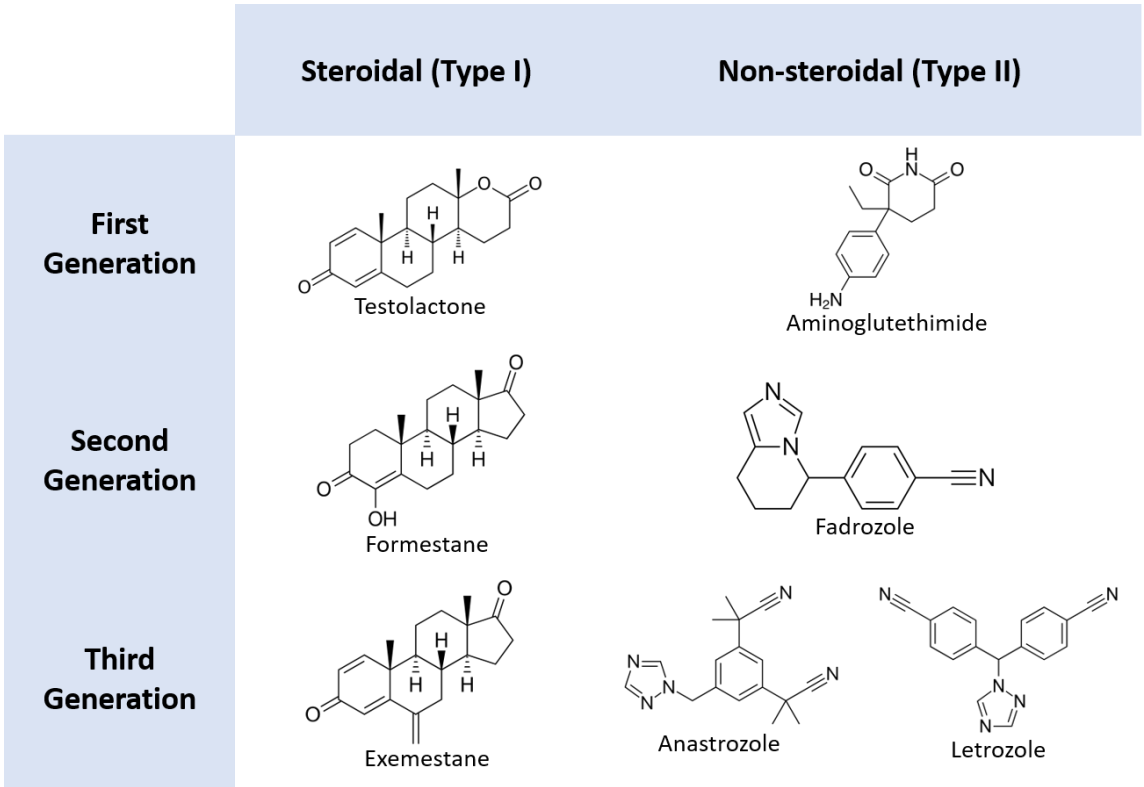

Figure 6: Chemical structures of the two types of AIs from the three generations.

In relation to the structural features of the AIs complexed with aromatase, some studies point that Asp309, Thr310, Ser478, Met374, Phe134, Phe221, Trp224, Ala306, Ala307, Val370, Leu372 and Leu477 are important residues for their binding to

aromatase (17). Furthermore, as well as in the ASD binding to aromatase, the residues Phe221, Trp224 and Met374 are also described to play key roles in the binding to AIs. However, the interaction is different depending on the type of AI (steroidal or non-steroidal) (8). In contrast with ASD, the mutations Phe221Tyr, Trp224Phe and Met374Thr induced a stronger binding of Let, probably because the mutated residues may re-arrange the binding pocket and reduce the steric clashes. In relation to Exe, the mutant Met374Thr, cause aromatase inhibition, but the mechanism-based inhibitor of this mutant is less effective than the wild-type (21). Moreover, for Exe, the residues Trp224, Glu302, Asp309 and Ser478 are also described to be deeply involved in the mechanism of aromatase inhibition (8). In addition, as steroidal AIs and non-steroidal AIs are structurally different, their binding to aromatase is also different, being the main difference the interaction with the heme group. While Exe, apparently, does not establish any interaction with the heme group, Let binds non-covalently to the heme group, being the distance between them of 3.7 Å (8, 21).

However, besides the huge therapeutic success of the third-generation AIs, their prolonged used is linked to a diversity of side effects, being the most common the hot flashes, headache, arthralgias, mood disorders, musculoskeletal pain, cardiovascular events, sexual dysfunction, dyslipidemia and thromboembolic side effects (11, 35, 70-72). Moreover, as these compounds induce a decrease in estrogen levels, they can lead to loss of bone mineral density, which increases the risk of bone fractures and the development of osteoporosis (60, 71, 73). Nevertheless, despite all these effects, the most concerning problem regarding AIs is the development of endocrine resistances, which is responsible for tumor-regrowth (35). Due to all of these side effects, several efforts have been done in order to develop and discover new and more potent steroidal (12, 74-76) and non-steroidal AIs (71, 77).

1.4.2. Anti-estrogens

As previously stated, anti-estrogens are compounds able to interfere, or even block, the interaction with estrogens and the activation of estrogen-dependent pathways. They can be classified as SERMs or SERDs.

Tamoxifen is the best known SERM **(Fig. 7A)**. It is a non-steroidal compound and is used in pre-menopausal women, acting as a partial ER antagonist by disrupting the ligand-receptor interaction, which prevents the normal action of estrogens (4). Tamoxifen binds to the ER in a similar manner as E_2, but AF-2 is not activated, reason why the transcription of target genes dependent on AF-2 is reduced (78). Nevertheless, AF-1

domain remains active. However, besides this antagonistic activity exerted mainly on breast tissue, tamoxifen is also capable of exerting agonistic effects, mainly on bone and endometrium. This dual action is modulated by the presence of co-activators and co-repressors (4, 79). Moreover, tamoxifen is responsible for some adverse effects. Due to its agonistic activity on endometrium, there is an increased probability to develop endometrium cancer. Besides that, other effects like chest pain, hot flashes, nausea, headache and depression can occur, which limits the use of this SERM (80).

Fulvestrant is a SERD that also acts as an ER antagonist, being commonly known as "pure" anti-estrogen, since the transcription is totally impaired **(Fig. 7B)**. This steroidal SERD acts by interacting with ERα, blocking its dimerization and DNA binding and thus, promoting its premature degradation, which consequently blocks estrogen signaling. As both AF-1 and AF-2 domains remain inactive, the result is a pure antagonistic effect with the full inhibition of estrogen-dependent pathways (78). Fulvestrant is used both in pre- and post-menopausal women when other therapies, like SERMs or AIs, are not effective (4, 79). Despite being a well-tolerated compound, fulvestrant causes also some side effects, namely nausea, vomiting, loss of appetite, headache, weakness and join and muscle pain. Furthermore, fulvestrant is administrated by intramuscular injection, which represents another disadvantage (81).

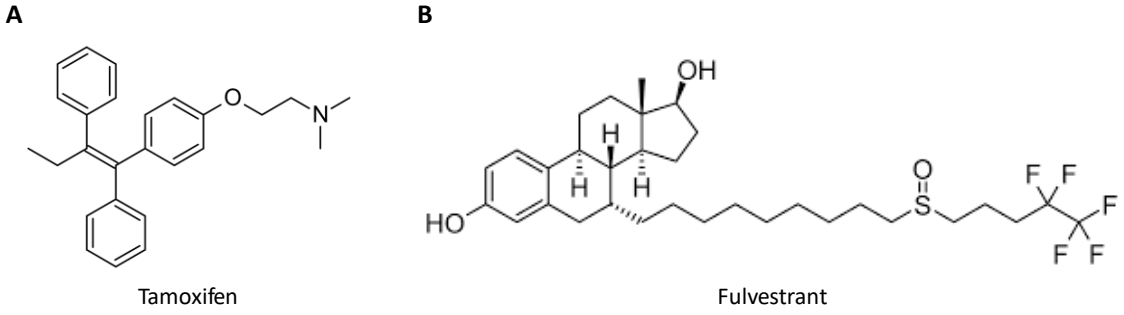

Figure 7: Structural representation of tamoxifen **(A)** and fulvestrant **(B)**.

Comparing the clinical efficacy of the three groups of therapies, AIs, SERMs and SERDs, the clinical studies already available point that AIs are more effective than tamoxifen, since they present higher prolonged disease free-survival, higher time to recurrence, as well as, lower side effects than this SERM. Nevertheless, AIs do not significantly improve the overall survival when compared to tamoxifen (35, 82). On the other hand, in relation to fulvestrant, data show that AIs are not better, since this SERD seems to increase disease free-survival and overall survival when compared with AIs (83, 84). However, the clinical use of fulvestrant is limited by its low solubility which impairs its oral delivery. Because of this, AIs remain the standard treatment option for

post-menopausal women with ER^+ breast cancer and, more recently, also to pre-menopausal women with ovary ablation (67, 68).

1.5. Resistance to Endocrine Therapy

As previously stated, endocrine therapy comprising anti-estrogenic compounds and AIs is the main therapeutic strategy for ER^+ breast cancer treatment. However, despite its clinical benefit, the main limitation regarding this therapy is the occurrence of endocrine resistances. In fact, it is estimated that about 20% of patients presenting early-stage disease do not respond to therapy, considered the primary/*de novo* resistance, and that 30% of the tumors that are initially responsive to endocrine therapy will eventually relapse, designated as secondary/acquired resistance (6, 35).

De novo resistance is defined as a relapse during the first 2 years of adjuvant endocrine therapy or as disease progression within the first 6 months of first-line endocrine therapy for metastatic breast cancer. Acquired resistance, in turn, is defined as a relapse during adjuvant endocrine therapy but after the first 2 years, or as a relapse within 12 months of completing adjuvant endocrine therapy or disease progression after 6 months of initiating endocrine therapy for metastatic breast cancer (67).

In the last years, several mechanisms responsible for the development of endocrine resistances have been described. One of the mechanisms involves the ER signaling pathway, as *ESR1*, the gene that encodes ERα, can suffer point mutations, translocations and amplifications (85-89). Furthermore, the deregulated activation of GFRs, IGFR-1, FGFR-1 and their downstream signaling pathways (6, 52, 90, 91), as well as, the deregulation of PI3K/Akt/mTOR or MAPK pathways (85, 88, 89, 91), and the hypersensitivity of the ERs to estrogens (35) can deregulate the activity of ERα and lead to endocrine resistance.

Other mechanisms of resistance involve the androgen receptor (AR) (35, 88), the aberrant expression or activation of molecules associated to the regulation of the cell cycle (35, 88, 92), apoptosis and autophagy (35, 93, 94) and, more recently, miRNAs (88, 95).

Considering all of these mechanisms, recent studies suggest the use of traditional endocrine therapy compounds in combination with other compounds such as CDK4/6 and mTOR inhibitors (6, 89, 96). Furthermore, keeping in mind how endocrine resistance limits the treatment of ER^+ breast cancer, it is crucial to discover and develop new therapies able to surpass this issue.

1.6. Multi-target Compounds for ER$^+$ Breast Cancer Treatment

ER$^+$ breast cancer treatment has evolved over time for the use of more efficient and selective compounds. Despite that, as previously referred, the therapies already available are associated with diverse side effects, being the most worrying the development of resistances. Because of this, in recent years, several studies have been focused on the discovery of new compounds and in the construction of better therapeutic approaches. Some of the studied approaches were the combination of AIs with SERMs, like the use of the AI Ana in combination with the SERM tamoxifen (97), or the combination of Let with the SERD fulvestrant (98). Both combinations proved to reduce the incidence of side effects. However, in relation to the former this was shown to be less effective than Ana alone (99). Besides that, the uptake of different drugs increases the risks of drug interactions that can lead to more pronounced side effects. Because of this, compounds with dual AI/SERM activity should be more effective than the combination of two different drugs (100).

The first multi-target compound identified for ER$^+$ breast cancer treatment was norendoxifen, a metabolite of tamoxifen, synthetized for the first time in 2013 (101). Besides its agonistic effects on ERα and ERβ, with EC_{50} values of 17 nM and 28 nM, respectively, this compound was also able to inhibit aromatase, with an IC_{50} value of 90 nM (102, 103). Although, until now, the biological effects of this compound are not yet described. Compounds like this are thought to exhibit an improved efficacy and lower side effects. In fact, taking into account the tissue-dependent actions of SERMs, it is expected that in cancerous cells, these compounds are able to simultaneously inhibit the production of estrogens, due to anti-aromatase activity, and block the effect of eventual residual estrogens through SERMs antagonistic action, if the compound act as an ERα antagonist. On the other hand, in noncancerous tissues, the agonistic action of SERMs would be able to alleviate the side effects induced by the depletion of estrogens (100, 102, 104).

Taking these evidences into account, the discovery and development of multi-target compounds would be crucial for the improvement of breast cancer treatment. For that, structural information about some molecules, like norendoxifen, already tested for that propose, as well as, the knowledge regarding the functions of important targets to be modulated are of pivotal importance. Thus, considering ER$^+$ breast cancer and the role of aromatase, ERα and ERβ on this type of tumors, the ideal would be the discovery of a multi-target compound able to inhibit aromatase and ERα and, at the same time, activate ERβ.

1.7. Virtual Screening

Drug discovery is a very complex and demanding process that aims to find a drug able to interact and modulate the function of a specific target, generally a protein, in order to modify its activity and, thus, be effective for the treatment of a specific disease. In fact, the discovery of a drug is a time-consuming process that is associated with very high costs. It is estimated that the whole process can take 14 to 17 years and costs hundreds of million dollars (105, 106). The most common technique used by the pharmaceutical industry to the identification of new leading compounds has being the physical screening of large libraries of chemicals against a biologically-relevant target, known as high-throughput screening (HTS). However, this approach presents many drawbacks. Besides the previously mentioned and related with time and costs, the other one is uncertainty of the mechanism of action of the compounds. Therefore, in general, it is crucial to develop new technologies to facilitate and reduce the hit-to-lead timeline, increase the number of potential compounds and save money and resources (105-108).

One of the most popular methods is virtual screening (VS). This method is used to select hit molecules with desirable properties, allowing the screening of millions of compounds and being faster and much less expensive than HTS. Therefore, it is a very useful technique that is able to reduce the number of compounds being tested with HTS (109, 110). VS can be divided into two distinct methodological classes: ligand-based VS and receptor-based VS methods. Ligand-based VS methods take into account the information regarding the compounds that are known to bind to the target in study, being applicable in the absence of structural information about the protein and in identifying the most common features among all of them. Considering that similar compounds may have similar effects, this information is then used to find other potential active compounds. On the other hand, receptor-based VS methods, also known as structure-based methods, requires the 3D structure of the target and use that information to select the compounds. In fact, these methods involve the explicit molecular docking of each ligand from a database into the binding site of the target, predicting the binding mode of each one and giving a measure related to the quality of the fit of the compound in the target-binding site (105, 106, 108-110).

The structure-based drug discovery is a fundamental tool in the search of novel therapeutic compounds. The application of a rational drug design taking into account, the molecular basis of a disease and the 3D structure of the biological target is more efficient than HTS (108). This approach encompasses several computational stages like, target and database preparation, docking and post-docking analysis and prioritization of the compounds for testing **(Fig. 8)**.

In relation to the target preparation, the most typical steps are: (i) selection of the best target; (ii) obtention of the respective 3D structure or construction of an homology model in case of the protein 3D structure is not available; (iii) evaluation of the *druggability* of the receptor, defined as its ability to bind molecules with drug-like properties; and (iv) identification of the binding site properties. Furthermore, general steps like the addition of hydrogen atoms, the definition of amino acid protonation states and the removal of solvent and ligands are also necessary to prepare the target for docking. In addition, when the structure is incomplete it must be constructed a more complete 3D model (105, 108).

As previously referred, with VS it is possible to easily test a huge number of compounds. However, it is necessary to restrict the number of compounds to be tested, so a good number of molecules can be analyzed in a reasonable period of time. Thus, several filters should be applied. The most common take into account that drugs need some crucial characteristics to be administered by patients and that some chemical groups display toxic properties or are not suitable in a drug. Additionally, counting methods like the Rule of Five developed by Christopher A. Lipinski (111) are also applied to assess the drug probability of a compound. The Rule of Five method is based on the features of the majority of drugs already available and states that a compound should present 5 or less hydrogen bond donors, 10 or less hydrogen bond acceptors, a molecular weight smaller than 500 and a log P (partition coefficient) smaller than 5 (111). Moreover, it is also important to keep in mind that the database to be used should be very diverse to increase the success of the VS (105, 106).

After the preparation of the target and library of compounds, the next step is the molecular docking. This is the step that requires more computational cost and time. Each compound is virtually docked into the target binding site in different conformations, in order to find the pose of the compound that results in the best interaction between the ligand and the target. For that, the docking programs use two different algorithms: the search algorithms and the scoring functions. The search algorithms provide degrees of freedom to the system allowing the generation of several poses to fit each ligand in the target binding site and can be classified as rigid-body search algorithms, flexible-ligand search algorithms and flexible-ligand and receptor search algorithms. Because of their good time-accuracy relation, flexible-ligand methods, which consider the target to be rigid, while ligands are flexible and able to explore conformational space, are the most common. The scoring functions are then used to rank the quality of each pose by calculating an energy value related to the affinity between the protein and the ligand. Furthermore, they can be organized into four categories as force field scoring functions, empirical scoring functions, knowledge-based potentials and machine learning methods.

The force-field scoring functions quantify the binding energy between the ligand and the receptor and, sometimes, the internal energy of the ligand. Empirical scoring functions are much simpler than the force-field scoring functions and assume that the binding energies are the sum of several contributing terms. Knowledge-based scoring functions are statistical methods used to reproduce experimental structures instead of binding affinities (105, 106, 108, 112). Finally, machine learning methods, which use pattern recognition algorithms to establish mathematical relationships between empirical observations, have gained a lot of attention in several areas including the development of scoring functions. However, in contrast to force field scoring functions, empirical scoring functions and knowledge-based potentials, which assume an additive functional form to represent the linear relationship between the binding affinity and the features of the complex protein-ligand, the machine learning methods do not establish this kind of assumptions. Since that linear relationship may not be always present, the non-linear methods introduced by machine learning should have a better performance (113, 114).

One of the most common methods to validate the docking program is evaluate its ability to discriminate between known active ligands and inactive molecules (decoys). It means that a good docking software should attribute a better score to the actives than to the inactive ligands. So, it is expected that the actives are on the top of the list resulting from the VS. This discrimination could be easily evaluated by the construction of a ROC (Receiver Operating Characteristic) curve and by the determination of the enrichment factor, defined as the ratio between recovered actives and the expected number of recovered actives using random scores (105, 115, 116).

Once the docking has been finished, it is necessary to choose the compounds to be experimentally tested. It is possible to choose the compounds based just in the rank, however, as the scoring functions are not absolutely accurate, some false positives could be among the top scored compounds. Because of this, it is useful to use additional post-analysis strategies to improve the choice of the compounds. Regarding this, visual analysis of the compounds is the most common additional analysis performed considering the knowledge about the target under study. However, it is impossible to visual analyze thousands of compounds, so additional strategies should be applied, like the clustering of the molecules and consensus scoring. With clusters, molecules are arranged in several groups according to their similarity and with this, it is possible to select the representative compound of each cluster and make a closer analysis of them. Consensus scoring means rescore de top docked poses with several different scoring functions and select the top compounds common to all functions (105, 106). These strategies increase the chances of finding a biologically relevant compound.

Besides the huge success and relevance of VS, this technique faces some limitations. Although the computational time is a big challenge for the finding of new compounds, flexibility is the major problem regarding these studies. Furthermore, as previously referred, the scoring functions still display some imperfections and physical phenomena such as entropy, and electrostatic interactions are not fully considered. Moreover, aspects like the solvent effect, the involvement of water molecules and, sometimes, the bad resolution of the crystallographic structures, bring additional complexity to this process (112, 117). Thus, much remains to be done to improve the VS techniques in order to reach a good methodology for an efficient drug discovery campaign.

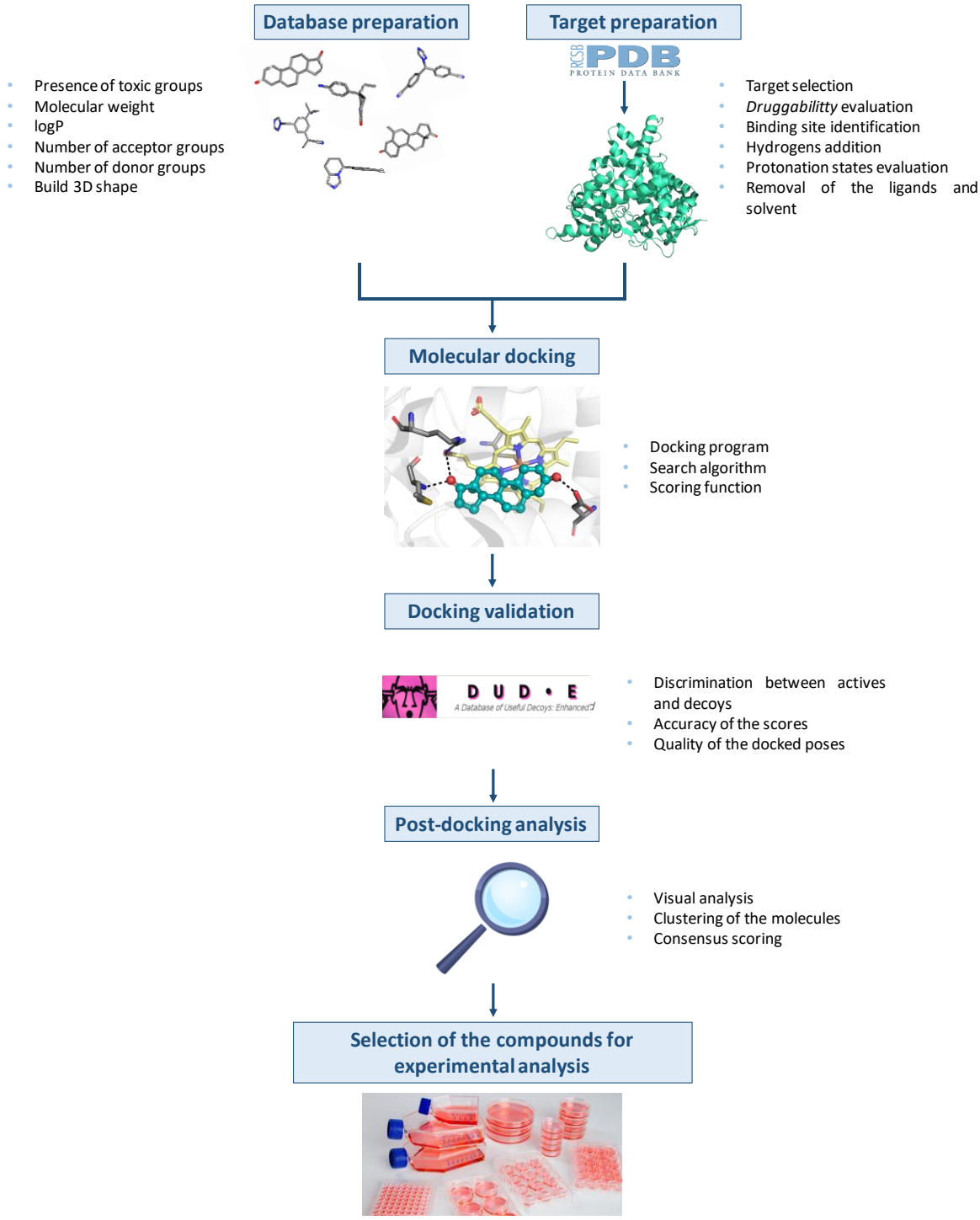

Figure 8: Receptor based VS workflow.

1.8. Objectives

Considering all this information and using VS techniques, we intent to discover a multi-target compound able to inhibit aromatase and, simultaneously, modulate ERα and ERβ actions. This approach seems to be very appealing as it may allow an improvement for the ER^+ breast cancer treatment and, on the other hand, there is very little information

about this matter. Additionally, other aim is to find novel non-steroidal AIs more potent than the AIs already available in the clinic.

First of all, we will perform structure-based VS, to select the best compounds, and make an extended analysis of the molecules already known to exhibit the desired effects in order to understand the specificities and features that the selected compounds should present. After selection, the compounds will be tested first in human placental microsomes, to assess their anti-aromatase activity. The compounds able to inhibit aromatase will be further studied on MCF-7aro and HFF-1 cells, in order to evaluate their *in vitro* effects on ER^+ breast cancer and on non-tumoral fibroblastic cells, respectively. Furthermore, for the non-toxic compounds in non-tumoral cells but able to impair proliferation of ER^+ breast cancer cells, it will be investigated if their effects on cells are dependent on aromatase, ERα and/or ERβ modulation. It will also be explored their effects on cell cycle progression and their ability to induce ER^+ breast cancer cell death.

For the best of our knowledge, this is the first attempt to discover multi-target compounds for ER^+ breast cancer treatment using this type of computational approaches.

2. Materials and Methods

2.1. Structure-based VS

2.1.1. Database preparation

The database used was created by Dr. Xavier Barril Laboratory. It is composed by 3.4 million non-steroidal, drug-like and purchasable compounds from several companies, namely Enamine, KeyOrganics, LifeChemicals, Princeton Biomolecular, Asinex and Specs. These compounds follow the Lipinski Rule of Five. These rules were stablished considering the main common molecular features among the drugs available in the market, in a certain country and year and for oral administration. They are very useful to evaluate the probability of a compound to be potentially orally bioavailable. For that, Lipinski states that the compound should have a molecular weight lower or equal to 500 Da, no more than 5 donors of hydrogen bonds, no more than 10 hydrogen bond acceptors and a log P lower than 5 (111, 118). Furthermore, there is a fifth rule that states that when the target is a substrate of a molecular transporter, the other four rules are not applicable. Moreover, these compounds respect the requirements of solubility and toxicity and are not frequent hitters, or false positives.

2.1.2. Target preparation

The crystal structure of aromatase used (3S79) was obtained from Protein Data Bank (PDB) (https://www.rcsb.org/). This structure was determined by D. Ghosh *et al* (16) using X-ray crystallography at 2.75 Å resolution (16) and consists of aromatase complexed with androstenedione, its natural substrate. In order to prepare the enzyme for docking, all water molecules were removed. This was made because no one of them was involved in the binding of the ligand and, besides that, the deletion of waters makes calculations easier and avoids their interference in the searching of poses. Furthermore, the ligand was also removed, and the protonation state of the residues evaluated by Propka 2.0.0 (http://nbcr-222.ucsd.edu/pdb2pqr_2.0.0/) (119). Considering the Propka results and earlier studies (18, 22), the residue Asp309 was modelled as neutral.

2.1.3. Docking validation[1]

Before running the VS, it is necessary to choose the best algorithm and software to do that. Thus, different software are evaluated, namely rDock, AutoDock Vina and

[1] This step was made by Dr. Ana Oliveira from the Theoretical Chemistry and Computational Biochemistry group of FCUP. I have only participated in the preparation of some data files as actives and decoys files.

AutoDock. One of the best ways to verify the performance of a docking software is to evaluate its ability to discriminate between known active ligands and similar inactive molecules (decoys). This means that a good docking software should attribute a better score to the actives than the structurally similar inactives. Here, the already known AIs, collected from ChEMBL (https://www.ebi.ac.uk/chembl/), and the respective decoys, generated with the free available DUD-E program (http://dude.docking.org/) (120), were used. To understand the effectiveness of the software, enrichment factors were determined. The software with the best enrichment factor was chosen to run the VS of 3.4 million compounds.

2.1.4. Molecular Docking

The docking program used in the VS was rDock (http://rdock.sourceforge.net/). rDock is an open available docking program, fast and versatile, that can be used to dock molecules against proteins and nucleic acids (121). The scoring function used by this software is a sum of intermolecular (S_{inter}), ligand intramolecular (S_{intra}), site intramolecular (S_{site}) and external restraint terms ($S_{restraint}$) **(Equation 1)**. S_{inter} is the most important term as it represents the protein-ligand interaction score. S_{intra} is related with the relative energy of the ligand conformation, while S_{site} represents the relative energy of the flexible regions of the binding site. Finally, $S_{restraint}$ is a collection of non-physical restraint functions that can be used to bias the docking in several useful ways.

During the VS, 5 conformations for each ligand were generated. Each one has a specific score value.

$$S_{total} = S_{inter} + S_{intra} + S_{site} + S_{restraint} \qquad \textbf{(1)}$$

2.1.5. Post-docking analysis[2]

After running the VS, it is necessary to choose the best compounds to be experimentally analyzed. In this study, when the VS was finished, the best pose of each compound was selected and then all those compounds were reordered by binding free energy value. After that, the 1000 compounds with the best score were selected and Extended Connectivity Fingerprints (ECFP) were generated for each one. ECFPs are topological fingerprints that represent the molecular structures by means of circular atom neighborhoods. They can be rapidly calculated and applied in molecular

[2] This step was made with Dr. Ana Oliveira from the Theoretical Chemistry and Computational Biochemistry group of FCUP.

characterization, similarity searching, structure-activity modeling and VS studies (122). Then, clusters based on chemical diversity were constructed with ECFP. This was made using JKlustor, available in ChemAxon software. Finally, the 3 compounds with the best binding free energy values of each cluster were selected to visual analysis and some compounds were chosen to be experimental tested.

2.2. Modelling of the ERs

For the study of ERα and ERβ, the structure of both receptors was modelled. First of all, using the database UniProt (https://www.uniprot.org/), it was possible to select the best structure of each receptor taking into account the resolution value of the structure, the existence of mutations and the receptor conformation. To know if the sequence of the selected structure was complete, each chosen structure was aligned with the respective *fasta* sequence in the VMD software through the MultiSeq analysis tool. Once the alignment was done, it was possible to verify which segments of the chosen structures were absent. Then, in order to complete the structure, the database BLAST (https://blast.ncbi.nlm.nih.gov/Blast.cgi) was used to find homologous receptors containing the missing parts of ERα and ERβ structures well resolved. This process was repeated for each segment to complete as much as possible the sequence. After searching for all the homologous structures, all of them were aligned with *fasta* and the best structure selected. The next step was the 3D modelling of the missing regions of the receptors. This was carried out with Modeller 9.20, a software that models three-dimensional structures of proteins. This software uses the alignment of the sequence to be modeled with known related structures and automatically construct several models for each receptor. The best models were chosen taking into account their score value and then were refined, also with Modeller 9.20, to obtain an even better model. Finally, the receptors were submitted to the software Propka 2.0.0 to evaluate their protonation states.

2.3. Alignment of the binding sites

In order to find a multi-target compound for hormone-dependent breast cancer, a close analysis of the binding sites of the three targets was made. The binding site residues of each target were selected taking into account the position of the ligand. For that, in PyMol, the ligand in the structures of aromatase (3S79), ERα (5FQP) and ERβ (5TOA) was selected and the binding site was defined considering all the residues in a

radius of 12 Å. Then, each binding site was saved as an independent molecule and in VMD the sequences of the three targets were aligned.

2.4. Compounds collection

The already known AIs, ERα antagonists and ERβ agonists were retrieved from ChEMBL in order to compare the different sets and find the differences and similarities among them. The final list contained 6985 compounds (2619 AIs, 3701 ERα antagonists and 665 ERβ agonists). In order to perform the analysis, these compounds were filtered by affinity with a cutoff of nanomolar (nM), which means that only the compounds with a nM IC_{50} or EC_{50} value were considered, being the IC_{50} the concentration of the compound able to induce an inhibition of 50% and the EC_{50} the concentration responsible for 50% of the maximum effect. Therefore, AIs and ERα antagonists were filtered by their IC_{50} value, while ERβ agonists were filtered by EC_{50}. The resulting list contained 1210 AIs, 1557 ERα antagonists and 73 ERβ agonists, counting for a total of 2840 compounds.

2.5. Molecular descriptors generation

Molecular descriptors are a set of values used to descript the molecular structure of the compounds in one, two or three dimensions (1D, 2D and 3D) and can be understand as an encoded representation of the chemical structures. They refer to all structural keys, hashed fingerprints, binary fingerprints, different pharmacophore fingerprints and scalar values and are very useful to quickly compare several compounds taking into account the values of the analyzed properties. In this study, the ChemAxon software was used to generate the molecular descriptors of the known ligands of aromatase, ERα and ERβ in order to compare the different sets.

To analyze the compounds, 1D and 2D molecular descriptors were generated. The 1D descriptors generated were molecular weight, molecular volume, number of rings, number of hydrogen bond acceptors, number of hydrogen bond donors, water-accessible surface area (ASA), Van Der Waals (VdW) interactions, logP and more. In relation to 2D descriptors, ECFPs were constructed.

2.6. Clusters construction

In order to group the several compounds according to their chemical similarity, clusters have been constructed. They were constructed according to similarity ranges

defined through the Tanimoto index and based on ECFP. Tanimoto index is a measure able to determine how similar (or different) two compounds are and is obtained dividing the number of common features by the total number of features (105). The cluster method used was Jarp, available in ChemAxon software.

2.7. Hierarchical clusters

Hierarchical clusters are very useful to evaluate the chemical evolution of a set of compounds. Here, these clusters were constructed for the members of the clusters previously identified as having compounds from the three targets. For that, Library MCS software, also available in ChemAxon, was used. This software searches for the maximum common substructures of a set of compounds in a hierarchical manner giving rise to a dendogram with several levels, being the first the smallest common substructure among all the compounds.

2.8. Pharmacophore construction

A pharmacophore is typically defined as a geometrical representation of the important chemical groups of a ligand that are needed to interact with the receptor. This model can be constructed in a ligand-based manner, by superposing a set of compounds that are known to exert the desired activity and extracting their common features, or in a structure-based manner, through the determination of the important points in the target to interact with ligands. Considering this, pharmacophores display important roles in VS and *de novo* drug design as they can increase the possibilities of finding a desired compound (123).

For the construction of the pharmacophore, the clusters presenting compounds from the three targets were used what account for a total of 78 compounds (26 AIs, 50 ERα antagonists, 1 ERβ agonist and 1 compound that is, at the same time, ERα antagonist and ERβ agonist). First, the best pose of each compound in aromatase was selected and all those poses were saved in the same mol2 file. Then this list was submitted to the free available online program PharmaGist (http://bioinfo3d.cs.tau.ac.il/PharmaGist/) that allows the construction of several pharmacophores at the same time in a simple and fast manner (124-126). This method is ligand-based and does not require any information about the target. After the pharmacophore generation, the best model was chosen considering its score value, the

representative molecule of the pharmacophore (pivot molecule) and the activity of the pivot molecule.

2.9. Biochemical and Biological studies

2.9.1. Materials

The MCF-7aro cells used in this study were kindly provided by Dr. Shiaun Chen (Beckman Research Institute, City of Hope, Duarte, CA, USA). The HFF-1 cells were obtained from ATCC (Manassas, VA, USA). To perform cell culture, it was used Eagle's minimum essential medium (MEM), Dulbecco's Modified Eagle's Medium (DMEM), fetal bovine serum (FBS), L-glutamine, antibiotic-antimycotic (10000 unit/mL of penicillin G sodium, 10000 mg/ml of streptomycin sulfate and 25 mg/ml of amphotericin B), Geneticin (G418), sodium pyruvate and trypsin, which were acquired from Gibco Invitrogen Co. (Paisley, Scotland, UK).

Other compounds like T, E_2, trypan blue, nicotinamide adenine dinucleotide phosphate (NADPH), ethylenediaminetetraacetic acid (EDTA), dimethyl sulfoxide (DMSO), Tween® 20, 3-(4,5-dimethylthiazol-2-yl)-2,5-diphenyltetrazolium (MTT), activated charcoal, protease inhibitor cocktail, 2',7'-dichlorodihydrofluorescein diacetate ($DCFH_2$-DA), Staurosporine (STS), ICI 182 780 (ICI), 4-[2-phenyl-5,7, bis (trifluoromethyl) pyrazol [1,5-a] pyrimidin-3-yl] phenol (PHTPP), DNase-free RNase A, Triton X-100 and propidium iodide (PI) were supplied by Sigma-Aldrich Co. (Saint Louis, USA). Caspase-Glo® 3/7, as well as, Caspase-Glo® 9 luminometric assays were obtained from Promega Corporation (Madison, USA). LDH Cytotoxicity Assay Kit was supplied by Thermo Scientific (Rockford, USA) and isopropanol by VWR Chemicals (Rador, Pennsylvania, USA). [1β-^{3}H]-androstenedione was obtained from Perkin-Elmer (Boston, MA, USA). The scintillation cocktail was purchased from ICN Radiochemicals (Irvine, CA, USA). Bradford reagent was provided by BioRad (Laboratories Melvile, NY, USA) and WesterBright^{TM} ECL chemiluminescent substrate by Advansta Inc. (Menlo Park, CA, USA). Triple Xtractor, Xpert cDNA Synthesis Mastermix and Xpert Fast SYBR were acquired from GRiSP Research Solutions (Porto, Portugal).

For reference or under study compounds, Exe was purchased from Sequoia Research Products Ltd. (Pangbourne, UK), Ana and Let were acquired to Sigma-Aldrich Co. (Saint Louis, USA), MT1 was obtained from Carbosynth (Compton, Berkshire, UK) and NS8 and NS16 were supplied by Enamine (Riga, Latvia).

In relation to the antibodies used, mouse monoclonal anti-ERα, mouse polyclonal anti-ERβ, goat polyclonal anti-CYP19 (aromatase), rabbit polyclonal p-ERαSer^{167} and

mouse polyclonal β-tubulin antibodies were provided by Santa Cruz Biotechnology (Dallas, TX, USA). Mouse polyclonal p-ERαSer^{118} was purchased by Cell Signalling (Danvers, MA, USA).

Stock solutions of T and E_2 were prepared in absolute ethanol, while stock solutions of Exe, ICI, PHTPP, MT1, NS8 and NS16 were prepared in 100% DMSO. All these compounds were stored at -20 ºC. Before beginning each experiment, dilutions of the compounds were prepared using fresh medium, being the final concentrations of DMSO and ethanol in culture medium lower than 0.05% and 0.01%, respectively.

2.9.2. Anti-aromatase activity

In order to screen the ability of the compounds to inhibit aromatase, we used a radiometric assay in which the anti-aromatase activity was measured in human placental microsomes, according to Thompson and Siiteri (127) and Heidrich et al. (128) modified (75) methods. After the aromatization reaction, the tritiated water released from [1β-^{3}H]-androstenedione was measured, being the amount of tritiated water proportional to the index of estrogen formation, and thus, to the activity of aromatase. For this assay, we used human placental microsomes, since they are a biological matrix rich in aromatase enzyme (129).

All the compounds tested were dissolved in DMSO and the subsequent dilutions were performed in 67 mM of potassium phosphate buffer (pH 7.4). The reaction was performed using 20 µg of microsomal protein, 15 µM of NADPH, 40 nM of [1β-^{3}H]-androstenedione and 2 µM of each compound under study, in a final reaction volume of 500 µL. First, the buffer was added, followed by the microsomes, the compounds, the [1β-^{3}H]-androstenedione and, lastly, the NADPH, which is responsible for initiating the aromatization reaction. The reaction occurred in a water bath at 37 ºC, during 15 min. After this time, the reaction was stopped by adding 500 µL of 20% trichloroacetic acid (TCA). In order to quantify only the tritiated water, the mixture was transferred to tubes containing a charcoal-activated pellet, vortexed and incubated for 1 hour. After incubation, the tubes were centrifuged at 14000 x*g* during 10 min, and the supernatants were then transferred to new charcoal-activated pellets, vortexed and incubated for 10 min. After centrifugation, 600 µL of the supernatant containing the tritiated water was transferred to scintillation tubes containing 3 mL of liquid scintillation cocktail. The scintillations were counted in a liquid scintillation counter (LS-6500, Beckman Coulter, Inc, Fullerton, CA).

All the experiments were performed in triplicate, in at least three independent experiments. The AIs Exe, Ana and Let at 1 µM were used as reference compounds.

2.9.3. Cell culture

To study the *in vitro* effects of the new compounds, we used MCF-7aro and HFF-1 cell lines, which grew at 37 ºC and 5% of CO_2.

MCF-7aro cells are an ER^+ aromatase-overexpressing human breast cancer cell line, which was prepared by stable transfection of MCF-7 cells with human placental aromatase gene and Geneticin selection (74, 130). Since these cells express high levels of aromatase, they are considered a good *in vitro* cell model to study ER^+ breast cancer and AIs (131). These cells were generally cultured in a MEM with phenol-red, 10% heat-inactivated FBS, 1 mmol/L of sodium pyruvate, 1% of penicillin-streptomycin-amphotericin B and 100 µg/mL of G418. To avoid the interference of the hormones present in FBS, as well as, the estrogen-like properties of phenol-red (132), three days before the beginning of the experiments, cells were cultured in an estrogen-free MEM without phenol red, containing 5% of pre-treated charcoal heat-inactivated fetal bovine serum (CFBS), 1 mmol/L of sodium pyruvate, 1% of penicillin-streptomycin-amphotericin B and 2 mmol/L of L-glutamine. All the experiments with MCF-7aro cells were performed in these conditions, but also in the presence of 1 nM of T, which was used as aromatase substrate and proliferation inducing agent (133), or with 1 nM of E_2, the aromatase product of the aromatization reaction (133).

The human foreskin fibroblast cell line (HFF-1) is a non-cancerous cell line that was used to evaluate the cytotoxicity of each compound. These cells were cultured in a glucose enriched DMEM medium, without phenol-red and supplemented with 1 mmol/L of sodium pyruvate, 1% of penicillin-streptomycin-amphotericin B, 2 mmol/L of L-glutamine and 10% of FBS.

2.9.4. Subcultures

Cell growth was monitored weekly and when cells reached a confluence of 70-80%, they were trypsinized. For this, the medium from the culture flasks was removed and, cells were washed with PBS (pH 7.4) and 0.25% Trypsin/1 mM EDTA solution was added, during 3 min at 37 ºC, to effectively detach the cells from the surface of the flask. After washing with PBS, the cells were collected to centrifugation tubes containing medium, in order to inactivate Trypsin/EDTA action, and were further submitted to centrifugation (300 x*g* during 5 min at 4 ºC). The supernatant was discarded, and cells were resuspended and homogenized in medium to be further plated in cell culture flasks.

To carry out the experiments and to know the cellular density of the cell suspension, after trypsinization the trypan blue (1:1) was added and the viable cells were

counted in a Neubauer's chamber. Trypan blue is a dye that crosses the membrane of the cells after membrane rupture, allowing the blue staining of non-viable cells. After this, cells were cultured in the appropriate cell culture plates, with the desired cell density, according to the type of the assay. After 12-16 hours of cell adhesion, the compounds were added at the desired concentrations (0.1-50 µM). Cells were maintained at 37 ºC and 5% CO_2, during 3 and 6 days of incubation, and the culture medium and compounds were refreshed every 3 days.

2.9.5. Cell viability

In order to evaluate the effects of the compounds on MCF-7aro and HFF-1 cell viability, the 3-(4,5-dimethylthiazol-2-yl)-2,5-difenyltetrazolium (MTT) assay was performed and the release of the enzyme lactate dehydrogenase (LDH) was also measured. The MTT assay allows the evaluation of the effects of the compounds on cell viability, based on the ability of the viable cells to metabolically reduce the MTT. This salt is a yellow water-soluble compound easily incorporated by viable cells. In viable cells, the reductases of mitochondria can reduce the MTT by the action of the NADH dehydrogenase enzyme. When MTT is reduced, it is converted in formazan crystals, a purple compound that is not soluble in water but soluble in an organic solution. The reduction of MTT to formazan is proportional to the mitochondrial activity and to the number of viable cells (134). On the other hand, the lactate dehydrogenase is a cytosolic enzyme involved in cell metabolism. Only cells with damage on cell membrane will release LDH, which will react with the enzyme substrate of the LDH Cytotoxicity Assay Kit (Thermo Scientific) (135).

To perform these assays, MCF-7aro and HFF-1 cells were cultured in 96-well plates at a cellular density of 2.0 x 10^4 cell/mL (for 3 days) and 1.0 x 10^4 cell/mL (for 6 days) for MCF-7aro cells, and 1.5 x 10^4 cell/mL (for 3 days) and 7.5 x 10^3 cell/mL (for 6 days) for HFF-1 cells. The cells were incubated with different concentrations (0.1-50 µM) of the compounds, and in case of MCF-aro cells, also in combination with T (1 nM), E_2 (1 nM), ICI (100 nM) or PHTPP (1 µM), during 3 or 6 days. MCF-7aro cells, stimulated only with T or E_2 with or without ICI or PHTPP, were considered as control. It should be pointed that MCF-7aro cells do not grow in the absence of T or E_2 (136) and that the selected concentrations of ICI and PHTPP were the ones previously used in this cell model (136, 137). For HFF-1 cells, the cells that were cultured without treatment were designated as control.

After each incubation time, 10% of the total volume corresponding to each well of the 3 days assays was withdrawn to a new 96-well plate, where an equal volume of LDH substrate reagent (LDH Cytotoxicity Assay Kit) was added. The plate was covered with aluminum, to protect from the light, during 30 min. After this period, to stop the reaction, the "stop solution" of the LDH Cytotoxicity Assay Kit was added and the air bubbles were removed. The absorbance was further determined at 450 nm in a Biotek Synergy HTX Multi-Mode Microplate Reader (Biotek Instruments, Vermont, USA).

MTT assay was performed with the remaining 90% volume of each well and, in order to have 1:10 dilution, 10% of total volume of an MTT solution (5 mg/ml), previously prepared, was added. The plate was incubated during 2 hours and 30 minutes at 37ºC in 5% of CO_2. After this time, the content of each well was collected and 200 µL of DMSO:isopropanol mixture (3:1) were added to solubilize the formazan crystals. The solubilization was performed on a stirred during 15 minutes and the absorbance was read at 540 nm in a Biotek Synergy HTX Multi-Mode Microplate Reader (Biotek Instruments, Vermont, USA).

All these experiments were performed in triplicate in, at least, three independent experiments. The results are expressed as relative percentage of the untreated control cells (100% of cell viability) for MTT assay and as relative unit (1) for LDH assay.

2.9.6. Cell cycle analysis

Cell cycle is the process responsible for DNA replication and division of the cells and consists in two distinct phases, interphase (G1, S, G2), and mitosis. During interphase, DNA duplication occurs and, after that, cells enter in mitosis (138).

In this study, we performed cell cycle analysis, by flow cytometry, in order to investigate the anti-proliferative effects of MT1 on MCF-7aro cells. For that, MCF-7aro cells (7×10^5 cells/mL) were cultured in 6-well plates and incubated with MT1 (5 and 10 µM), for 3 days, in a medium containing T (1 nM). Cells only treated with T were designated as control. After the incubation period, the medium was removed and the cells were washed with PBS and trypsinised. Subsequently, cells were transferred to centrifugation tubes and centrifuged at 300 *xg*, for 5 minutes at 4 ºC. The supernatant was removed and the cells washed with PBS, resuspended and centrifuged. After that, the supernatant was once again removed, and cells resuspended in 500 µL of PBS and 4.5 mL of 70% cold ethanol, which was added to fix the cells. After at least 48 hours of cell fixation at 4 ºC, the samples were centrifuged and cells washed two times with PBS, being then resuspended in 500 µL of a PBS/PI staining solution, containing 5 µg/mL of PI, 0.1% of Triton X-100 and 200 µg/mL of RNAse A. The Triton X-100 permeabilizes

the cell membrane allowing PI to cross the cell membrane to bind and to intercalate with DNA. The RNAse A is important to ensure that only DNA is analyzed during this process.

To analyze the DNA content of the cells it was used the BD Accuri™ C6 cytometer with a BD Accuri™ C6 analysis software® (San Jose, CA, USA). The detectors of the three fluorescence channels (FL-1, FL-2 and FL-3) were set on a linear scale, as well as, the forward and side light scatter (FSC and SSC, respectively). Using a two-parameter plot of FL-2-Area to FL-2-Width of PI fluorescence, cell debris, doublets and aggregates were removed. The results were analyzed using a BD Accuri™ C6 software® and the anti-proliferative effects of MT1 were presented as percentage of cells in the G_0/G_1, S and G_2/M phases, in relation to the control cells. Data correspond to three independent experiments performed, at least, in triplicate.

2.9.7. Analysis of apoptosis

Caspases are a family of protease enzymes with a cysteine residue and capable of cleaving a target protein only after an aspartic acid residue. They have essential roles in the apoptotic programmed cell death, occurring widely during development, and throughout life to maintain cell homeostasis (139). To evaluate the activity of caspases, luminescent assays with Caspase-Glo® 3/7 and Caspase-Glo® 9 kits, were performed according to the manufacturer's instruction. However, as MCF-7aro cells are deficient in caspase-3 (133), only the activity of caspase-7 was evaluated. MCF-7aro cells were plated on a 96-well white plate with a cell density of 2 x 10^4 cells/mL and incubated with MT1 (5 and 10 µM) in the presence of T (1 nM), for 2 days. Cells only treated with T (1 nM) were designated as control, while cells treated with STS at 10 µM were used as positive control. STS was added to cells 3 hours before adding caspase-7 and caspase-9 solutions. Luminescence was measured in a Biotek Synergy HTX Multi-Mode Microplate Reader (Biotek Instruments, Vermont, USA). The results are expressed relative to untreated control cells and data were presented as relative luminescence units (RLU). All the assays were performed in triplicate, in at least, three independent experiments.

2.9.8. Intracellular reactive oxygen species measurement

Intracellular reactive oxygen species (ROS) are chemical species containing oxygen that have important roles in cell signaling and homeostasis, but under stress conditions, their levels can increase dramatically, which may result in considerable damage of cell structures (140, 141).

The $DCFH_2$-DA method was used to detect the intracellular levels of ROS. $DCFH_2$-DA is a lipophilic non-fluorescent compound that crosses the cell membrane and once inside the cell it is metabolized by intracellular esterases to form 2',7'-dichlorodihydrofluorescein ($DCFH_2$). Then, $DCFH_2$ reacts with intracellular ROS to form the fluorescent compound 2',7'-dichlorofluorescein (DCF) (142).

MCF-7aro cells were plated at a cell density of 2 x 10^4 cell/mL in a 96-well black plate and, then, incubated with MT1 (5 and 10 µM) in the presence of T (1 nM) for 30 minutes, 1 hour, 2 hours, 6 hours, 1 day, 2 days and 3 days. A group control of cells treated just with T (1 nM) were also performed. As a positive control, cells were incubated with Exe (10 µM), which is known to induce the production of ROS in this cell line (133). After incubation, cells were labeled with $DCFH_2$-DA (50 µM), during 30 minutes at 37 ºC. Fluorescence was measured with an excitation wavelength of 480 nm and an emission filter of 530 nm in a Biotek Synergy HTX Multi-Mode Microplate Reader (Biotek Instruments, Vermont, USA).

The results are expressed as mean fluorescence intensity (MFI) and in relation to untreated control cells. All the assays were performed in triplicate in, at least, three independent experiments.

2.9.9. Western-Blot analysis

The Western-Blot is a widely used analytical technique that allows the study of the expression levels of specific proteins in a biological matrix. The proteins of the samples are separated according to their molecular weight on an SDS-PAGE electrophoresis, transferred to a nitrocellulose membrane and, then, incubated with specific antibodies against the proteins under study. The proteins are detected and the intensity levels of the bands correspond to the levels of the protein present. Thus, a standard should be used as a loading control, in order to normalize the amount of the protein present in the sample (143).

The effects of MT1 (5 and 10 µM) on the expression levels of aromatase, ERα and ERβ, as well as on the ERα phosphorylated on Ser^{118} and Ser^{167} were investigated by Western-Blot. The MCF-7aro cells were plated in a 6-well plate, at a cell density of 7 x 10^6 cells/mL during 8 hours, to study aromatase levels, or at 7 x 10^5 cells/mL, during 3 days, to study ERα, ERβ and p-ERα levels. Cells only treated with T (1 nM) were designated as control, while cells treated with ICI (100 nM) or PHTPP (1 µM) or Exe (10 µM) were used as positive controls. After incubation, cells were lysed with cold TNTE lysis buffer (20 mM Tris-HCl, 150 mM NaCl, 0.3% Triton X-100 and 5 mM EDTA) containing an appropriate protease inhibitor cocktail (1:100) and centrifuged at 14000 x*g*

for 10 minutes, at 4 ºC. The supernatants were stored at -80 ºC and protein concentrations of each sample were determined using Bradford assay. A total of 50 µg of protein per sample were subjected to electrophoresis using a 12% Bis-Tris gel and transferred to nitrocellulose membranes using a transfer buffer solution (48 mM Tris-Base, 39 mM glycine and 20% methanol at pH 9.2). After the transfer, the membranes were blocked during 1 hour with 5% milk in TBS-Tween (0,1%) and further incubated overnight at 4 ºC with the primary antibodies mouse monoclonal anti-ERα antibody (1:200), mouse polyclonal anti-ERβ antibody (1:200), rabbit polyclonal anti-p-Ser^{167} antibody (1:200), mouse polyclonal anti-p-Ser^{118} antibody (1:200) and goat polyclonal anti-CYP19 (aromatase) antibody (1:200). Membranes were, then, washed twice with TBS-Tween (0.1%) and incubated for 1 hour, at room temperature, with the secondary antibodies goat anti-mouse (1:2000), goat anti-rabbit (1:2000) and rabbit anti-goat (1:2000). The mouse polyclonal anti-β-tubulin antibody (1:500) was used to control loading variations. After incubation with primary and secondary antibodies, the membranes were further washed twice with TBS-Tween (0.1%) and, then, twice with TBS. A WesterBright^{TM} ECL chemiluminescent substrate (Advansta Inc.; Menlo Park, CA, USA) was used to visualize the immunoreactive bands and an appropriate software (BioRad) was used to quantify the intensity levels of each band.

For each target protein, at least, three independent experiments were performed.

2.9.10. Polymerase Chain Reaction analysis

Polymerase chain reaction (PCR) is an enzymatic, very sensitive, simple and widely used technique, that allows the quick amplification of a specific DNA segment, resulting in billions of copies. For that, this assay requires the presence of DNA sample, primers, nucleotides and DNA polymerase. DNA polymerase is the key enzyme of this assay, as it is the responsible for the linking of individual nucleotides together to form the PCR product, while the primers are short DNA fragments with a sequence complementary to the target DNA segment that we want to detect and amplify. First, the PCR reaction mixture is heated above the melting point of the two complementary DNA strands of the target DNA in order to separate them (denaturation). Then, the temperature is lowered allowing the primers to bind to the specific DNA segments, a process known as hybridization or annealing. After that, temperature is raised again in order to DNA polymerase synthetize a DNA strand. Quantitative real-time, or qRT-PCR, allows the detection and quantification of the PCR product, while it is being synthetized (real-time). This version can be combined with reverse transcription allowing the use of mRNA that is converted to cDNA which is further quantified by qRT-PCR (144).

Here, qPCR was performed to analyze the effects of MT1 on the transcription levels of *CYP19A1* gene in MCF-7aro cells. Cells were plated in a 6-well plate at a cell density of 7 x 10^6 cells/mL, during 8 hours. After that, the total RNA content of the cells was collected and extracted using the TripleXtractor reagent according to the manufacturer's protocol. RNA quality was assessed with the Experion RNA StdSens Kit (Bio-Rad Laboratories), by the Experion analytical software (Bio-Rad Laboratories), and further quantified at 230 nm, using the NanoDrop ND-1000 Spectrophotometer (NanaDrop Technologies, Inc, Wilmington, DE, USA). Furthermore, the ratio between 260 nm and 280 nm was also considered, since it is related to the purity of RNA, as well as the ratio between 260 nm and 230 nm, which is related to the purity of the nucleic acids. Further, RNA was converted into cDNA using the GRiSP Xpert cDNA Synthesis Mastermix containing reverse transcriptase, according to the manufacturer's protocol. By using a specific mastermix, containing an appropriate intercalating dye (GRiSP Xpert Fast SYBR) and the specific primers for the gene under study, it was possible to amplify the desired sequence. This process was performed in MiniOpticon Real-Time PCR Detection System (Bio-Rad Laboratories, USA), according to the manufacturer's protocol. For qPCR reactions, the enzyme activation was performed at 95 ºC for 40 seconds, the denaturation at 95 ºC for 3 seconds and the annealing for 30 seconds, followed by 40 cycles of denaturation. The sequences of the primers used, and the respective annealing temperatures are listed in **Table 1**. Through the melting curve it was evaluated the specificity of PCR product amplification. The amplification is represented as relative mRNA expression. The fold change in gene expression was calculated using the $2^{-\Delta\Delta Ct}$ method (145) and considering the housekeeping genes *β-Actin* and *α-Tubulin*, to normalize *CYP19A1* gene expression, as well as, two independent experiments.

Table 1: Primer sequences and annealing temperatures for housekeeping and target genes.

Symbol	Primers	Annealing Temperature
CYP19A1	Forward: 5′-GATGATGTAATCGATGGCTAC-3′ Reverse: 5′-TTCATCATCACCATGGCGAT-3′	58 ºC
β-Actin	Forward: 5′-TACAGCTTCACCACCACAGC-3′ Reverse: 5′- AAGGAAGGCTGGAAGAGAGC-3′	55 ºC
α-Tubulin	Forward: 5′-CTGGAGCACTCTGATTGT-3′ Reverse: 5′-ATAAGGCGGTTAAGGTTAGT-3′	55 ºC

2.10. Statistical analysis

The statistical analysis of all data was carried out with GraphPad Prism 7® software and by the analysis of variance (ANOVA), followed by Bonferroni and Tukey post-hoc tests for multiple comparisons (Two-way ANOVA and One-way ANOVA, respectively). Values of $p < 0.05$ were considered statistically significant. All the data were expressed as the mean ± standard error of the mean (SEM), with exception of preliminary results.

3. Results

3.1. Multi-target approach for ER$^+$ breast cancer treatment

Aromatase, ERα and ERβ display important roles in the development and progression of ER$^+$ breast cancer. Taking this into account, the discovery and development of compounds able to simultaneously modulate these three targets is a very promising therapeutic approach. Considering the functions of each target in breast tumor environment, it would be ideal to discover a compound capable to inhibit aromatase and ERα and, at the same time, activate ERβ.

3.1.1. ERs modulation

Considering that none of the LBD ER structures deposited in PDB are totally complete, the first step was to build a model structure of each receptor, using Modeller 9.20. For ERα, the template structures chosen to build the model were 2JFA and 5FQP **(Table 2)**, both in an inactivated conformation. In relation to ERβ, the structures used were 5TOA, 2I0G, 1QKM, 1U9E, 2GIU, 1X76 and 1ZAF **(Table 3)**. All the seven structures are in an active conformation.

Table 2: Information about the structures used to build ERα models.

Code	Resolution (Å)	Ligand	Conformation	References
2JFA	2.55	Raloxifene	Inactive	(146)
5FQP	1.88	Tetrahydroisoquinoline phenol 1	Inactive	(147)

For each receptor, the three best models, with appropriate conformation, were chosen taking into account, their score value. In relation to ERα, the best models presented a score of -5977, -5459 and -5416, while the best ERβ models had score values of -3535, -3378 and -3364. The best model of each receptor is represented in **Fig. 9**.

Table 3: Information about the structures used to build ERβ models.

Code	Resolution (Å)	Ligand	Conformation	References
5TOA	2.5	Estradiol	Active	(58)
2I0G	2.5	Benzopyran	Active	(148)
1QKM	1.8	Genistein	Active	(149)
1U9E	2.4	WAY-397	Active	(150)
2GIU	2.2	Compound 45	Active	(151)
1X76	2.2	WAY-697	Active	(150)
1ZAF	2.2	3-Bromo-6-hydroxy-2-(4-hydroxyphenyl)-inden-1-one	Active	(152)

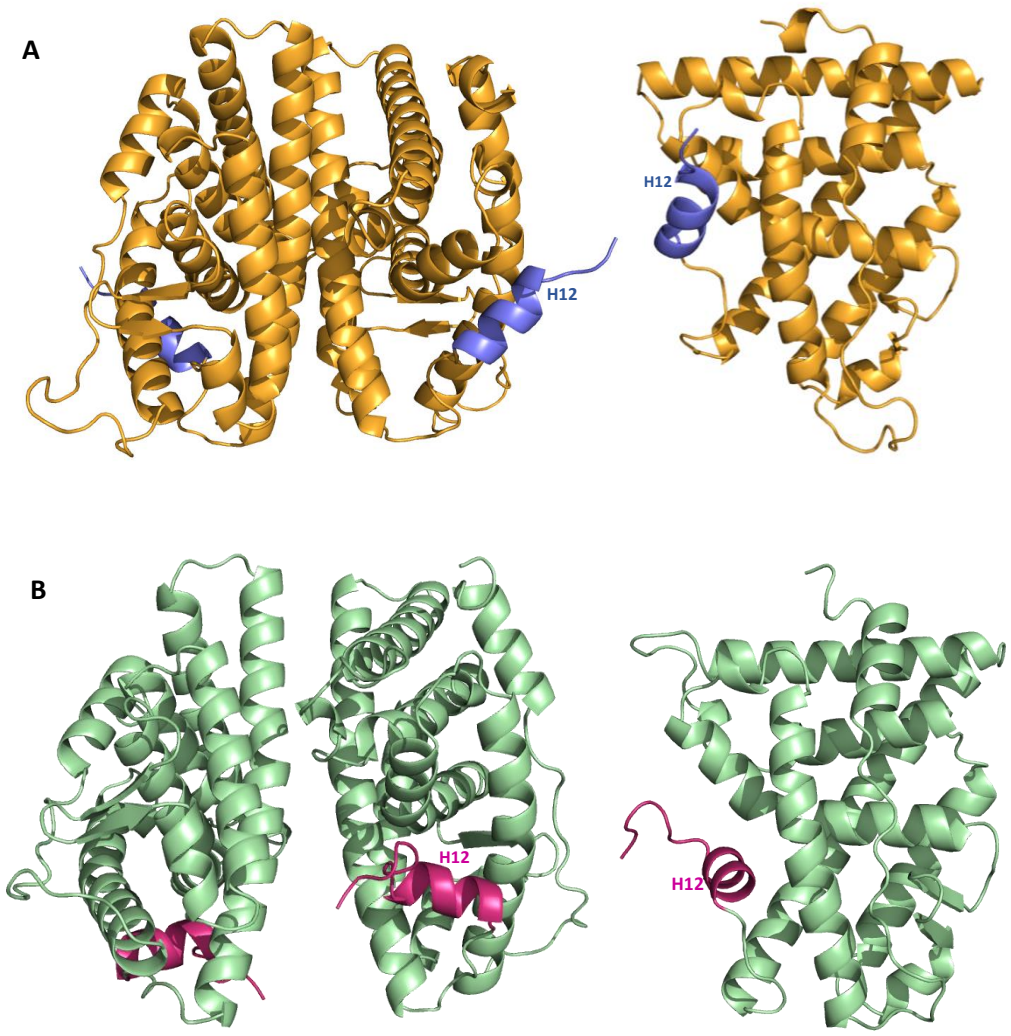

Figure 9: Structural representations of ERα **(A)** and ERβ **(B)** generated with Modeller. Both receptors are represented in dimeric and monomeric forms. In ERα, H12 exhibit a position that avoids the binding of co-activators and, because of that, that conformation is known as inactive. On the other hand, in ERβ, H12 is positioned in a way that allows the binding of co-activators. That conformation is known as active.

Each model was further submitted to Propka 2.0.0 to evaluate the protonation state of the residues. According to Propka results, the residue Glu49 of ERα had a pka of 5.47, 6.48 and 5.75 in the three different models, while the pattern pka value of Glu is 4.4. Considering the higher pka values determined, we decided to evaluate the effect of different protonation states of this residue in the three models. The same occurred with Glu46 and Glu78 in ERβ, as the values determined for Glu46 were 6.64, 6.08 and 6.18 and for Glu78 were 6.64, 6.44 and 6.11.

3.1.2. Binding site alignment

In order to understand how similar the binding sites of aromatase, ERα and ERβ are, we aligned in VMD the primary sequence of the protein. Through the alignment analysis, it was possible to verify that some of the residues crucial for the *druggability* are conserved among the three targets **(Fig. 10)**. One of those residues is an aspartate (Asp309), critical for substrate binding and aromatase catalysis (18).

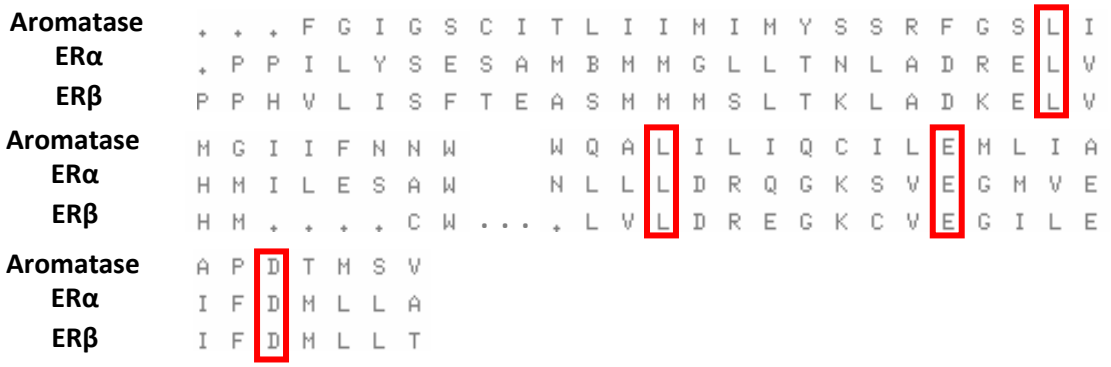

Figure 10: Alignment of the binding sites of aromatase, ERα and ERβ. The binding site of each target was defined considering all the residues in a radius of 12 Å.

3.1.3. Comparison of the known aromatase inhibitors, ERα antagonists and ERβ agonists

Considering the similarities found among the binding sites of aromatase, ERα and ERβ, we decided to evaluate how similar the AIs, ERα antagonists and ERβ agonists already described in literature are. For that purpose, we started to construct several 1D descriptors with ChemAxon software **(Fig. 11)**. According to the results **(Fig. 11A)**, it is possible to conclude that the majority of the AIs has a molecular weight between 100 g/mol and 300 g/mol and that more than 80% of the ERβ agonists have a molecular weight between 100 g/mol and 200 g/mol. Furthermore, as expected, ERα antagonists

have typically higher molecular weights, mainly between 301 g/mol and 400 g/mol. Similarly, the volume values of AIs and ERβ agonists vary, mainly, between 301 $Å^3$ and 600 $Å^3$, while the majority of ERα antagonists has higher molecular volumes, typically between 601 $Å^3$ and 800 $Å^3$ **(Fig. 11B)**. In relation to the number of rings, most of the compounds have 3 or 4 rings **(Fig. 11C)**. The analysis of the number of donors reveals that the majority of the compounds has between 2 and 5 donor groups **(Fig. 11D)**. However, in relation to the number of acceptor groups, they differ among the three sets. While most of the ERα antagonists and ERβ agonists have typically 2 acceptor groups, more than 60% of the AIs do not have any acceptor group **(Fig. 11E)**. In relation to VdW interactions, the majority of the AIs and ERβ agonists exhibit values between 100 $Å^2$ and 200 $Å^2$, while the ERα antagonists present values between 100 $Å^2$ and 400 $Å^2$ **(Fig. 11F)**. ASA values exhibit, once again, differences among the three sets of compounds. AIs and ERβ agonists have ASA values mainly between 200 $Å^2$ and 400 $Å^2$, while most of the ERα antagonists have values typically between 301 $Å^2$ and 600 $Å^2$ **(Fig. 11G)**. Finally, in relation to log P values, it is possible to see that there is a considerable distribution of them. Nevertheless, the majority of the AIs have log P values between 1.0 and 3.0, while around 70% of the ERβ agonists have log P values between 2.1 and 3.0 and the ERα antagonists have typically higher values, mainly between 2.1 and 5.0 **(Fig. 11H)**.

In addition, 2D descriptors were also generated to analyze the compounds. For that, ECFP were chosen. They were then used to generate clusters according to Tanimoto index, in order to group the compounds according to their similarity and to find clusters containing compounds from the three sets. For a Tanimoto index between 0.6 and 0.9, 2840 compounds were grouped in 175 clusters. Two of those clusters had compounds from the three targets. Cluster 1 is composed by 75 compounds (25 AIs, 49 ERα antagonists and 1 ERβ agonist) and cluster 2 by 3 compounds (1 AI, 1 ERα antagonist and 1 compound that is simultaneously an ERα antagonist and ERβ agonist) **(Fig. 12)**.

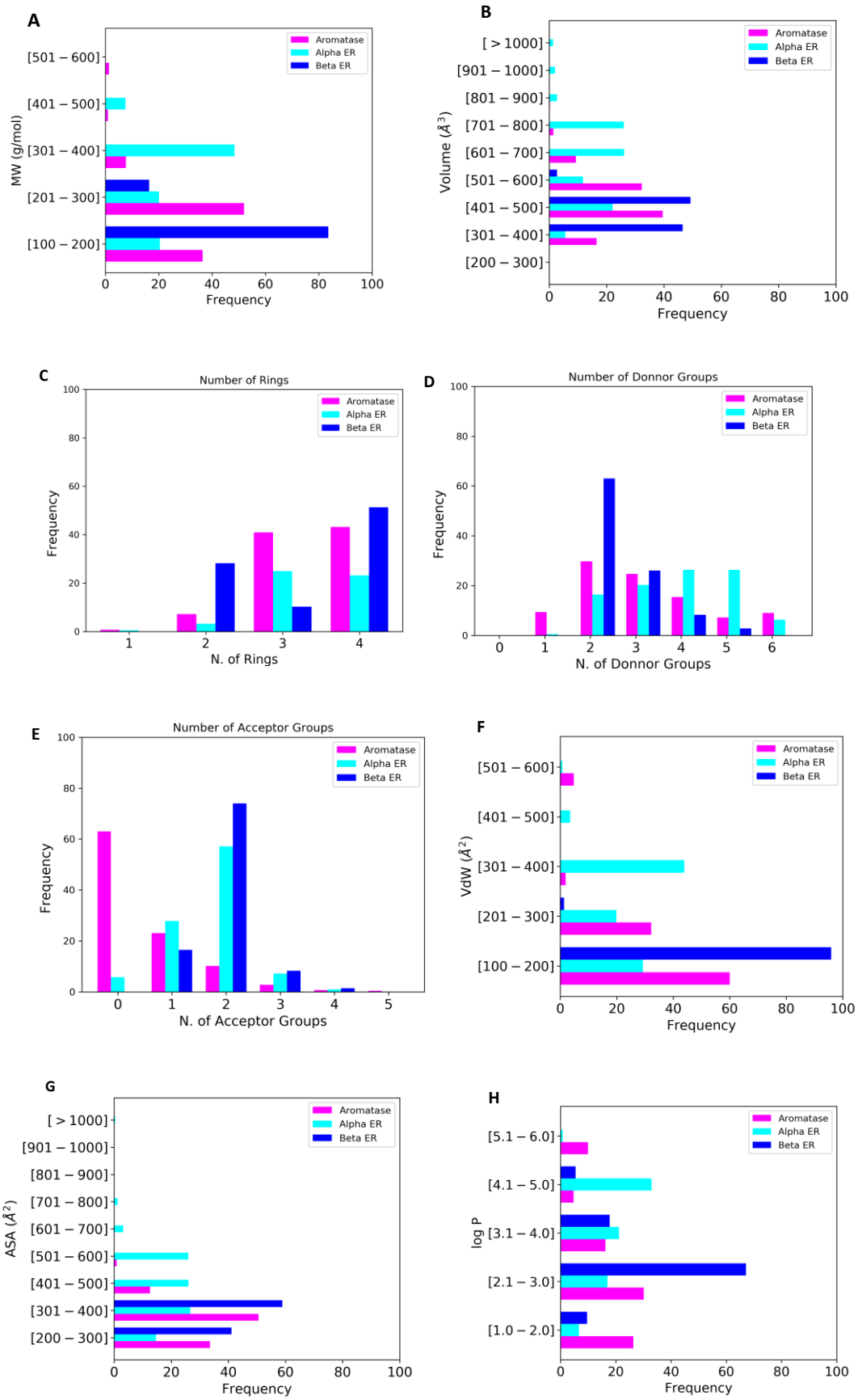

Figure 11: 1D descriptors for the sets of AIs (pink), ERα antagonists (cyan) and ERβ agonists (blue). The descriptors represented are molecular weight **(A)**, volume **(B)**, number of rings **(C)**, number of donors **(D)**, number of acceptors **(E)**, VdW interactions **(F)**, ASA **(G)** and log P **(H)**.

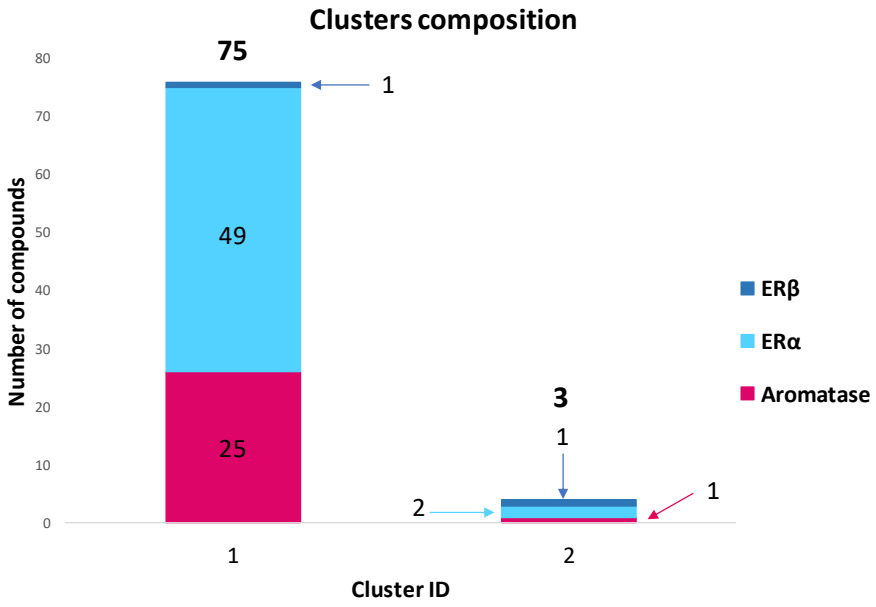

Figure 12: Composition of the two clusters containing members of the three sets of compounds.

3.1.4. Chemical evolution of the compounds of the clusters

In order to understand the chemical evolution of the compounds of the two clusters containing AIs, ERα antagonists and ERβ agonists, the hierarchical cluster method Library MCS (LibMDS), available in ChemAxon, was used. The hierarchical cluster of cluster 1 is represented in **Figure 13**. As it is possible to observe, the minimum common sub-structure is composed by 2 aromatic rings, while all the 75 members of this cluster have 3 aromatic rings differently substituted.

In relation to cluster 2 **(Fig. 14)**, its chemical evolution is much simpler than the previous one. The minimum common sub-structure and the 3 cluster members have 3 aromatic rings differently substituted.

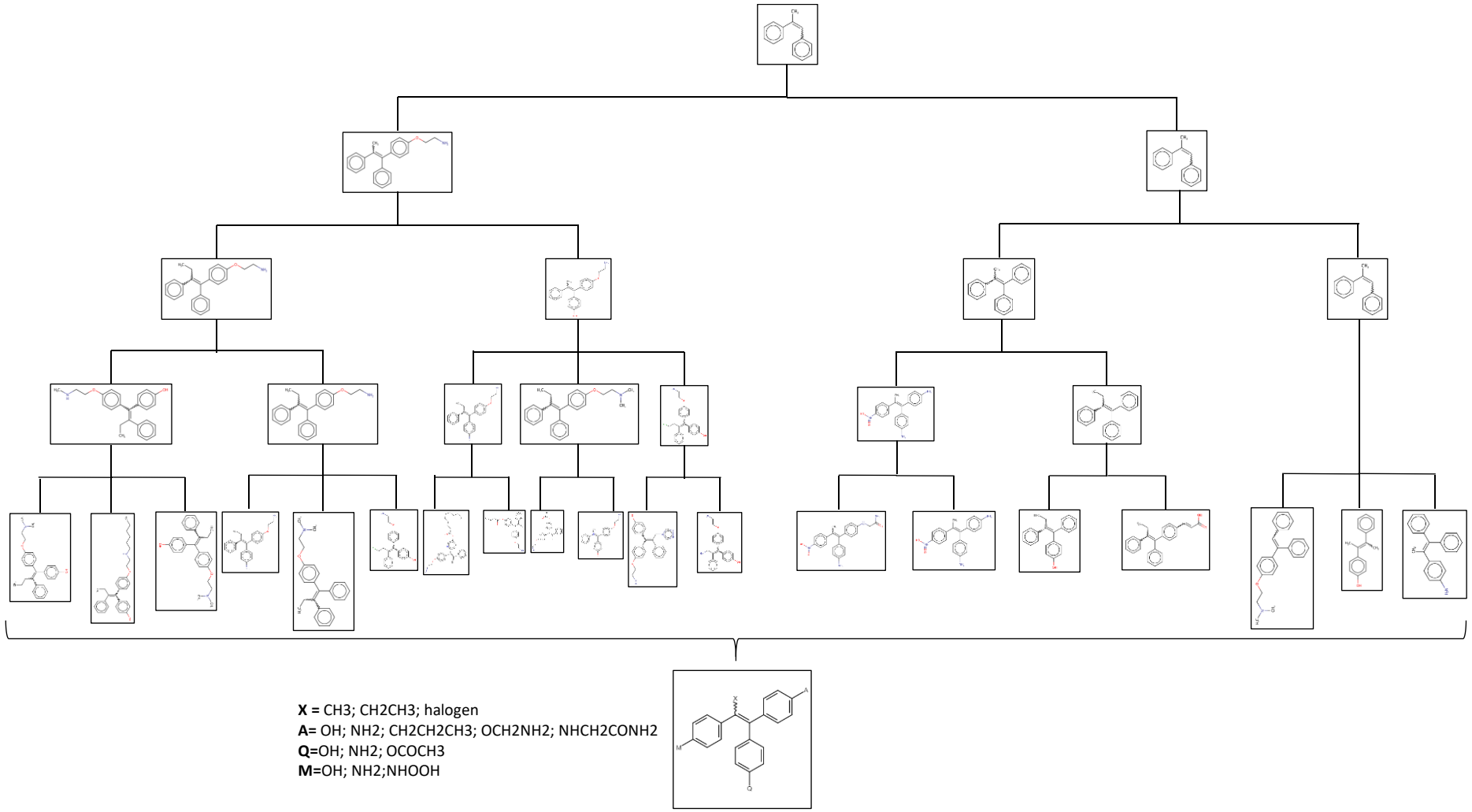

Figure 13: Hierarchical clusters of cluster 1.

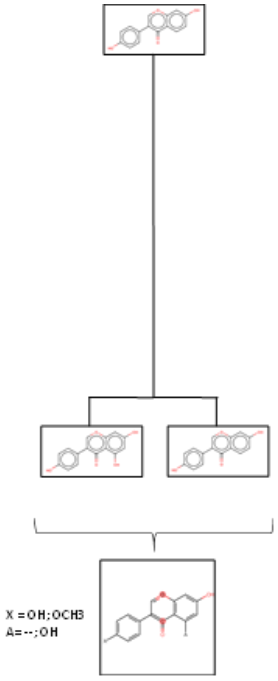

Figure 14: Hierarchical clusters of cluster 2.

3.1.5. Pharmacophore construction

Considering the similarity of the compounds of the 2 clusters, we decided to construct a pharmacophore model. This model was constructed taking into account the structural information of the 78 compounds and using the online program PharmaGist. The pharmacophore chosen has a score value of 55.537 and its pivot molecule, randomly selected by the software, is an AI with an IC_{50} of 30 nM. Furthermore, this model is a representation of the common features among all the 78 compounds and through its analysis, it is possible to conclude that the majority of the 78 compounds has 2 donor groups, 3 aromatic rings and 4 hydrophobic groups in specific positions **(Fig. 15)**.

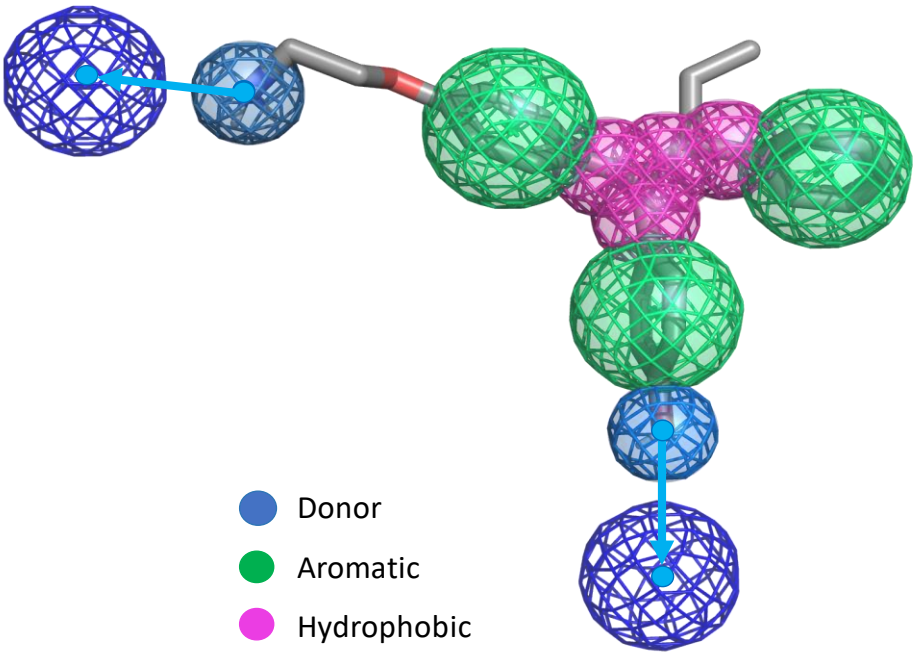

Figure 15: Representation of the pharmacophore model constructed. It is composed by 2 donor groups (blue), 3 aromatic rings (green) and 4 hydrophobic groups (pink).

3.1.6. Visual analysis of the compounds

In order to find a multi-target compound, we have also decided to verify how the ERs ligands of the 78 compounds fit in aromatase. For that we performed docking studies to evaluate if those compounds could bind to the binding site of aromatase. We verified that three of those compounds fit very well in the enzyme, establishing interactions with Arg115, Phe221, Trp224, Asp309, Thr310, Leu372, Val373 and Leu477, residues that are described as important for aromatase inhibition (17). However, after a literature search on information related to these compounds, we found that one of the compounds, diethylstilbestrol, was removed from the market in 2000, by FDA, as serious side effects have been associated with this compound (153, 154). Because of this, this compound was not selected for the biochemical and biological studies. Another compound was genistein, an isoflavone present in soya. This compound has already been studied, at biochemical and biological level, by the Biochemistry group of FFUP and results for the anti-aromatase activity in human placental microsomes showed an aromatase inhibition lower than 30%, being, thus, considered a weak inhibitor (155). Because of this, this compound was not selected for the subsequent studies. Finally, for the third compound, nominated MT1, there is no controversial information, reason why, this compound was selected for the biochemical and biological studies.

3.1.7. Anti-aromatase activity of MT1

Once a promising multi-target compound, MT1, has been identified the anti-aromatase activity of MT1, in human placental microsomes was evaluated, according to the Thompson and Siiteri (127) and Heidrich (128) methods, with modifications (75), by measuring the tritiated water released from [1β-^{3}H]-androstenedione, during the aromatization reaction. The results showed that MT1 was not able to inhibit aromatase and, on the contrary, it seems to stimulate aromatase reaction in 2.81% **(Table 4)**. As reference AIs, it was used all the three AIs used in clinic, the steroidal AI Exe and the non-steroidal AIs Ana and Let. As expected, and contrary to MT1, all these reference AIs presented very high anti-aromatase activity (≥ 97%).

Table 4: Percentage of anti-aromatase activity of MT1 in human placental microsomes.

Compound	Anti-aromatase activity (%)
MT1	-2.81 ± 3.05
Exe	97.86 ± 0.52
Ana	99.12 ± 0.02
Let	99.69 ± 0.06

Microsomes (20 µg) were incubated with NADPH (15 µM), MT1 (2 µM) and [1β-^{3}H]-androstenedione (40 nM), during 15 minutes at 37 ºC. Results are presented as a percentage of tritiated water released, in relation to control, and are represented as the mean ± SEM of three independent experiments carried out in triplicate. The reference AIs, Exe, Ana and Let, at 1 µM, were used as positive controls.

3.1.8. Effects of MT1 on non-cancerous cells

One of the most concerning and limiting questions about anti-cancer therapies are the effects of the new drugs in non-cancerous cells. A drug, to be secure and successfully used in clinic, should not affect non-cancerous cells. In order to verify if MT1 was able to induce undesired effects on non-tumour cells, an MTT assay was performed using a non-cancerous human foreskin fibroblastic cell line (HFF-1). For that, cells were treated with MT1 (0.1 - 50 µM), during 3 and 6 days, and cells without MT1 treatment were considered as control. After 3 days of MT1 treatment, no effects on cell viability were observed (data not shown). The results presented in **Figure 16** showed that MT1, after 6 days of treatment, only induced a significant ($p < 0.01$) decrease in HFF-1 cell viability at 50 µM. Considering these results, this concentration was no longer used in the further experiments.

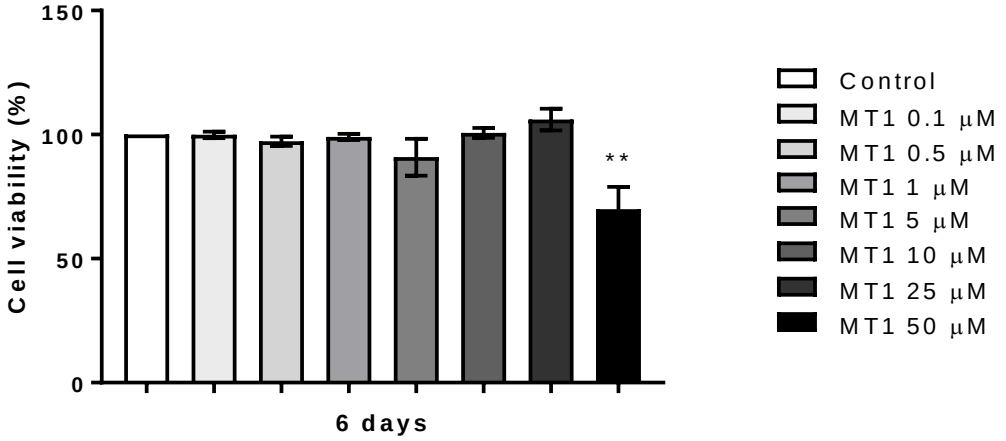

Figure 16: Effects of MT1 on HFF-1 cell viability. Cells were treated with different concentrations of MT1 (0.1 – 50 µM), during 6 days. Cells without MT1 treatment were used as control, representing 100% of cell viability. The results are presented as mean ± SEM of at least three independent experiments, performed in triplicate. Statistically significant differences between MT1-treated cells and control cells are expressed as ** ($p < 0.01$).

3.1.9. Effects of MT1 on ER$^+$ breast cancer cells: MTT and LDH assays

After studying the effects of MT1 in non-cancerous cells, we investigated its effects on the viability of MCF-7aro cells, an ER$^+$ aromatase-overexpressing human breast cancer cell line that expresses high levels of aromatase, being thus, considered a good *in vitro* cell model to study ER$^+$ breast cancer and AIs (74).

The MCF-7aro cells were treated with different concentrations of MT1 (0.1 – 25 µM) and the effects were evaluated after 3 and 6 days of treatment, through the MTT assay. For that, these cells were stimulated with 1 nM of T, which is a natural substrate of aromatase that is converted by this enzyme in E_2 and was used as a cell proliferation inducing agent, to better mimic the microenvironment of ER$^+$ breast tumors (136). The results, represented in **figure 17**, showed that MT1 was able to induce a significant ($p < 0.05$; $p < 0.01$; $p < 0.001$) decrease on MCF-7aro cell viability in a dose- and time-dependent manner, being their effects more pronounced after 6 days of treatment.

Thus, considering these results, it is possible to conclude that besides MT1 was not able to inhibit aromatase, it was capable to reduce the viability of ER$^+$ breast cancer cells.

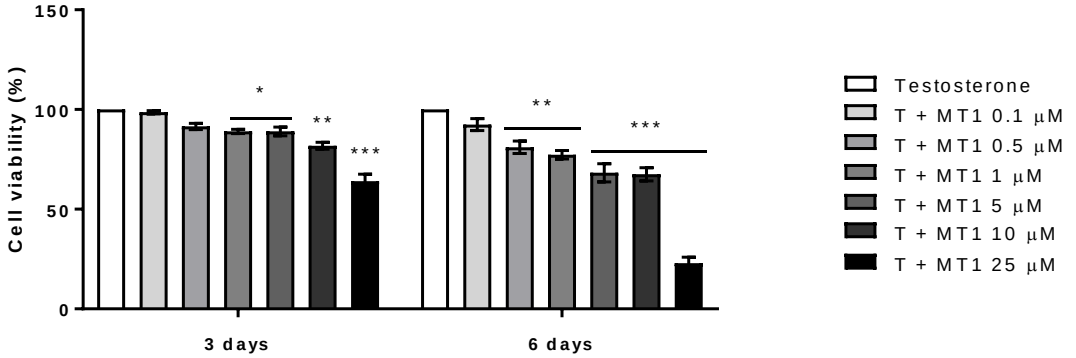

Figure 17: Effects of MT1 on MCF-7aro cell viability. Cells were treated with different concentrations of MT1 (0.1 – 25 µM), during 3 or 6 days in the presence of T (1 nM). Cells treated only with T were considered as control, representing 100% of cell viability. The results are presented as mean ± SEM of at least three independent experiments, performed in triplicate. Statistically significant differences between MT1-treated cells and control cells are expressed as * ($p < 0.05$), ** ($p < 0.01$) and *** ($p < 0.001$).

In order to evaluate the potential effects at the cell membrane integrity of MCF-7aro cells, we analyzed the release of LDH, as it is suggestive of loss of cell membrane integrity. For that, MCF-7aro cells stimulated with T (1 nM) were treated with MT1, at the same concentrations used in the MTT assay (1 - 25 µM), during 3 days. The results showed that MT1, at the concentrations studied, did not induced LDH release **(Fig. 18)**, which means that, at these conditions, the MT1 does not induce cell membrane rupture, being not cytotoxic.

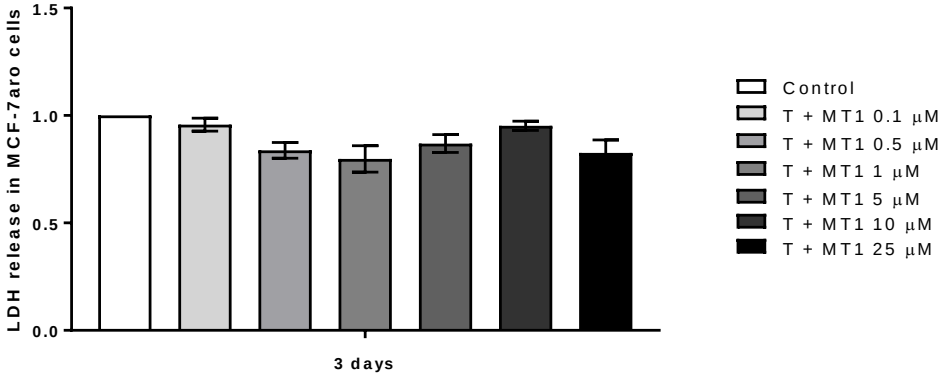

Figure 18: Effects induced by MT1 on MCF-7aro cell cytotoxicity, evaluated by LDH-release assay. Cells were treated with different concentrations of MT1 (0.1 – 25 µM), during 3 days, in the presence of T (1 nM). Cells treated only with T were considered as control, representing 100% of cell membrane integrity. The results are presented as mean ± SEM of at least three independent experiments performed in triplicate.

3.1.10. Understanding the involvement of aromatase on the effects induced by MT1 on ER+ breast cancer cells

Although the studies in human placental microsomes have shown that MT1 was not able to inhibit aromatase, we decided to analyze the possible involvement of aromatase in the reduction of MCF-7aro cell viability induced by MT1. To address this issue, MCF-7aro cells were incubated during 3 or 6 days with MT1 (1 -25 µM) in the presence of 1 nM of E_2, which is the product of the aromatization reaction of testosterone by aromatase (136). Through its interaction with ERs, E_2 is responsible for breast cancer cell proliferation (156). In this case, cells treated only with E_2 were considered as control.

Curiously, by comparing the results obtained in the presence of E_2 with those obtained in the presence of T, it is possible to conclude that MT1 affected MCF-7aro cell viability in the presence of T, but not in the presence of E_2. In fact, significant differences were observed between E_2- and T-stimulated cells **(Fig. 19)**. In T-stimulated cells there was a dose- and time-dependent reduction in cell viability, mainly at 10 µM and 25 µM, while in E_2-stimulated cells no significant effects in cell viability were induced by MT1. These results suggested that the effects of MT1 may be aromatase-dependent.

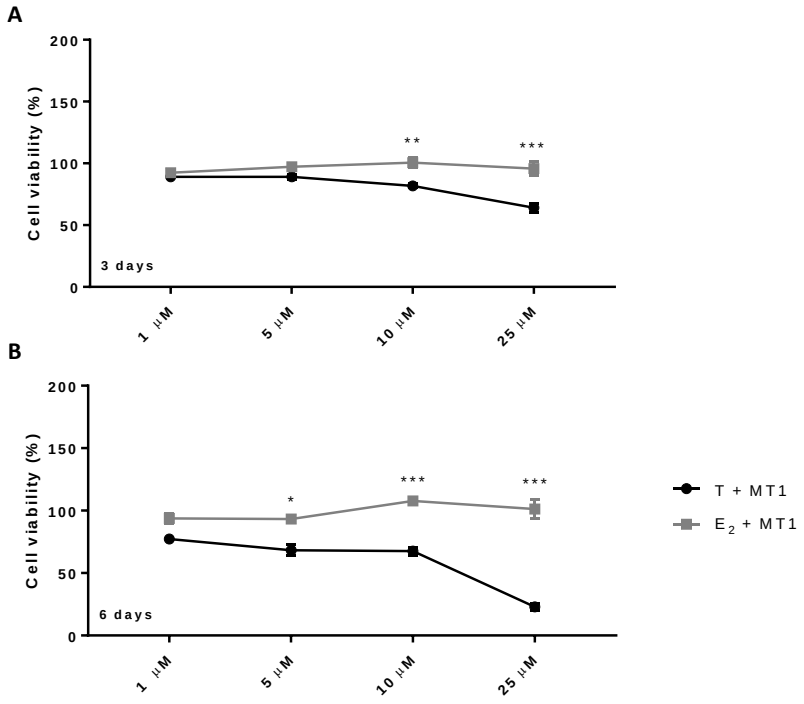

Figure 19: Comparison of the effects of MT1 on MCF-7aro cells treated with T or E2. Cells were treated with different concentrations of MT1 (1 – 25 µM), during 3 **(A)** or 6 days **(B)**, in the presence of T (1 nM) or E2 (1 nM). Cells treated only with T or E2 were considered as control, representing 100% of cell viability. The results are presented as mean ± SEM of at least three independent experiments, performed in triplicate. Statistically significant differences between T-treated cells and E_2-treated cells are expressed as * ($p < 0.05$), ** ($p < 0.01$) and *** ($p < 0.001$).

As it was observed that aromatase may be involved on the effects induced by MT1 and to better understand this relationship, we investigated the effects of this compound on aromatase protein levels, by Western-Blot, after 8 hours of MT1 (10 μM) treatment, which is a time point where it was described that the reference AI Exe induces aromatase degradation (157). Cells treated just with medium were considered as control, while cells treated with Exe (10 μM) were used as positive control. Our results demonstrated that MT1 was able to induce a decrease of 44% on aromatase expression levels ($p < 0.001$) and, as expected, the positive control Exe also induced a significant ($p < 0.001$) reduction (72%) on aromatase levels **(Fig. 20)**.

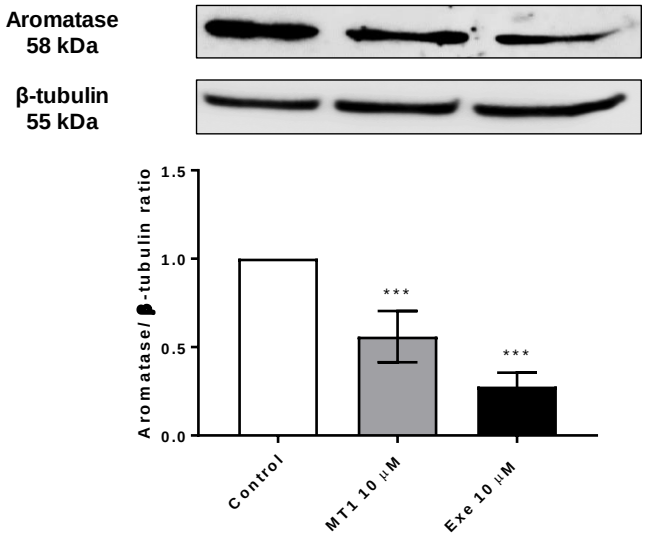

Figure 20: Aromatase protein expression levels in MCF-7aro cells treated with MT1. Cells were treated with MT1 (10 μM) for 8 hours. Cells without MT1 treatment were considered as control and cells treated with Exe (10 μM), a reference AI, were considered as positive control. A representative Western-Blot of aromatase and β-tubulin, as well as, densitometric analysis of aromatase expression levels after normalization with β-tubulin levels, are shown. β-tubulin was used as loading control. The results are the mean ± SEM of at least three independent experiments. Statistically significant differences between MT1-treated cells or Exe-treated cells and control cells are expressed as *** ($p < 0.001$).

Considering the Western-Blot results, the question that arises is: are the effects induced by MT1 on aromatase protein expression levels a result of a decreased *CYP19A1* gene transcription or a consequence of aromatase degradation? To answer this question, we performed a PCR analysis. After mRNA extraction and consequent conversion to cDNA, *CYP19A1* mRNA was amplified and quantified using an appropriate dye that intercalates with DNA. Our preliminary results demonstrated that MT1 in MCF-7aro cells did not induce any significant change in *CYP19A1* mRNA transcript levels **(Fig. 21)**. Nevertheless, contrary to what was observed for the housekeeping gene *α-tubulin* **(Fig. 21B)**, when the reference gene considered was *β-actin* **(Fig. 21A)**, there

was a non-significant increase in the mRNA levels of *CYP19A1* for cells treated with MT1 and Exe. As this is a preliminary data, this assay needs to be repeated to confirm these results. Still, altogether, these results suggest that MT1 may have an aromatase-dependent effect on cells, by affecting aromatase protein levels and not the mRNA transcription of aromatase.

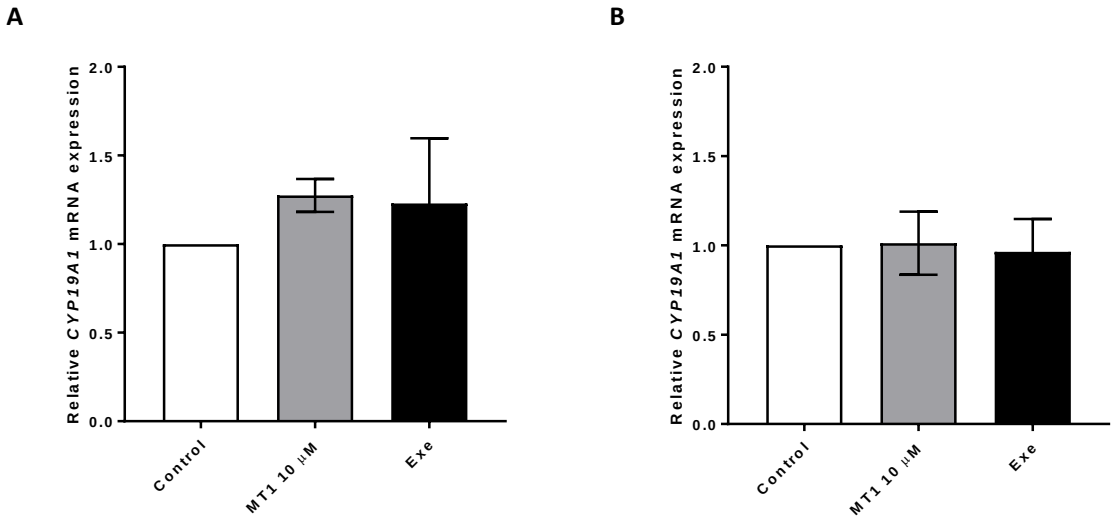

Figure 21: *CYP19A1* mRNA transcript levels in MCF-7aro cells treated with MT1. MCF-7aro cells were treated with MT1 (10 µM) for 8 hours. Cells without MT1 treatment were considered as control, whereas cells treated with Exe (10 µM), a reference AI, were considered as positive control. To quantify the mRNA transcript levels of *CYP19A1* it was used the housekeeping genes: *β-actin* **(A)** and *α-tubulin* **(B)**. The results are presented as mean ± SEM of two independent experiments.

3.1.11. Understanding the involvement of ERα on the effects induced by MT1 on ER⁺ breast cancer cells

In order to investigate the involvement of ERα in the reduction of MCF-7aro cell viability, we evaluated, by MTT assay, the effects of MT1 when ERα is blocked with ICI 182 780, also known as fulvestrant. ICI is a SERD that binds irreversibly to the receptor avoiding its dimerization and leading it to proteolytic degradation (78). Studies demonstrated that these effects are only exerted in ERα and that in ERβ, ICI exerts opposite effects (158). Thus, considering ICI action, MCF-7aro cells were stimulated with T (1 nM) and MT1 (1 – 25 µM) with or without ICI (100 nM). As presented in **Figure 22**, by comparing the results obtained with and without ERα blockade, significant differences between treatments, after 3 ($p < 0.05$; $p < 0.01$; $p < 0.001$) and 6 days ($p < 0.01$; $p < 0.001$) were observed. In the presence of ICI, the inhibitory growth observed in the presence of MT1 was totally reversed, suggesting that the ERα may be involved in the MT1-induced effect.

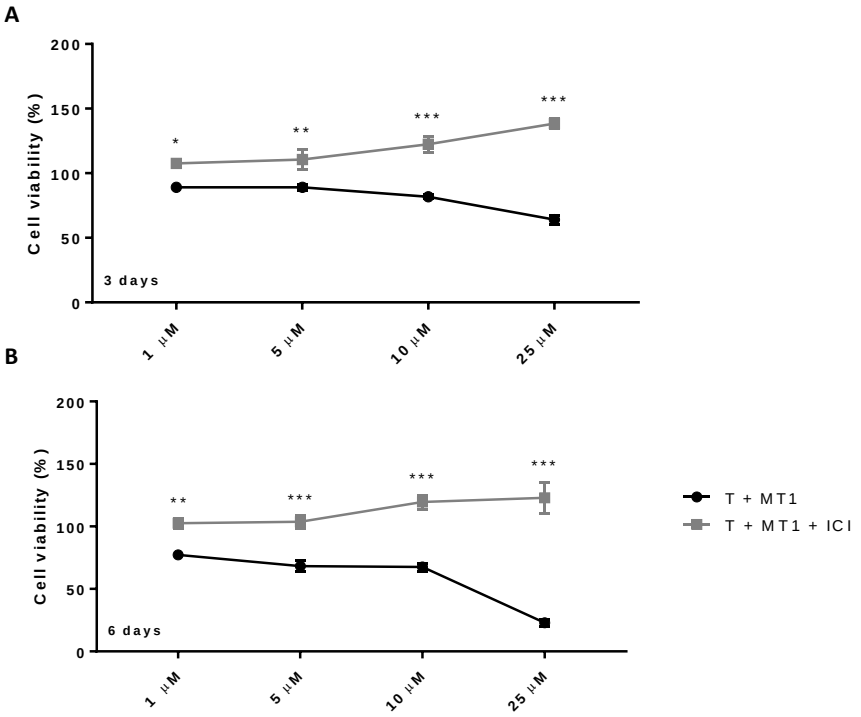

Figure 22: Comparison of the effects of MT1 on MCF-7aro cells treated with or without ICI. Cells stimulated with T (1 nM) were treated with different concentrations of MT1 (1 – 25 µM) in combination with ICI (100 nM), during 3 **(A)** or 6 days **(B)**. Cells treated only with T with or without ICI were considered as control, representing 100% of cell viability. The results are presented as mean ± SEM of at least three independent experiments performed in triplicate. Statistically significant differences between MT1-treated cells with or without ICI are expressed as * ($p < 0.05$), ** ($p < 0.01$) and *** ($p < 0.001$).

Taking these results into account, we investigated the effects of MT1 on ERα protein expression levels, through Western-Blot. Cells were treated with MT1 (10 µM) in a medium containing T (1 µM), for 3 days. Cells treated with T and ICI (100 nM) were considered as controls. As presented in **figure 23**, MT1 induced a significant ($p < 0.001$) increase of 2-fold on the expression levels of ERα. On the contrary, and as expected, ICI induced a significant ($p < 0.01$) decrease on the expression levels of ERα (reduction of 54%).

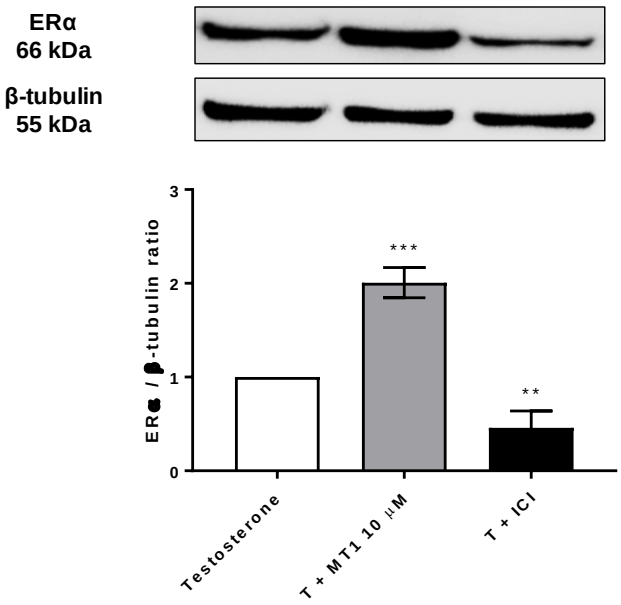

Figure 23: ERα protein expression levels in MCF-7aro cells treated with MT1. Cells stimulated with T (1 nM) were treated with MT1 (10 μM) for 3 days. Cells treated only with T were considered as control, while cells treated with T and ICI (100 nM) were considered as positive control. A representative Western-Blot of ERα and β-tubulin, as well as, densitometric analysis of ERα expression levels after normalization with β-tubulin levels, is shown. β-tubulin was used as loading control. The results are presented as mean ± SEM of at least three independent experiments. Statistically significant differences between MT1-treated cells or ICI-treated cells and control cells are expressed as ** ($p < 0.01$) and *** ($p < 0.001$).

In order to obtain more insights related to the specific action of MT1 in ERα, we investigated the phosphorylation pattern of two key residues of ERα: Ser118 and Ser167, which are both located on the AF-1 domain. Ser118 is the principal residue being phosphorylated in response to E_2 and can also be phosphorylated in response to the activation of the MAPK pathway. On the other hand, Ser167 can also be phosphorylated through the activation of MAPK pathway and by the PI3k/Akt pathway (159). The phosphorylation of these two serine residues leads to the activation of ERα and consequent transcription of target genes. Because of that, their pattern of phosphorylation could be very useful to understand if MT1 acts as an agonist or as an antagonist of ERα, on our cell model. Therefore, the phosphorylation of Ser118 and Ser167 was evaluated by Western-Blot on MCF-7aro cells treated with T (1 nM) and MT1 (10 μM), during 3 days. Cells without MT1 were considered as control. Our results demonstrated that MT1 induced a pronounced and significant ($p < 0.01$; $p < 0.001$) decrease on the phosphorylation of both ERα serine residues **(Fig. 24)**. Nevertheless, the reduction on Ser118 phosphorylation **(Fig. 24A)** was lower (35%) than the reduction on Ser167 phosphorylation (69%; **Fig. 24B**). Together, these results suggest that MT1 may act as an ERα antagonist on MCF-7aro cells.

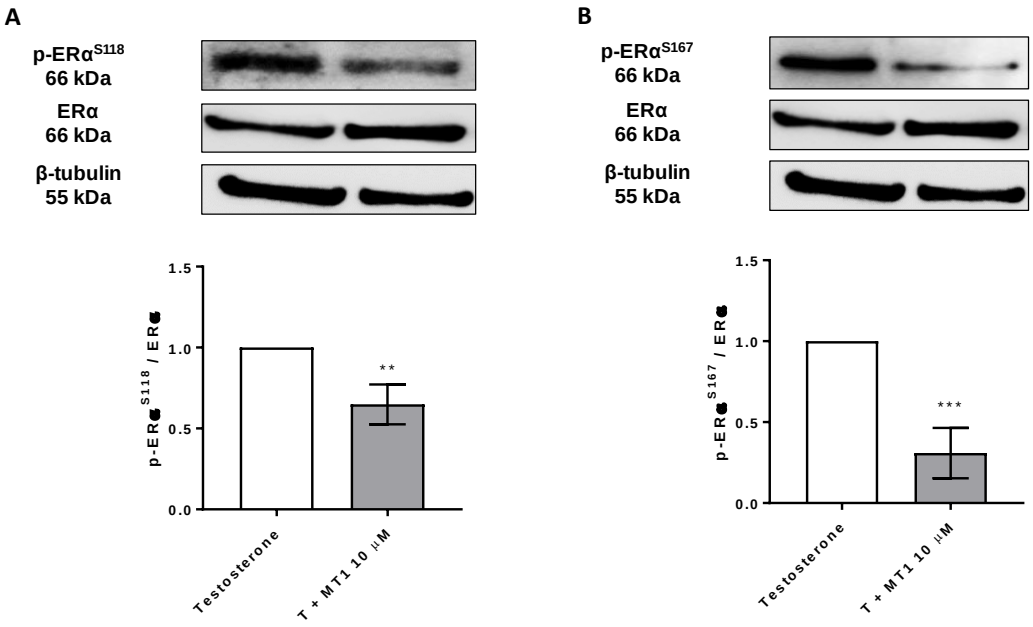

Figure 24: Effects of MT1 on phosphorylated ERα expression levels at Ser118 **(A)** and Ser167 **(B)**. Cells were stimulated with T (1 nM) and treated with MT1 (10 μM) for 3 days. Cells treated only with T were considered as control. A representative Western-Blot of p-ERα^{S118}, ERα and β-tubulin, as well as, of p-ERα^{S167}, ERα and β-tubulin are presented. Densitometric analysis of p-ERα^{S118} or p-ERα^{S167} expression levels after normalization with ERα levels, are shown. ERα and β-tubulin were used as a loading controls. The results are presented as mean ± SEM of at least three independent experiments. Statistically significant differences between MT1-treated cells and control cells are expressed as ** ($p < 0.01$) and *** ($p < 0.001$).

3.1.12. Understanding the involvement of ERβ on the effects induced by MT1 on ER$^+$ breast cancer cells

Finally, after analyzing the involvement of aromatase and ERα in the effects exerted by MT1, we investigated the role of ERβ in the MT1-induced effects on MCF-7aro cells. In order to achieve that, we studied, through the MTT assay, the effects of MT1 in combination with 4-[2-phenyl-5,7,bis(trifluoromethyl)pyrazol-[1,5-a]pyrimidin-3-yl]-phenol (PHTPP). PHTPP is an ERβ antagonist with 36 x more affinity to ERβ than to ERα. This compound antagonizes the effect of E_2 by preventing gene transcription, since PHTPP interferes with the interaction between ERβ and the ERE (160, 161). To perform this assay, MCF-7aro cells were treated with T (1 nM) and MT1 (1 – 25 μM) in combination with PHTPP (1 μM), during 3 and 6 days. Comparing these results with those of the cells treated just with MT1 in the presence of T (1 nM), PHTPP totally reversed the effects caused by MT1 **(Fig. 25)**. These results suggest that ERβ may also be involved in the MT1-induced growth inhibitory action.

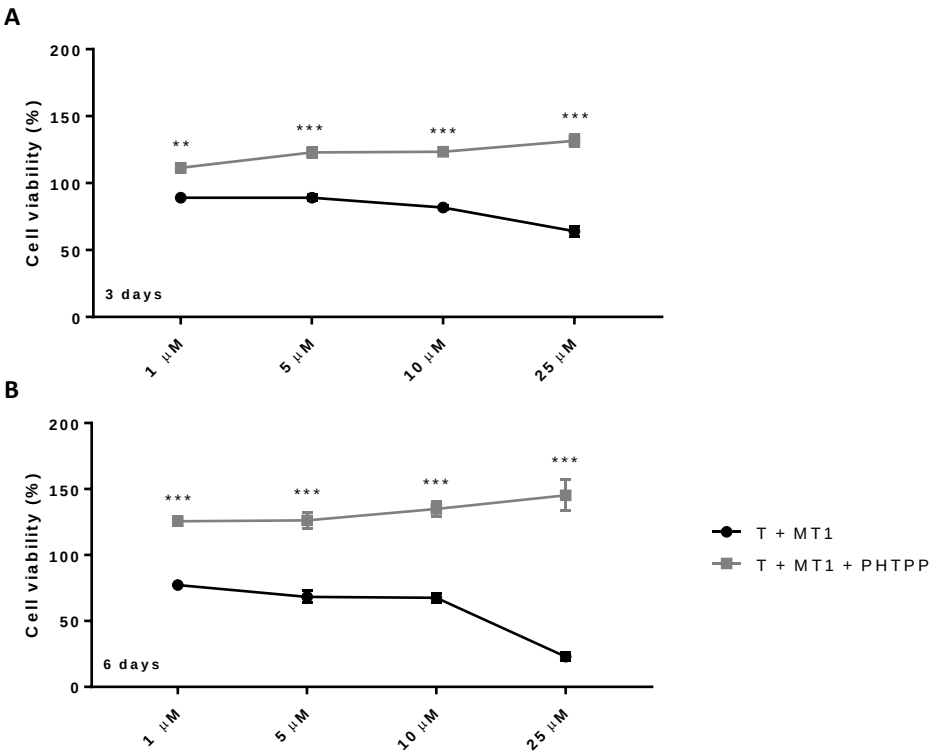

Figure 25: Comparison of the effects of MT1 on MCF-7aro cells treated with or without PHTPP. Cells stimulated with T (1 nM) were treated with different concentrations of MT1 (1 – 25 µM) in combination with PHTPP (1 µM), during 3 **(A)** or 6 days **(B)**. Cells treated only with T with or without PHTPP were considered as control, representing 100% of cell viability. The results are presented as mean ± SEM of at least three independent experiments performed in triplicate. Statistically significant differences between MT1-treated cells with or without PHTPP are expressed as ** ($p < 0.01$) and *** ($p < 0.001$).

Considering these results, we also explored the effects of MT1 on ERβ protein expression levels, by Western-Blot. Cells were stimulated with T (1 nM) and treated with MT1 (10 µM), for 3 days. Cells treated only with T with or without PHTPP (1 µM) were used as controls. As presented in **figure 26**, the preliminary results did not show any significant difference between the control and MT1-treated cells.

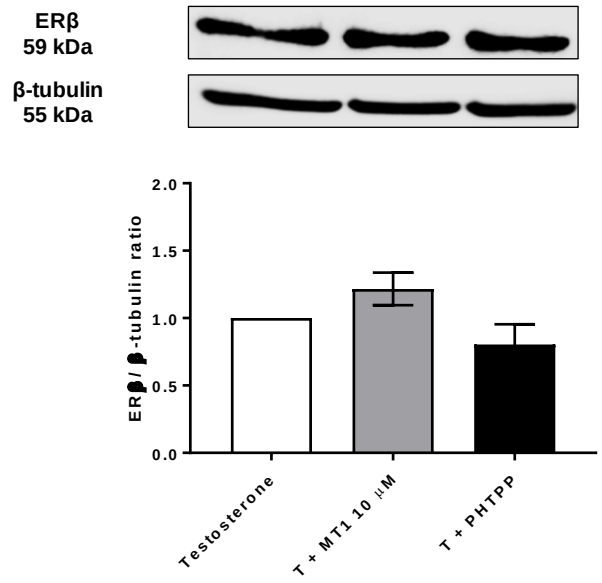

Figure 26: ERβ protein expression levels in MCF-7aro cells treated with MT1. Cells stimulated with T (1 nM) were treated with MT1 (10 μM), for 3 days. Cells treated only with T were considered as control, while cells treated with T and PHTPP (1 μM) were also considered as positive control. A representative Western-Blot of ERβ and β-tubulin, as well as, densitometric analysis of ERβ expression levels after normalization with β-tubulin levels, is shown. β-tubulin was used as loading control. The results are presented as mean ± SEM of at least two independent experiments.

3.1.13. Effects of MT1 on MCF-7aro cell cycle progression

In order to understand if the effects induced by MT1 on MCF-7aro cell viability, are due to a cell cycle deregulation, we explored the effects of MT1 on cell cycle progression by flow cytometry. MCF-7aro cells were treated with T (1 nM) and MT1 (5 and 10 μM), for 3 days. After the 3 days of treatment, cells were fixed with ethanol (70%) and stained with PI, which is a fluorescent dye that binds and intercalates into the DNA, allowing the determination of DNA content within the cells and thus, the cell cycle phase. Comparing the results of MT1 with control, it was possible to observe that MT1 treatment provoked a significant ($p < 0.05$; $p < 0.001$) decrease in the number of cells in G_0/G_1 phase, as well as, a significant ($p < 0.001$) decrease of the number of cells in S phase. On the other hand, MT1 also induced a significant ($p < 0.001$) increase in the number of cells in G_2/M phase. These effects were more pronounced with increasing concentrations **(Table 5)**.

Table 5: Effects of MT1 on MCF-7aro cell cycle progression.

	G_0/G_1	S	G_2/M
Testosterone	82.44 ± 0.47	7.16 ± 0.14	9.97 ± 0.33
T + MT1 5 µM	81.19 ± 0.42 *	2.99 ± 0.18 ***	14.45 ± 0.48 ***
T + MT1 10 µM	78.79 ± 0.21 ***	2.83 ± 0.21 ***	16.68 ± 0.27 ***

MCF-7aro cells were stimulated with T (1 nM) and treated with MT1 (5 and 10 µM), during 3 days. Cells treated only with T (1 nM) were considered as control. After staining the cells with PI (5 µg/ml), they were analyzed by flow cytometry. Values are represented as a percentage of single cell events in each stage of the cell cycle and are the mean ± SEM of at least three independent experiments performed in triplicate. Statistically significant differences between MT1-treated cells and control cells are expressed as * ($p < 0.05$) and *** ($p < 0.001$).

3.1.14. Analysis of MCF-7aro cell death

As the reduction in MCF-7aro cell viability induced by MT1 can also be a result of different mechanisms of cell death, it was investigated the involvement of apoptosis on MCF-7aro cells treated with MT1, by evaluating the activities of caspase-7 and caspase-9. Caspases are a family of protease enzymes which display pivotal roles in the apoptotic cell death. Caspase-7 is an effector caspase responsible for the overall apoptotic process, while caspase-9 is an initiator caspase, specifically involved in the intrinsic pathway of apoptosis which is mediated by mitochondria (162).

The caspase activities were evaluated after 2 days of treatment with MT1 (5 and 10 µM). Cells treated with Staurosporine (STS; 10 µM) were used as positive control. As expected, STS induced a significant ($p < 0.001$) increase in caspase-7 and caspase-9 activities **(Fig. 27)**. In relation to MT1, it caused a significant ($p < 0.01$) increase in caspase-7 activation, both at 5 µM (43.08%) and 10 µM (47.57%) **(Fig. 27A)**. However, the same was not verified in relation to caspase-9 activation, as MT1 did not induce any significative change in the activation profile of this caspase **(Fig. 27B)**.

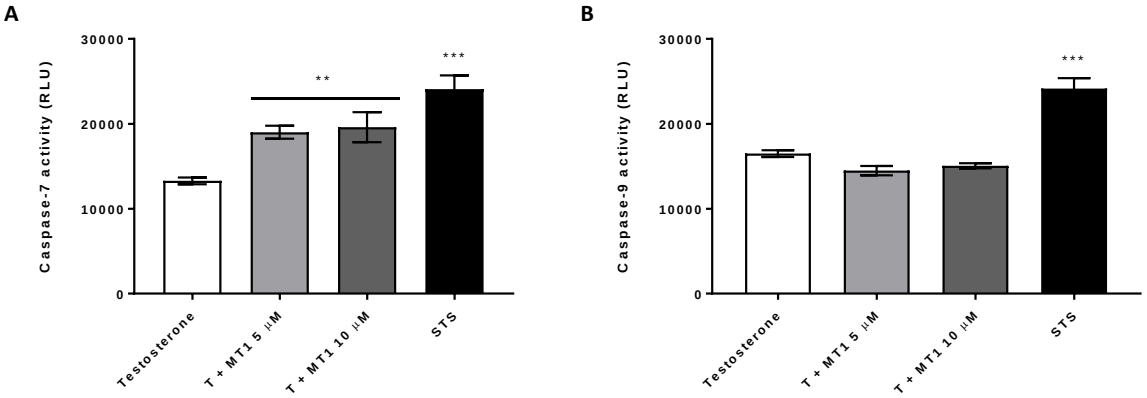

Figure 27: Effects of MT1 on caspase-7 **(A)** and caspase-9 **(B)** activation levels in MCF-7aro cells. Cells were stimulated with T (1 nM) and treated with MT1 (5 and 10 µM), for 2 days. Cells treated only with T were considered as control, while cells treated with STS (10 µM) were used as positive control. The results are presented as mean ± SEM of at least three independent experiments, performed in triplicate. Statistically significant differences between MT1-treated cells and control cells are expressed as ** ($p < 0.01$) and *** ($p < 0.001$).

Although these results suggest that mitochondria is not involved in the apoptotic process, ROS production was also evaluated, as this is one of the features of the apoptotic process that is generally associated with mitochondrial disfunction. ROS production was measured at different time points (30 minutes, 1 hour, 2 hours, 6 hours, 1 day, 2 days and 3 days), using $DCFH_2$-DA. This is a non-fluorescent dye which once inside the cell is oxidized in the presence of ROS into a fluorescent compound, DCF. Cells treated with Exe (10 µM) were used as positive control. Our results, presented in **figure 28** showed that MT1, after 30 min of treatment, induced a significant ($p < 0.001$) increase in the levels of ROS, both at 5 µM (52,87%) and 10 µM (56,69%). Furthermore, as expected, Exe also induced a significant ($p < 0.001$; 38,50%) increase in ROS production **(Fig. 28)**.

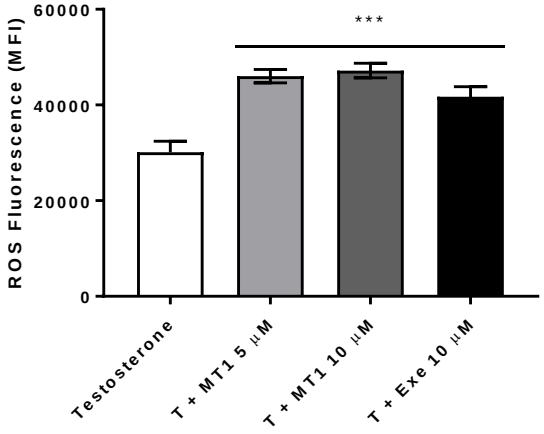

Figure 28: Effects induced by MT1 on ROS production. MCF-7aro cells were stimulated with T (1 nM) and treated with MT1 (5 and 10 µM), for 30 min. Cells treated only with T were considered as control and cells treated with Exe (10 µM) were used as positive control. The results are presented as mean ± SEM of at least three independent experiments, performed in triplicate. Statistically significant differences between MT1- or Exe-treated cells and control cells are expressed as *** ($p < 0.001$).

3.2. Discovery of new non-steroidal AIs

Nowadays, AIs are the first-line therapy to treat hormone-dependent breast cancer cases both in pre- and post-menopausal women patients (68). However, the occurrence of side effects and, especially, the development of resistances are very worrying and limiting. Given this, the discovery of more potent AIs with lower side effects is crucial to improve therapies.

3.2.1. Structure-based virtual screening

Here, we developed a virtual screening approach to discover new potential non-steroidal AIs.

The structure of aromatase complexed with its natural substrate, androstenedione (3S79), was used as target to perform the VS of the 3.4 million of compounds. They were docked using the program rDock and 5 different poses were generated for each compound. rDock was the program chosen because it presented an enrichment factor of 10.3, while AutoDock Vina and AutoDock presented an enrichment factor of 4.6 and 3.7, respectively. All the docked poses were ranked according to the rDock scoring function and the best scored pose of each compound was chosen. After that, the top-scoring 1000 compounds, whose fitness scores ranged from -220.92 to -44.06, were selected for further analysis. In order to select different compounds, ECFP

descriptors were generated for the best 1000 compounds and, then, used to construct 50 chemical diverse clusters using JKlustor available in ChemAxon software. With this type of cluster method, the compounds were grouped according to their structural similarity and the different clusters had compounds chemically different. After that, the 3 top-scoring compounds of each cluster were selected, counting for a total of 128 compounds, and a visual analysis of all of them was done.

Firstly, the best 25 compounds were chosen considering their structure and the interactions that they can establish with aromatase. Furthermore, 10 of those compounds were selected according to their score value, information available in literature, their chemical diversity and the docking in ERs. Finally, and due to time limitations, only 2 of those compounds were selected for experimental analysis at the biochemical and biological levels.

3.2.2. Anti-aromatase activity of NS8 and NS16

The two compounds selected through VS were nominated as NS8 and NS16. Their ability to inhibit aromatase in human placental microsomes was investigated as previously referred for MT1. The results showed that neither NS8 nor NS16 were able to inhibit aromatase in microsomes **(Table 6)**. In fact, NS8 seems to activate aromatase in 5.89%, while NS16 induced an inhibition of 3.04%. Thus, both compounds were not considered AIs. As expected, and contrary to NS8 and NS16, the reference AIs used presented higher anti-aromatase activity (≥ 97%).

Table 6: Percentage of anti-aromatase activity of NS8 and NS16 in human placental microsomes.

Compound	Anti-aromatase activity (%)
NS8	-5.89 ± 2.21
NS16	3.04 ± 2.43
Exe	97.86 ± 0.52
Ana	99.12 ± 0.02
Let	99.69 ± 0.06

Microsomes (20 µg) were incubated with NADPH (15 µM), NS8 (2 µM) or NS16 (2 µM) and [1β-^{3}H]-androstenedione (40 nM), during 15 minutes at 37 ºC. Results are presented as a percentage of tritiated water released in relation to control and are represented as the mean ± SEM of three independent experiments, carried out in triplicate. The reference AIs, Exe, Ana and Let, at 1 µM were used as positive controls.

3.2.3. Effects of NS8 and NS16 on HFF-1 cells

Although our results have demonstrated that NS8 and NS16 were not able to inhibit aromatase, we decided to evaluate the effects of these compounds on cells. First, we investigated the effects on the viability of HFF-1 cells through an MTT assay. For that, cells were treated with NS8 (5 – 25 µM) or NS16 (5 – 25 µM), for 6 days. Our preliminary results showed that neither NS8 nor NS16 exerted effects on the viability of HFF-1 cells **(Fig. 29)**. Despite that, it is possible to see that these compounds induced a slight decrease on the viability of these cells, results that should be confirmed with more assays.

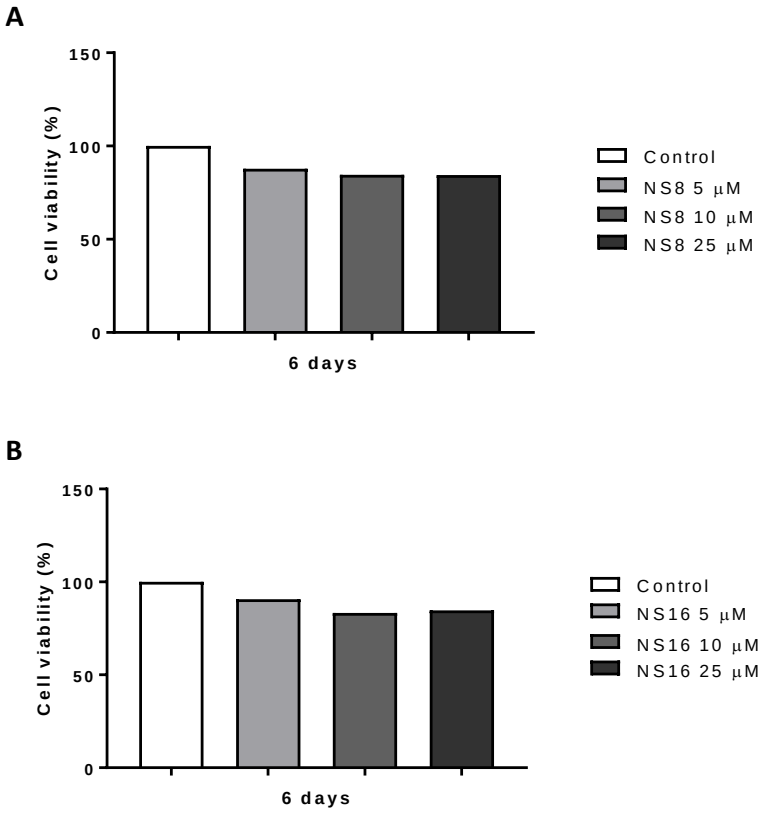

Figure 29: Effects of NS8 **(A)** and NS16 **(B)** on HFF-1 cell viability. Cells were treated with different concentrations of NS8 (5 – 25 µM) or NS16 (5 – 25 µM), for 6 days. Cells without NS8 or NS16 treatment were used as control, representing 100% of cell viability. The results are presented as mean of one experiment performed in triplicate.

3.2.4. Effects of NS8 and NS16 on ER$^+$ breast cancer cells: MTT and LDH assays

After studying the effects of NS8 and NS16 in the viability of non-tumoral cells, we analyzed their effects on MCF-7aro cell viability, as previously referred. For that, cells were treated with NS8 (1 – 25 µM) or NS16 (1 – 25 µM), for 3 and 6 days. NS8 did not

induce any significant decrease on MCF-7aro cell viability, at 3 or at 6 days of treatment **(Fig. 30A)**. However, at the lowest dose (1 µM), after 3 days of treatment, NS8 induced a significant ($p < 0.001$) increase on the number of viable cells (34%). A similar effect was also observed for NS16 (32%) **(Fig. 30B)**. Nevertheless, and contrary to NS8, NS16 induced a significant ($p < 0.01$; $p < 0.001$) decrease on MCF-7aro cell viability after 3 and 6 days, being more pronounced in the latter case. Thus, NS16 presented anti-proliferative effects on MCF-7aro cells in a dose- and time-dependent manner.

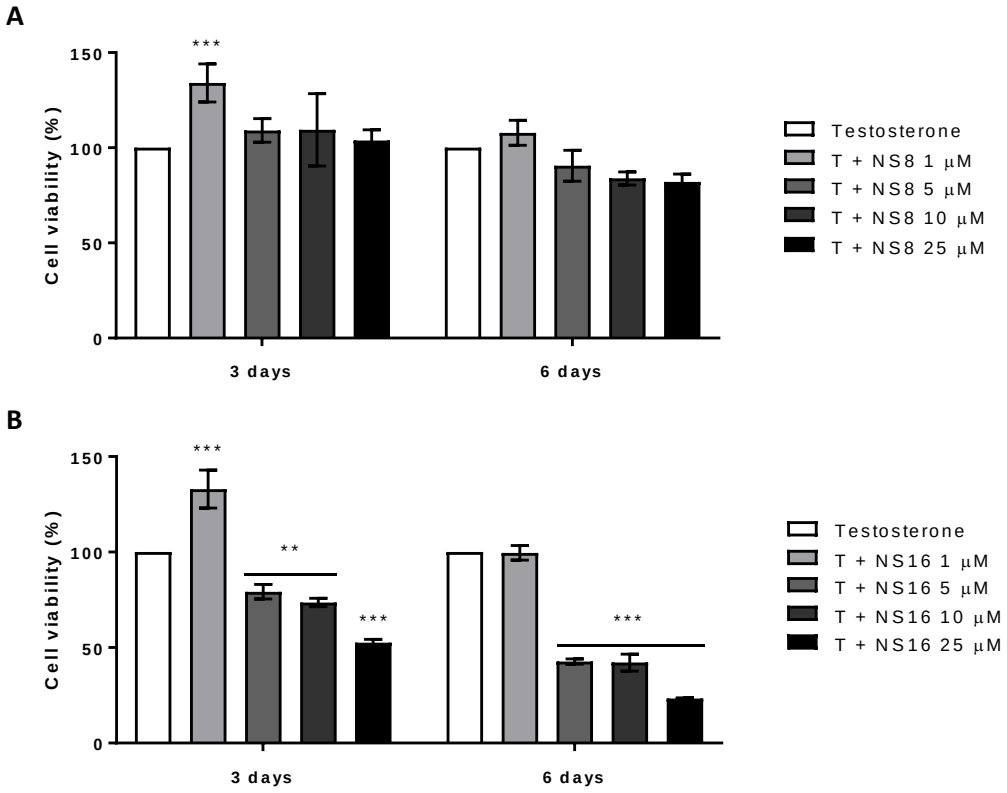

Figure 30: Effects of NS8 **(A)** and NS16 **(B)** on MCF-7aro cell viability. Cells in the presence of T (1 nM) were treated with different concentrations of NS8 (1 – 25 µM) or NS16 (1 – 25 µM), during 3 or 6 days. Cells treated only with T were considered as control, representing 100% of cell viability. The results are presented as mean ± SEM of at least three independent experiments performed in triplicate. Statistically significant differences between NS8- or NS16-treated cells and control cells are expressed as ** ($p < 0.01$) and *** ($p < 0.001$).

As only NS16 reduced cell viability and in order to evaluate the effects on cell membrane integrity, we analyzed the release of LDH, as previously referred. The results demonstrated that NS16 **(Fig. 31)**, did not induce a significant increase in LDH release, at the concentrations studied, which means that at those conditions, the cell membrane of MCF-7aro cells remains intact, being the compound not cytotoxic.

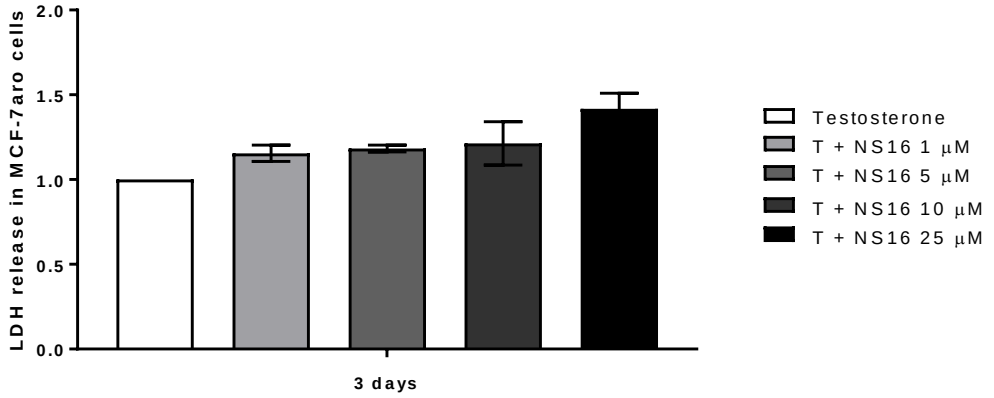

Figure 31: Effects induced by NS16 on MCF-7aro cell cytotoxicity, evaluated by LDH-release assay. Cells were treated with different concentrations of NS16 (1 – 25 μM) in the presence of T (1 μM), during 3 days. Cells treated only with T were considered as control, representing 100% of cell membrane integrity. The results are presented as mean ± SEM of at least three independent experiments, performed in triplicate. Statistically significant differences between NS16-treated cells and control cells are expressed as ** ($p < 0.01$).

4. Discussion

Breast cancer is currently the most frequently diagnosed cancer in women worldwide (1). Around 2/3 of the total breast cancer cases are hormone-dependent (ER^+) therefore, estrogens are crucial for the proliferation and survival of these tumors (5). Estrogens are produced by aromatase, through the aromatization of androgenic compounds, like ASD and T, and exert their effects by binding to ERs in order to induce the transcription of specific target genes (5, 16). Considering the key role of estrogens in tumor growth and survival, the endocrine therapies target aromatase, which prevents the estrogens synthesis, or target ERs, thereby, controlling the transcription of target genes (6, 7). Initially, the SERM tamoxifen was used as a standard therapy both in pre- and post-menopausal women with ER^+ breast cancer. Nowadays, the third-generation of AIs, which comprises the non-steroidal Ana and Let and the steroidal Exe, are recommended to be used as first-line therapy in post-menopausal women and, more recently, also in pre-menopausal women after ovaries ablation, since these AIs proved to be superior to the other endocrine therapies, like tamoxifen (68). However, despite their clinical success, acquired resistance may develop, causing tumor relapse (35). Therefore, many efforts have been made in order to develop novel therapeutic options, more potent and with lower side effects.

In the last decade, computational tools have strongly emerged as a powerful option able to help in drug discovery demand. With the determination of the crystallographic structure of aromatase, in 2009 (19), and using receptor-based VS methods, the discovery of new potential AIs may strongly evolve, since millions of compounds can be simultaneously studied. Considering this, one of the goals of this work was to discover new potential non-steroidal AIs using computational and biological approaches. Moreover, we also aimed to discover possible multi-target compounds able to inhibit aromatase and, simultaneously, modulate the actions of ERα and ERβ. In recent years, this strategy is becoming attractive due to its therapeutic advantages. For that, molecular docking and VS studies were performed. In addition, the biological effects of the selected compounds were studied on ER^+ aromatase-overexpressing breast cancer cells (MCF-7aro cells), the best *in vitro* cell model to study ER^+ breast cancer and AIs, since these cells overexpress aromatase, mimicking, in that way, the microenvironment of this type of tumor (131).

In relation to the multi-target approach, considering aromatase, ERα and ERβ targets, the first step was to evaluate the similarity among the binding sites of these three targets. Our results showed that key residues, including an aspartic acid, which displays critical roles in the catalytic activity of aromatase (18), are conserved among them. This suggests that aromatase, ERα and ERβ can possibly accommodate the same ligands in their binding sites and, consequently, that the discovery of a multi-target compound may

be possible. Furthermore, considering that our goal was to find a multi-target compound able to simultaneously inhibit aromatase and ERα, but also activate ERβ, we analyzed the properties of the AIs, ERα antagonists and ERβ agonists already described in literature, in order to understand their similarities. Together, it was analyzed 2840 compounds, namely 1210 AIs, 1557 ERα antagonists and 73 ERβ agonists. The reduced number of ERβ agonists is explained by the fact that there are many more studies related to ERα than to ERβ. In addition, as previously referred, 1210 AIs were used to study the properties of AIs. Though, because of the high number of compounds used, it was difficult to collect all the information related to each compound, reason why, we do not know if some of these compounds are not competitive inhibitors, which means that they may not interact with the aromatase binding site directly but, rather, being allosteric modulators. Considering this, it would be better to know all the features and mechanisms of action of those AIs, in order to guarantee a more accurate analysis. Still, the results showed that, for the properties studied, the AIs and ERβ agonists have typically similar values, while the values determined for ERα antagonists are, for the majority of the properties studied, higher. In fact, antagonists of the ERs are typically larger than the agonists, which is directly associated to their biological functions, since the conformation of the ERs, related to the position of H12, is dependent on the type of ligand bonded (31, 59). In concordance with these results, there are the log P values in which ERα antagonists exhibit higher values, making these compounds less soluble in aqueous solutions than the other compounds, which may compromise their bioavailability. Moreover, the main difference among the three sets of compounds relies on the number of acceptor groups, as ERα antagonists and ERβ agonists have typically two acceptor groups, while most of the AIs do not have any acceptor group. This is, certainly, related to the type of interactions that each type of compound establishes with the respective target. Nevertheless, it is important to note that there are many compounds of the three sets that exhibit the same properties. This highlights the possibility of discover a multi-target compound.

In order to group all the compounds according to their similarity, ECFP were generated and clusters constructed with the aim of finding clusters containing compounds from the three sets. For a similarity range between 0.6 and 0.9, 175 clusters have been constructed. Although this number can be high, it guarantees that only very similar compounds are grouped together. Two of those clusters were found to contain members of the three sets and these 78 compounds were then used to construct a pharmacophore model. This model is very useful, since it represents the most common features among the 78 compounds selected and, besides that, this pharmacophore can be used in the future as a filter in a VS demand, in order to increase the probabilities of

finding compounds with the desired features. However, due to lack of time, this VS was not performed. Instead, we decided to analyze from the 78 compounds selected, how the 52 ERα antagonists and ERβ agonists fit the aromatase active site. We have only investigated the ERs modulators because we wanted to find novel aromatase inhibitors able to act as multi-target compounds. This procedure leads us to find three compounds able to establish important interactions with Arg115, Phe221, Trp224, Asp309, Thr310, Leu372, Val373 and Leu477 residues of aromatase known to be crucial for the inhibition of this enzyme (17). However, only one of the compounds was suitable to be studied, since the other two compounds have already been explored in this type of cancer, being one of them already known for its undesired side effects. Thus, the biochemical and biological studies proceeded just with one potential multi-target compound, which was nominated as MT1.

MT1 has been already described as an ERα antagonist in MCF-7-2a cells, an estrogen-independent MCF-7 breast cancer cell line (163). Moreover, there is also a study that states that this compound can act as an AI, but the assay was done using recombinant enzymes and the IC_{50} value was 24880 nM. Unexpectedly, in our conditions and using a biological matrix rich in aromatase (129), our results proved that MT1 was not able to inhibit aromatase in human placental microsomes. Nevertheless, we proceeded with its study, by exploring the *in vitro* effects of this compound on breast cancer cells, in order to elucidate its anti-cancer properties. First of all, it was explored its cytotoxic effects in a non-cancerous cell line, HFF-1, and only for the highest concentration studied it was observed a cytotoxic behavior. These are considered good results, since a drug to be used as an anti-cancer agent and be applied in the clinic, should not affect the non-cancerous cells. Considering these results, the studies proceeded for the evaluation of the biological effects of MT1 on ER^+ aromatase-overexpressing breast cancer cells, MCF-7aro cells. Our results demonstrated that MT1 significantly reduced the viability of MCF-7aro cells, in a dose- and time-dependent manner, without causing disruption of cell membrane. These results suggest that although MT1 is not able to inhibit aromatase, it presents anti-cancer growth-inhibitory properties.

In order to understand the mechanism of action behind the anti-cancer properties and besides MT1 did not exhibit anti-aromatase activity and, to discard any involvement of aromatase in those effects, we evaluated the effects of MT1 in cells treated with E_2 and compared these results with the ones of cells stimulated with T and treated with MT1. Interestingly, the results clearly demonstrated that the effects exerted by MT1 may be dependent on aromatase because, in contrast with T, E_2 treatment did not induce any significant alteration on MCF-7aro cell viability. To understand these results, we

investigated by, Western-Blot, the effects of MT1 on aromatase protein expression levels. Interestingly, like Exe (157), MT1 treatment, reduced aromatase expression levels by 44%, when compared to control. Considering these results, we evaluated the effects of MT1 on *CYP19A1* mRNA transcript levels to understand if the reduction on aromatase protein levels was a result of a decrease in *CYP19A1* gene transcription or a consequence of aromatase degradation. Our preliminary results did not reveal any significant alteration in the relative *CYP19A1* mRNA transcript levels upon MT1 treatment. This suggests that, like Exe, MT1 may induce degradation of aromatase. It is known that Exe has the ability to induce aromatase degradation by the proteasome (157), however, to confirm this hypothesis for MT1, more studies should be performed.

Since MT1 was selected as a possible multi-target compound, it was also investigated its effects on ERα and ERβ. For that, it was used the ERα antagonist ICI, a SERD, which induces the degradation of ERα, without affecting ERβ (78), and the antagonist PHTPP, which exhibits 36-fold more selectivity for ERβ than ERα (164). Results demonstrate that ERα blockage impaired the anti-cancer growth-inhibitory properties induced by MT1, suggesting that ERα may be involved on the effects induced by MT1 in breast cancer cells, by acting as an ERα antagonist. Nevertheless, to better understand this possible mechanism of action, we also analyzed the effects of MT1 on protein expression and ERα activation levels. Although the results revealed an increase in ERα expression levels, a significant decrease in the phosphorylation of both residues, Ser118 and Ser167, indicative of ERα activation, was also observed. Taking into account the antagonistic behavior that MT1 seems to exert on cells, this augment on the ERα expression levels may occur as a compensation mechanism. It could be hypothesized that MT1, by binding to ERα, could destabilize the receptor, which could lead to its degradation. As this possible mechanism may occur in a very short period of time and as we are studying protein levels after 3 days of MT1 treatment, we may not detect these alterations on ERα protein expression levels. Moreover, if this occurs, there may be *de novo* synthesis of this receptor to compensate the hypothetical effect. Still, together, these results suggest that, in our cell model, MT1 may act as an ERα antagonist, by preventing ERα phosphorylation and consequent activation, which is a desired effect and a therapeutic advantage, considering that ERα is directly involved in the growth and survival of ER^+ breast tumors.

Furthermore, our data also suggests that MT1 may act as an ERβ agonist, since, when ERβ is inactivated by PHTPP, the growth-inhibitory action of MT1 is impaired. Similarly to ERα, the expression levels of ERβ were also investigated after MT1 treatment. Our results indicated that MT1 did not affect the expression levels of ERβ. Interestingly, PHTPP treatment also did not induce a significant difference on the

expression levels of ERβ, which suggests that this ERβ antagonist may act only by destabilizing ERβ without inducing its degradation. Despite that, together our results suggest that MT1 may also mediates its effects via ERβ, but without interfering with ERβ expression levels. Nevertheless, as these are preliminary results, further studies should be performed in order to clarify the role of ERβ in MT1-treated cells.

Several studies have demonstrated that new steroidal anti-cancer compounds that act as AIs (136, 165, 166), as well as the AIs used in clinic (133, 167), exert their effects on ER^+ breast cancer cells by causing cell cycle arrest. The results of cell cytometry showed that MT1 was able to induce cell cycle arrest in the G_2/M phase, causing a consequent reduction on the number of cells in both G_0/G_1 and S phases. This indicates that the effects exerted by MT1 on ER^+ breast cancer cells can be explained by a disruption on cell cycle progression. In fact, a G_2/M arrest has already been observed for Exe after 6 days of treatment (133), while in the case of the non-steroidal Ana and Let, as well as, for the anti-estrogens tamoxifen and fulvestrant, an arrest in the G_0/G_1 phase was detected (131, 167). However, as an increase in the number of cells arrested in G_2/M phase may be indicative of an apoptotic process (168), it was also explored the involvement of apoptosis in the reduction of MCF-7aro cell viability induced by MT1. For that, the activation of caspase-7 and caspase-9 and the production of intracellular ROS were evaluated. Caspase-7 is an effector caspase responsible for the apoptotic process, while caspase-9 is an initiator caspase involved in the intrinsic pathway of apoptosis, that is mediated by mitochondria (162). In turn, increased ROS production can lead to oxidative stress, which is frequently associated to mitochondrial disfunction and apoptosis (169). MT1 treatment induced, in breast cancer cells, a significant increase in the activation of caspase-7, but not in the activation of caspase-9. This suggests that MT1, as the AIs used in clinic (133, 167), induced apoptosis in ER^+ breast cancer cells, but that this process is caspase-9 independent, which suggests that the activation of apoptosis may be not mediated by mitochondria. The activation of apoptosis can occur mainly by the involvement of the extrinsic or death receptor pathway and/or the intrinsic or mitochondrial pathway. However, there is evidence of an additional perforin/granzyme pathway able to activate apoptosis, by converging on the same terminal or execution as extrinsic and intrinsic pathways (170). Moreover, it is known that endonuclease G is a protein that can potentially be involved in both caspase-independent and caspase-dependent apoptotic cell death (171). Additionally, endoplasmic reticulum stress can also trigger apoptosis through caspase-12 activation, or through the involvement of the classic apoptotic mitochondrial pathway or by the activation of caspase-independent cell death (171).

Besides the activation of caspase-7, MT1 also induced a significant increase in the intracellular levels of ROS, suggesting that the activation of apoptosis is ROS-dependent. ROS production occurs essentially in mitochondria, however, other factors and cellular sources are involved in their production. In fact, ROS can also be produced by endoplasmic reticulum, peroxisomes and cytosolic enzymes (172-174). Considering this, the effects induced by MT1 on ROS levels can be a result of the activation of some of these pathways, though further studies should be performed to clarify the mechanism. Furthermore, it is important to note that the effects of MT1 observed on caspase-7, caspase-9 and ROS levels can be a result of the involvement of several pathways, being the major ones previously described. For example, it is known that exemestane metabolites induced an increase in the levels of ROS, caspase-9, but also caspase-8, which suggests that the apoptotic pathway is mediated simultaneously by mitochondria and through the activation of caspase-8, by a crosstalk not fully understood (166). In relation to the AIs used in clinic, different studies suggest only the involvement of the intrinsic pathway (133, 167), though microarray analysis also suggests an up-regulation of caspase-8 in the case of Ana (131). In the case of tamoxifen, different studies described that this SERM induces apoptosis through the involvement of caspase-9 (167) or independently on caspase-9 activation (175). Moreover, for tamoxifen, it was also reported that the induction of apoptosis might also occur through the involvement of tyrosine kinase receptors (TKR), through the $ERK_{1}/_{2}$ pathway (164). In the case of the SERD fulvestrant, it was only reported the involvement of the mitochondrial pathway (167). Thus, considering all this information, future studies should be performed in order to better understand the underlying mechanisms by which MT1 activates the apoptotic process.

Overall, this study provided crucial information regarding multi-target compounds capable of modulating aromatase, ERα and ERβ, being this information important for the development of novel therapeutic approaches. For the best of our knowledge, this is the first attempt to discover multi-target compounds for ER^{+} breast cancer treatment using computational approaches. For the three targets under investigation, only norendoxifen has been pointed as capable to inhibit aromatase and activate ERα and ERβ (102, 103). Polyphenolic compounds have also been described as modulators of both ERα and ERβ (176). One of those compounds, genistein, an isoflavone present in soya, has been described as presenting dual-function, being able to act as an ERα antagonist and, simultaneously, as an ERβ agonist (177). Furthermore, it has been referred that genistein is able to inhibit aromatase and induce its degradation (177), however, these results are controversial, since our group showed that genistein is a weak AI (155). Indeed, studies for the development of multi-target compounds have been steadily increasing, as these

compounds are capable of simultaneously modulate more than one target, being thus more effective and promising than single-target compounds (178, 179). In fact, these compounds are pointed as more effective, more potent, less toxic and associated with fewer side effects (178-180). In this field, computational tools display a fundamental role in the identification of novel compounds able to regulate the function of several targets. Tools like molecular docking, pharmacophore construction, combination methods and structure-activity relationships (SAR), as well as, quantitative structure-activity relationship (QSAR) are some of the most important and used (180, 181).

In relation to the VS approach for the discovery of novel non-steroidal AIs, a database of 3.4 million compounds and the docking program rDOCK were used. The top 1000 compounds ranked in the VS approach have the probability of being potential AIs. Thus, the compounds were organized in 50 clusters, according to their chemical similarities. The three best scored compounds from each cluster were then selected. The best 25 compounds were chosen taking into account their structure and the interactions that they established with aromatase, namely with Phe221, Trp224, Asp309, Thr310, Leu372, Met374 and L477 (17). In this study, only 2 of those 25 compounds were selected to be experimentally analyzed. The non-steroidal compounds were designated as NS8 and NS16 and, similarly to what was done with MT1, the first step was to evaluate their ability to inhibit aromatase, in human placental microsomes. Unexpectedly, our results demonstrated that neither NS8 nor NS16 were able to inhibit aromatase. These results emphasize that, although these compounds have been selected after an exhaustive VS procedure and analysis, only two compounds were tested, which limits the success of the demand. Thus, more compounds should be tested to find a compound with the desired properties. In spite of that, the biological effects of these compounds were explored in non-cancerous and in ER^+ breast cancer cells. Preliminary results demonstrated that, in our conditions, neither NS8 nor NS16 affected the viability of the non-cancerous HFF-1 cells, though only NS16 caused a significant decrease in MCF-7aro cell viability in a dose- and time-dependent manner.

Despite the VS approach for the discovery of novel non-steroidal AIs did not lead to the discovery of any compound able to inhibit aromatase, NS16 presented growth-inhibitory properties in ER^+ breast cancer cells and as MT1, NS16 may affect the levels of the enzyme aromatase. If this is the case, less estrogen will be synthetized which, consequently, may explain the NS16-induced growth-inhibitory effects. Therefore, although the mechanisms underlying this reduction in cell viability have not been studied, further studies should be performed.

5. Conclusion

The discovery of novel drugs for cancer treatment is one of the main concerns of the scientific community. In this field, *in silico* tools display crucial contributions allowing a better understanding and a more realistic representation of the protein structures and of the interactions involved in a certain function. Because of that, they represent a more efficacious way to develop novel therapeutic strategies, like in the finding of multi-target compounds, which are gaining a lot of interest, since this type of compounds are considered to be better than single-target compounds. Here, we discovered MT1, a multi-target compound with anti-cancer growth-inhibitory properties for ER^+ breast cancer treatment. Although MT1 did not inhibit aromatase, it was able to induce a decrease of its protein levels and to act as an ERα antagonist and, simultaneously, as an ERβ agonist. This may represent an advantage for the treatment of this subtype of breast cancer, since the key targets responsible for estrogen production and function are modulated. Besides that, this multi-target compound was able to impair the cell cycle progression of ER^+ breast cancer cells and also induced apoptotic cell death. Therefore, MT1 is, for the best of our knowledge, the first multi-target compound with anti-cancer properties for ER^+ breast cancer, discovered through this type of computational approaches, making this study an important landmark in this field.

In relation to the discovery of new non-steroidal AIs, the two candidates studied in this work were not able to inhibit aromatase. However, one of these compounds, NS16, presented growth-inhibitory properties in MCF-7aro cells. Considering this, it is possible that NS16 effects on breast cancer cells may also be a result of the modulation of the ERs or like MT1 be due to the induction of aromatase degradation, though, future studies should be performed to understand its mechanism of action. In addition, it is important to note that the VS demand is a theoretical approach that does not guarantee the immediate success of the study. For a successful demand, several compounds must be experimentally and simultaneously tested.

In conclusion, the overall study provides crucial structural insights related to the inhibition of aromatase, ERα antagonists and ERβ agonists, through the analysis of molecular descriptors, which helped to discover a multi-target compound. Furthermore, it also reveals the strong potential of multi-target compounds for the treatment of ER^+ breast cancer, through the discovery of MT1.

6. References

1. Lukong KE. Understanding breast cancer - The long and winding road. BBA Clin. 2017;7:64-77.
2. Ferlay J, Soerjomataram I, Dikshit R, Eser S, Mathers C, Rebelo M, et al. Cancer incidence and mortality worldwide: sources, methods and major patterns in GLOBOCAN 2012. Int J Cancer. 2015;136(5):E359-86.
3. Bray F, Ferlay J, Soerjomataram I, Siegel RL, Torre LA, Jemal A. Global cancer statistics 2018: GLOBOCAN estimates of incidence and mortality worldwide for 36 cancers in 185 countries. CA Cancer J Clin. 2018;68(6):394-424.
4. Wu VS, Kanaya N, Lo C, Mortimer J, Chen S. From bench to bedside: What do we know about hormone receptor-positive and human epidermal growth factor receptor 2-positive breast cancer? J Steroid Biochem Mol Biol. 2015;153:45-53.
5. Chen S. An "omics" approach to determine the mechanisms of acquired aromatase inhibitor resistance. OMICS. 2011;15(6):347-52.
6. Ballinger TJ, Meier JB, Jansen VM. Current Landscape of Targeted Therapies for Hormone-Receptor Positive, HER2 Negative Metastatic Breast Cancer. Front Oncol. 2018;8:308.
7. Brufsky AM, Dickler MN. Estrogen Receptor-Positive Breast Cancer: Exploiting Signaling Pathways Implicated in Endocrine Resistance. Oncologist. 2018;23(5):528-39.
8. Chan HJ, Petrossian K, Chen S. Structural and functional characterization of aromatase, estrogen receptor, and their genes in endocrine-responsive and -resistant breast cancer cells. J Steroid Biochem Mol Biol. 2016;161:73-83.
9. Hong Y, Li H, Yuan Y-C, Chen S. Molecular Characterization of Aromatase. Annals of the New York Academy of Sciences. 2009;1155(1):112-20.
10. Di Nardo G, Cimicata G, Baravalle R, Dell'Angelo V, Ciaramella A, Catucci G, et al. Working at the membrane interface: Ligand-induced changes in dynamic conformation and oligomeric structure in human aromatase. Biotechnol Appl Biochem. 2018;65(1):46-53.
11. Chumsri S, Brodie A. Aromatase inhibitors and breast cancer. Horm Mol Biol Clin Investig. 2012;9(2):119-26.
12. Varela CL, Amaral C, Correia-da-Silva G, Carvalho RA, Teixeira NA, Costa SC, et al. Design, synthesis and biochemical studies of new 7alpha-allylandrostanes as aromatase inhibitors. Steroids. 2013;78(7):662-9.
13. Chumsri S, Howes T, Bao T, Sabnis G, Brodie A. Aromatase, aromatase inhibitors, and breast cancer. J Steroid Biochem Mol Biol. 2011;125(1-2):13-22.
14. Hua H, Zhang H, Kong Q, Jiang Y. Mechanisms for estrogen receptor expression in human cancer. Exp Hematol Oncol. 2018;7:24.
15. Brueggemeier RW. Aromatase inhibitors: new endocrine treatment of breast cancer. Semin Reprod Med. 2004;22(1):31-43.
16. Ghosh D, Lo J, Morton D, Valette D, Xi J, Griswold J, et al. Novel aromatase inhibitors by structure-guided design. J Med Chem. 2012;55(19):8464-76.
17. Suvannang N, Nantasenamat C, Isarankura-Na-Ayudhya C, Prachayasittikul V. Molecular Docking of Aromatase Inhibitors. Molecules. 2011;16(5):3597-617.
18. Di Nardo G, Breitner M, Bandino A, Ghosh D, Jennings GK, Hackett JC, et al. Evidence for an elevated aspartate pK(a) in the active site of human aromatase. J Biol Chem. 2015;290(2):1186-96.
19. Ghosh D, Griswold J, Erman M, Pangborn W. Structural basis for androgen specificity and oestrogen synthesis in human aromatase. Nature. 2009;457(7226):219-23.
20. Shoombuatong W, Schaduangrat N, Nantasenamat C. Towards understanding aromatase inhibitory activity via QSAR modeling. EXCLI J. 2018;17:688-708.
21. Hong Y, Rashid R, Chen S. Binding features of steroidal and nonsteroidal inhibitors. Steroids. 2011;76(8):802-6.
22. Park J, Czapla L, Amaro RE. Molecular simulations of aromatase reveal new insights into the mechanism of ligand binding. J Chem Inf Model. 2013;53(8):2047-56.

23. Ghosh D, Egbuta C, Lo J. Testosterone complex and non-steroidal ligands of human aromatase. J Steroid Biochem Mol Biol. 2018;181:11-9.
24. Brzozowski AM, Pike AC, Dauter Z, Hubbard RE, Bonn T, Engstrom O, et al. Molecular basis of agonism and antagonism in the oestrogen receptor. Nature. 1997;389(6652):753-8.
25. Ascenzi P, Bocedi A, Marino M. Structure-function relationship of estrogen receptor alpha and beta: impact on human health. Mol Aspects Med. 2006;27(4):299-402.
26. Salum LB, Polikarpov I, Andricopulo AD. Structure-based approach for the study of estrogen receptor binding affinity and subtype selectivity. J Chem Inf Model. 2008;48(11):2243-53.
27. Chen L, Wu D, Bian HP, Kuang GL, Jiang J, Li WH, et al. Selective ligands of estrogen receptor beta discovered using pharmacophore mapping and structure-based virtual screening. Acta Pharmacol Sin. 2014;35(10):1333-41.
28. Reinert T, Goncalves R, Bines J. Implications of ESR1 Mutations in Hormone Receptor-Positive Breast Cancer. Curr Treat Options Oncol. 2018;19(5):24.
29. Russo J, Russo IH. The role of estrogen in the initiation of breast cancer. J Steroid Biochem Mol Biol. 2006;102(1-5):89-96.
30. Yue W, Wang JP, Li Y, Fan P, Liu G, Zhang N, et al. Effects of estrogen on breast cancer development: Role of estrogen receptor independent mechanisms. Int J Cancer. 2010;127(8):1748-57.
31. Huang P, Chandra V, Rastinejad F. Structural overview of the nuclear receptor superfamily: insights into physiology and therapeutics. Annu Rev Physiol. 2010;72:247-72.
32. Zhao C, Dahlman-Wright K, Gustafsson JA. Estrogen receptor beta: an overview and update. Nucl Recept Signal. 2008;6:e003.
33. Sever R, Glass CK. Signaling by nuclear receptors. Cold Spring Harb Perspect Biol. 2013;5(3):a016709.
34. Ruff M, Gangloff M, Wurtz JM, Moras D. Estrogen receptor transcription and transactivation: Structure-function relationship in DNA- and ligand-binding domains of estrogen receptors. Breast Cancer Res. 2000;2(5):353-9.
35. Augusto TV, Correia-da-Silva G, Rodrigues CMP, Teixeira N, Amaral C. Acquired resistance to aromatase inhibitors: where we stand! Endocr Relat Cancer. 2018;25(5):R283-R301.
36. Schulman IG, Heyman RA. The flip side: Identifying small molecule regulators of nuclear receptors. Chem Biol. 2004;11(5):639-46.
37. Leclercq G, Gallo D, Cossy J, Laios I, Larsimont D, Laurent G, et al. Peptides targeting estrogen receptor alpha-potential applications for breast cancer treatment. Curr Pharm Des. 2011;17(25):2632-53.
38. Yasar P, Ayaz G, User SD, Gupur G, Muyan M. Molecular mechanism of estrogen-estrogen receptor signaling. Reprod Med Biol. 2017;16(1):4-20.
39. Shiau AK, Barstad D, Loria PM, Cheng L, Kushner PJ, Agard DA, et al. The structural basis of estrogen receptor/coactivator recognition and the antagonism of this interaction by tamoxifen. Cell. 1998;95(7):927-37.
40. Walter P, Green S, Greene G, Krust A, Bornert JM, Jeltsch JM, et al. Cloning of the human estrogen receptor cDNA. Proc Natl Acad Sci U S A. 1985;82(23):7889-93.
41. Kuiper GG, Enmark E, Pelto-Huikko M, Nilsson S, Gustafsson JA. Cloning of a novel receptor expressed in rat prostate and ovary. Proc Natl Acad Sci U S A. 1996;93(12):5925-30.
42. Lee HR, Kim TH, Choi KC. Functions and physiological roles of two types of estrogen receptors, ERalpha and ERbeta, identified by estrogen receptor knockout mouse. Lab Anim Res. 2012;28(2):71-6.
43. Niu AQ, Xie LJ, Wang H, Zhu B, Wang SQ. Prediction of selective estrogen receptor beta agonist using open data and machine learning approach. Drug Des Devel Ther. 2016;10:2323-31.

44. Manas ES, Xu ZB, Unwalla RJ, Somers WS. Understanding the selectivity of genistein for human estrogen receptor-beta using X-ray crystallography and computational methods. Structure. 2004;12(12):2197-207.
45. Dong X, Hilliard SG, Zheng W. Structure-based quantitative structure--activity relationship modeling of estrogen receptor beta-ligands. Future Med Chem. 2011;3(8):933-45.
46. Paterni I, Granchi C, Katzenellenbogen JA, Minutolo F. Estrogen receptors alpha (ERalpha) and beta (ERbeta): subtype-selective ligands and clinical potential. Steroids. 2014;90:13-29.
47. Qin W, Xie M, Qin X, Fang Q, Yin F, Li Z. Recent advances in peptidomimetics antagonists targeting estrogen receptor alpha-coactivator interaction in cancer therapy. Bioorg Med Chem Lett. 2018;28(17):2827-36.
48. Haldosen LA, Zhao C, Dahlman-Wright K. Estrogen receptor beta in breast cancer. Mol Cell Endocrinol. 2014;382(1):665-72.
49. Tuccinardi T, Poli G, Dell'Agnello M, Granchi C, Minutolo F, Martinelli A. Receptor-based virtual screening evaluation for the identification of estrogen receptor beta ligands. J Enzyme Inhib Med Chem. 2015;30(4):662-70.
50. Wolff M, Kosyna FK, Dunst J, Jelkmann W, Depping R. Impact of hypoxia inducible factors on estrogen receptor expression in breast cancer cells. Arch Biochem Biophys. 2017;613:23-30.
51. Farooq A. Structural and Functional Diversity of Estrogen Receptor Ligands. Curr Top Med Chem. 2015;15(14):1372-84.
52. AlFakeeh A, Brezden-Masley C. Overcoming endocrine resistance in hormone receptor-positive breast cancer. Curr Oncol. 2018;25(Suppl 1):S18-S27.
53. Prossnitz ER, Maggiolini M. Mechanisms of estrogen signaling and gene expression via GPR30. Mol Cell Endocrinol. 2009;308(1-2):32-8.
54. Prossnitz ER, Arterburn JB, Sklar LA. GPR30: A G protein-coupled receptor for estrogen. Mol Cell Endocrinol. 2007;265-266:138-42.
55. Bjornstrom L, Sjoberg M. Mechanisms of estrogen receptor signaling: convergence of genomic and nongenomic actions on target genes. Mol Endocrinol. 2005;19(4):833-42.
56. Lee S, Barron MG. Structure-Based Understanding of Binding Affinity and Mode of Estrogen Receptor alpha Agonists and Antagonists. PLoS One. 2017;12(1):e0169607.
57. Pavlin M, Spinello A, Pennati M, Zaffaroni N, Gobbi S, Bisi A, et al. A Computational Assay of Estrogen Receptor alpha Antagonists Reveals the Key Common Structural Traits of Drugs Effectively Fighting Refractory Breast Cancers. Sci Rep. 2018;8(1):649.
58. Souza PCT, Textor LC, Melo DC, Nascimento AS, Skaf MS, Polikarpov I. An alternative conformation of ERbeta bound to estradiol reveals H12 in a stable antagonist position. Sci Rep. 2017;7(1):3509.
59. Ng HL. Simulations reveal increased fluctuations in estrogen receptor-alpha conformation upon antagonist binding. J Mol Graph Model. 2016;69:72-7.
60. Awan A, Esfahani K. Endocrine therapy for breast cancer in the primary care setting. Curr Oncol. 2018;25(4):285-91.
61. Lumachi F, Luisetto G, Basso SM, Basso U, Brunello A, Camozzi V. Endocrine therapy of breast cancer. Curr Med Chem. 2011;18(4):513-22.
62. Altundag K, Ibrahim NK. Aromatase inhibitors in breast cancer: an overview. Oncologist. 2006;11(6):553-62.
63. Pingaew R, Prachayasittikul V, Anuwongcharoen N, Prachayasittikul S, Ruchirawat S, Prachayasittikul V. Synthesis and molecular docking of N,N'-disubstituted thiourea derivatives as novel aromatase inhibitors. Bioorg Chem. 2018;79:171-8.
64. Sobral AF, Amaral C, Correia-da-Silva G, Teixeira N. Unravelling exemestane: From biology to clinical prospects. J Steroid Biochem Mol Biol. 2016;163:1-11.
65. Dutta U, Pant K. Aromatase inhibitors: past, present and future in breast cancer therapy. Med Oncol. 2008;25(2):113-24.

66. Schneider R, Barakat A, Pippen J, Osborne C. Aromatase inhibitors in the treatment of breast cancer in post-menopausal female patients: an update. Breast Cancer (Dove Med Press). 2011;3:113-25.
67. Cardoso F, Costa A, Senkus E, Aapro M, Andre F, Barrios CH, et al. 3rd ESO-ESMO international consensus guidelines for Advanced Breast Cancer (ABC 3). Breast. 2017;31:244-59.
68. Cardoso F, Senkus E, Costa A, Papadopoulos E, Aapro M, Andre F, et al. 4th ESO-ESMO International Consensus Guidelines for Advanced Breast Cancer (ABC 4)dagger. Ann Oncol. 2018;29(8):1634-57.
69. Hamadeh IS, Patel JN, Rusin S, Tan AR. Personalizing aromatase inhibitor therapy in patients with breast cancer. Cancer Treat Rev. 2018;70:47-55.
70. Mao H, Bao T, Shen X, Li Q, Seluzicki C, Im EO, et al. Prevalence and risk factors for fatigue among breast cancer survivors on aromatase inhibitors. Eur J Cancer. 2018;101:47-54.
71. Adhikari N, Amin SA, Saha A, Jha T. Combating breast cancer with non-steroidal aromatase inhibitors (NSAIs): Understanding the chemico-biological interactions through comparative SAR/QSAR study. Eur J Med Chem. 2017;137:365-438.
72. Fabian CJ. The what, why and how of aromatase inhibitors: hormonal agents for treatment and prevention of breast cancer. Int J Clin Pract. 2007;61(12):2051-63.
73. Tseng OL, Spinelli JJ, Gotay CC, Ho WY, McBride ML, Dawes MG. Aromatase inhibitors are associated with a higher fracture risk than tamoxifen: a systematic review and meta-analysis. Ther Adv Musculoskelet Dis. 2018;10(4):71-90.
74. Zhou DJ, Pompon D, Chen SA. Stable expression of human aromatase complementary DNA in mammalian cells: a useful system for aromatase inhibitor screening. Cancer Res. 1990;50(21):6949-54.
75. Roleira FMF, Varela C, Amaral C, Costa SC, Correia-da-Silva G, Moraca F, et al. C-6alpha- vs C-7alpha-Substituted Steroidal Aromatase Inhibitors: Which Is Better? Synthesis, Biochemical Evaluation, Docking Studies, and Structure-Activity Relationships. J Med Chem. 2019;62(7):3636-57.
76. Cepa MM, Tavares da Silva EJ, Correia-da-Silva G, Roleira FM, Teixeira NA. Structure-activity relationships of new A,D-ring modified steroids as aromatase inhibitors: design, synthesis, and biological activity evaluation. J Med Chem. 2005;48(20):6379-85.
77. Sahin Z, Ertas M, Berk B, Biltekin SN, Yurttas L, Demirayak S. Studies on non-steroidal inhibitors of aromatase enzyme; 4-(aryl/heteroaryl)-2-(pyrimidin-2-yl)thiazole derivatives. Bioorg Med Chem. 2018;26(8):1986-95.
78. Carlson RW. The History and Mechanism of Action of Fulvestrant. Clinical Breast Cancer. 2005;6:S5-S8.
79. Abdel-Razeq H. Current frontline endocrine treatment options for women with hormone receptor-positive, Human Epidermal Growth Factor Receptor 2 (HER2)-negative advanced-stage breast cancer. Hematol Oncol Stem Cell Ther. 2018.
80. Mourits MJ, De Vries EG, Willemse PH, Ten Hoor KA, Hollema H, Van der Zee AG. Tamoxifen treatment and gynecologic side effects: a review. Obstet Gynecol. 2001;97(5 Pt 2):855-66.
81. Vergote I, Abram P. Fulvestrant, a new treatment option for advanced breast cancer: tolerability versus existing agents. Ann Oncol. 2006;17(2):200-4.
82. Chumsri S. Clinical utilities of aromatase inhibitors in breast cancer. Int J Womens Health. 2015;7:493-9.
83. Robertson JFR, Bondarenko IM, Trishkina E, Dvorkin M, Panasci L, Manikhas A, et al. Fulvestrant 500 mg versus anastrozole 1 mg for hormone receptor-positive advanced breast cancer (FALCON): an international, randomised, double-blind, phase 3 trial. The Lancet. 2016;388(10063):2997-3005.
84. Ellis MJ, Llombart-Cussac A, Feltl D, Dewar JA, Jasiowka M, Hewson N, et al. Fulvestrant 500 mg Versus Anastrozole 1 mg for the First-Line Treatment of Advanced Breast Cancer: Overall Survival Analysis From the Phase II FIRST Study. J Clin Oncol. 2015;33(32):3781-7.

85. Vidula N, Rugo HS. Emerging data on improving response to hormone therapy: the role of novel targeted agents. Expert Rev Anticancer Ther. 2018;18(1):3-18.
86. Niu J, Andres G, Kramer K, Kundranda MN, Alvarez RH, Klimant E, et al. Incidence and clinical significance of ESR1 mutations in heavily pretreated metastatic breast cancer patients. Onco Targets Ther. 2015;8:3323-8.
87. Ma CX, Reinert T, Chmielewska I, Ellis MJ. Mechanisms of aromatase inhibitor resistance. Nat Rev Cancer. 2015;15(5):261-75.
88. Daldorff S, Mathiesen RM, Yri OE, Odegard HP, Geisler J. Cotargeting of CYP-19 (aromatase) and emerging, pivotal signalling pathways in metastatic breast cancer. Br J Cancer. 2017;116(1):10-20.
89. Mills JN, Rutkovsky AC, Giordano A. Mechanisms of resistance in estrogen receptor positive breast cancer: overcoming resistance to tamoxifen/aromatase inhibitors. Curr Opin Pharmacol. 2018;41:59-65.
90. Mosly D, Turnbull A, Sims A, Ward C, Langdon S. Predictive markers of endocrine response in breast cancer. World J Exp Med. 2018;8(1):1-7.
91. Cortes J, Im SA, Holgado E, Perez-Garcia JM, Schmid P, Chavez-MacGregor M. The next era of treatment for hormone receptor-positive, HER2-negative advanced breast cancer: Triplet combination-based endocrine therapies. Cancer Treat Rev. 2017;61:53-60.
92. Hole S, Pedersen AM, Lykkesfeldt AE, Yde CW. Aurora kinase A and B as new treatment targets in aromatase inhibitor-resistant breast cancer cells. Breast Cancer Res Tr. 2015;149(3):715-26.
93. Amaral C, Varela C, Azevedo M, da Silva ET, Roleira FM, Chen S, et al. Effects of steroidal aromatase inhibitors on sensitive and resistant breast cancer cells: aromatase inhibition and autophagy. J Steroid Biochem Mol Biol. 2013;135:51-9.
94. Amaral C, Augusto TV, Tavares-da-Silva E, Roleira FMF, Correia-da-Silva G, Teixeira N. Hormone-dependent breast cancer: Targeting autophagy and PI3K overcomes Exemestane-acquired resistance. J Steroid Biochem Mol Biol. 2018;183:51-61.
95. Muluhngwi P, Klinge CM. Identification of miRNAs as biomarkers for acquired endocrine resistance in breast cancer. Mol Cell Endocrinol. 2017;456:76-86.
96. Peddi PF. Hormone receptor positive breast cancer: state of the art. Curr Opin Obstet Gynecol. 2018;30(1):51-4.
97. Baum M, Budzar AU, Cuzick J, Forbes J, Houghton JH, Klijn JG, et al. Anastrozole alone or in combination with tamoxifen versus tamoxifen alone for adjuvant treatment of postmenopausal women with early breast cancer: first results of the ATAC randomised trial. Lancet. 2002;359(9324):2131-9.
98. Jelovac D, Macedo L, Goloubeva OG, Handratta V, Brodie AM. Additive antitumor effect of aromatase inhibitor letrozole and antiestrogen fulvestrant in a postmenopausal breast cancer model. Cancer Res. 2005;65(12):5439-44.
99. Baum M, Buzdar A, Cuzick J, Forbes J, Houghton J, Howell A, et al. Anastrozole alone or in combination with tamoxifen versus tamoxifen alone for adjuvant treatment of postmenopausal women with early-stage breast cancer: results of the ATAC (Arimidex, Tamoxifen Alone or in Combination) trial efficacy and safety update analyses. Cancer. 2003;98(9):1802-10.
100. Zhao LM, Jin HS, Liu J, Skaar TC, Ipe J, Lv W, et al. A new Suzuki synthesis of triphenylethylenes that inhibit aromatase and bind to estrogen receptors alpha and beta. Bioorg Med Chem. 2016;24(21):5400-9.
101. Lv W, Liu J, Lu D, Flockhart DA, Cushman M. Synthesis of mixed (E,Z)-, (E)-, and (Z)-norendoxifen with dual aromatase inhibitory and estrogen receptor modulatory activities. J Med Chem. 2013;56(11):4611-8.
102. Lv W, Liu J, Skaar TC, Flockhart DA, Cushman M. Design and synthesis of norendoxifen analogues with dual aromatase inhibitory and estrogen receptor modulatory activities. J Med Chem. 2015;58(6):2623-48.

103. Lu WJ, Xu C, Pei Z, Mayhoub AS, Cushman M, Flockhart DA. The tamoxifen metabolite norendoxifen is a potent and selective inhibitor of aromatase (CYP19) and a potential lead compound for novel therapeutic agents. Breast Cancer Res Treat. 2012;133(1):99-109.
104. Lv W, Liu J, Skaar TC, O'Neill E, Yu G, Flockhart DA, et al. Synthesis of Triphenylethylene Bisphenols as Aromatase Inhibitors That Also Modulate Estrogen Receptors. J Med Chem. 2016;59(1):157-70.
105. Cerqueira NM, Gesto D, Oliveira EF, Santos-Martins D, Bras NF, Sousa SF, et al. Receptor-based virtual screening protocol for drug discovery. Arch Biochem Biophys. 2015;582:56-67.
106. PD L. Structure-based virtual screening: an overview. 2002.
107. Shoichet BK. Virtual screening of chemical libraries. Nature. 2004;432(7019):862-5.
108. Lionta E, Spyrou G, Vassilatis DK, Cournia Z. Structure-based virtual screening for drug discovery: principles, applications and recent advances. Curr Top Med Chem. 2014;14(16):1923-38.
109. Kalaszi A, Szisz D, Imre G, Polgar T. Screen3D: a novel fully flexible high-throughput shape-similarity search method. J Chem Inf Model. 2014;54(4):1036-49.
110. Ghemtio L, I. Perez-Nueno V, Leroux V, Asses Y, Souchet M, Mavridis L, et al. Recent Trends and Applications in 3D Virtual Screening. Combinatorial Chemistry & High Throughput Screening. 2012;15(9):749-69.
111. Lipinski CA. Drug-like properties and the causes of poor solubility and poor permeability. Journal of Pharmacological and Toxicological Methods. 2000;44(1):235-49.
112. Sousa SF, Fernandes PA, Ramos MJ. Protein-ligand docking: current status and future challenges. Proteins. 2006;65(1):15-26.
113. Ain QU, Aleksandrova A, Roessler FD, Ballester PJ. Machine-learning scoring functions to improve structure-based binding affinity prediction and virtual screening. Wiley Interdiscip Rev Comput Mol Sci. 2015;5(6):405-24.
114. Shen C, Ding J, Wang Z, Cao D, Ding X, Hou T. From machine learning to deep learning: Advances in scoring functions for protein–ligand docking. Wiley Interdisciplinary Reviews: Computational Molecular Science. 2019.
115. Triballeau N, Acher F, Brabet I, Pin JP, Bertrand HO. Virtual screening workflow development guided by the "receiver operating characteristic" curve approach. Application to high-throughput docking on metabotropic glutamate receptor subtype 4. J Med Chem. 2005;48(7):2534-47.
116. Kirchmair J, Markt P, Distinto S, Wolber G, Langer T. Evaluation of the performance of 3D virtual screening protocols: RMSD comparisons, enrichment assessments, and decoy selection--what can we learn from earlier mistakes? J Comput Aided Mol Des. 2008;22(3-4):213-28.
117. Sousa SF, Ribeiro AJM, Coimbra JTS, Neves RPP, Martins SA, Moorthy NSHN, et al. Protein-Ligand Docking in the New Millennium – A Retrospective of 10 Years in the Field. Current Medicinal Chemistry. 2013;20(18):2296-314.
118. Lipinski CA, Lombardo F, Dominy BW, Feeney PJ. Experimental and computational approaches to estimate solubility and permeability in drug discovery and development settings 1PII of original article: S0169-409X(96)00423-1. The article was originally published in Advanced Drug Delivery Reviews 23 (1997) 3–25. 1. Advanced Drug Delivery Reviews. 2001;46(1-3):3-26.
119. Dolinsky TJ, Nielsen JE, McCammon JA, Baker NA. PDB2PQR: an automated pipeline for the setup of Poisson-Boltzmann electrostatics calculations. Nucleic Acids Res. 2004;32(Web Server issue):W665-7.
120. Mysinger MM, Carchia M, Irwin JJ, Shoichet BK. Directory of Useful Decoys, Enhanced (DUD-E): Better Ligands and Decoys for Better Benchmarking. Journal of Medicinal Chemistry. 2012;55(14):6582-94.
121. Ruiz-Carmona S, Alvarez-Garcia D, Foloppe N, Garmendia-Doval AB, Juhos S, Schmidtke P, et al. rDock: a fast, versatile and open source program for docking ligands to proteins and nucleic acids. PLoS Comput Biol. 2014;10(4):e1003571.

122. Rogers D, Hahn M. Extended-connectivity fingerprints. J Chem Inf Model. 2010;50(5):742-54.
123. Yang SY. Pharmacophore modeling and applications in drug discovery: challenges and recent advances. Drug Discov Today. 2010;15(11-12):444-50.
124. Schneidman-Duhovny D, Dror O, Inbar Y, Nussinov R, Wolfson HJ. PharmaGist: a webserver for ligand-based pharmacophore detection. Nucleic Acids Res. 2008;36(Web Server issue):W223-8.
125. Dror O, Schneidman-Duhovny D, Inbar Y, Nussinov R, Wolfson HJ. Novel approach for efficient pharmacophore-based virtual screening: method and applications. J Chem Inf Model. 2009;49(10):2333-43.
126. Inbar Y S-DD, Dror O, Nussinov R, Wolfson HJ. Deterministic Pharmacophore Detection via Multiple Flexible Alignment of Drug-Like Molecules. Lecture Notes in Computer Science. 3692. Springer Verlag ed2007. p. 423-34.
127. Thompson EA, Jr., Siiteri PK. The involvement of human placental microsomal cytochrome P-450 in aromatization. J Biol Chem. 1974;249(17):5373-8.
128. Heidrich DD, Steckelbroeck S, Klingmuller D. Inhibition of human cytochrome P450 aromatase activity by butyltins. Steroids. 2001;66(10):763-9.
129. Varela C, Tavares da Silva EJ, Amaral C, Correia da Silva G, Baptista T, Alcaro S, et al. New Structure–Activity Relationships of A- and D-Ring Modified Steroidal Aromatase Inhibitors: Design, Synthesis, and Biochemical Evaluation. Journal of Medicinal Chemistry. 2012;55(8):3992-4002.
130. Sun X-Z, Zhou D, Chen S. Autocrine and paracrine actions of breast tumor aromatase. A three-dimensional cell culture study involving aromatase transfected MCF-7 and T-47D cells. The Journal of Steroid Biochemistry and Molecular Biology. 1997;63(1-3):29-36.
131. Itoh T, Karlsberg K, Kijima I, Yuan YC, Smith D, Ye J, et al. Letrozole-, anastrozole-, and tamoxifen-responsive genes in MCF-7aro cells: a microarray approach. Mol Cancer Res. 2005;3(4):203-18.
132. Berthois Y, Katzenellenbogen JA, Katzenellenbogen BS. Phenol red in tissue culture media is a weak estrogen: implications concerning the study of estrogen-responsive cells in culture. Proc Natl Acad Sci U S A. 1986;83(8):2496-500.
133. Amaral C, Borges M, Melo S, da Silva ET, Correia-da-Silva G, Teixeira N. Apoptosis and autophagy in breast cancer cells following exemestane treatment. PLoS One. 2012;7(8):e42398.
134. Stockert JC, Blazquez-Castro A, Canete M, Horobin RW, Villanueva A. MTT assay for cell viability: Intracellular localization of the formazan product is in lipid droplets. Acta Histochem. 2012;114(8):785-96.
135. Chan FK, Moriwaki K, De Rosa MJ. Detection of necrosis by release of lactate dehydrogenase activity. Methods Mol Biol. 2013;979:65-70.
136. Amaral C, Varela CL, Mauricio J, Sobral AF, Costa SC, Roleira FMF, et al. Anti-tumor efficacy of new 7alpha-substituted androstanes as aromatase inhibitors in hormone-sensitive and resistant breast cancer cells. J Steroid Biochem Mol Biol. 2017;171:218-28.
137. Masri S, Lui K, Phung S, Ye J, Zhou D, Wang X, et al. Characterization of the weak estrogen receptor alpha agonistic activity of exemestane. Breast Cancer Res Treat. 2009;116(3):461-70.
138. Otto T, Sicinski P. Cell cycle proteins as promising targets in cancer therapy. Nat Rev Cancer. 2017;17(2):93-115.
139. McIlwain DR, Berger T, Mak TW. Caspase functions in cell death and disease. Cold Spring Harb Perspect Biol. 2013;5(4):a008656.
140. Droge W. Free radicals in the physiological control of cell function. Physiol Rev. 2002;82(1):47-95.
141. Chandel NS, Schumacker PT. Cellular oxygen sensing by mitochondria: old questions, new insight. J Appl Physiol (1985). 2000;88(5):1880-9.

142. Chen X, Zhong Z, Xu Z, Chen L, Wang Y. 2',7'-Dichlorodihydrofluorescein as a fluorescent probe for reactive oxygen species measurement: Forty years of application and controversy. Free Radic Res. 2010;44(6):587-604.
143. Mahmood T, Yang PC. Western blot: technique, theory, and trouble shooting. N Am J Med Sci. 2012;4(9):429-34.
144. Garibyan L, Avashia N. Polymerase chain reaction. J Invest Dermatol. 2013;133(3):1-4.
145. Livak KJ, Schmittgen TD. Analysis of relative gene expression data using real-time quantitative PCR and the 2(-Delta Delta C(T)) Method. Methods. 2001;25(4):402-8.
146. Heldring N, Pawson T, McDonnell D, Treuter E, Gustafsson JA, Pike AC. Structural insights into corepressor recognition by antagonist-bound estrogen receptors. J Biol Chem. 2007;282(14):10449-55.
147. Scott JS, Bailey A, Davies RD, Degorce SL, MacFaul PA, Gingell H, et al. Tetrahydroisoquinoline Phenols: Selective Estrogen Receptor Downregulator Antagonists with Oral Bioavailability in Rat. ACS Med Chem Lett. 2016;7(1):94-9.
148. Norman BH, Dodge JA, Richardson TI, Borromeo PS, Lugar CW, Jones SA, et al. Benzopyrans are selective estrogen receptor beta agonists with novel activity in models of benign prostatic hyperplasia. J Med Chem. 2006;49(21):6155-7.
149. Pike AC, Brzozowski AM, Hubbard RE, Bonn T, Thorsell AG, Engstrom O, et al. Structure of the ligand-binding domain of oestrogen receptor beta in the presence of a partial agonist and a full antagonist. EMBO J. 1999;18(17):4608-18.
150. Manas ES, Unwalla RJ, Xu ZB, Malamas MS, Miller CP, Harris HA, et al. Structure-based design of estrogen receptor-beta selective ligands. J Am Chem Soc. 2004;126(46):15106-19.
151. Wilkening RR, Ratcliffe RW, Tynebor EC, Wildonger KJ, Fried AK, Hammond ML, et al. The discovery of tetrahydrofluorenones as a new class of estrogen receptor beta-subtype selective ligands. Bioorg Med Chem Lett. 2006;16(13):3489-94.
152. McDevitt RE, Malamas MS, Manas ES, Unwalla RJ, Xu ZB, Miller CP, et al. Estrogen receptor ligands: design and synthesis of new 2-arylindene-1-ones. Bioorg Med Chem Lett. 2005;15(12):3137-42.
153. Hoover RN, Hyer M, Pfeiffer RM, Adam E, Bond B, Cheville AL, et al. Adverse health outcomes in women exposed in utero to diethylstilbestrol. N Engl J Med. 2011;365(14):1304-14.
154. Wise LA, Palmer JR, Rowlings K, Kaufman RH, Herbst AL, Noller KL, et al. Risk of benign gynecologic tumors in relation to prenatal diethylstilbestrol exposure. Obstet Gynecol. 2005;105(1):167-73.
155. Amaral C, Toloi MRT, Vasconcelos LD, Fonseca MJV, Correia-da-Silva G, Teixeira N. The role of soybean extracts and isoflavones in hormone-dependent breast cancer: aromatase activity and biological effects. Food Funct. 2017;8(9):3064-74.
156. Tian JM, Ran B, Zhang CL, Yan DM, Li XH. Estrogen and progesterone promote breast cancer cell proliferation by inducing cyclin G1 expression. Braz J Med Biol Res. 2018;51(3):1-7.
157. Wang X, Chen S. Aromatase destabilizer: novel action of exemestane, a food and drug administration-approved aromatase inhibitor. Cancer Res. 2006;66(21):10281-6.
158. Peekhaus NT1 CT, Hayes EC, Wilkinson HA, Mitra SW, Schaeffer JM, Rohrer SP. Distinct effects of the antiestrogen Faslodex on the stability of estrogen receptors-alpha and -beta in the breast cancer cell line MCF-7. Journal of Molecular Endocrinology. 2004;32:987-95.
159. Lannigan DA. Estrogen receptor phosphorylation. Steroids. 2003;68(1):1-9.
160. Compton DR, Sheng S, Carlson KE, Rebacz NA, Lee IY, Katzenellenbogen BS, et al. Pyrazolo[1,5-a]pyrimidines: estrogen receptor ligands possessing estrogen receptor beta antagonist activity. J Med Chem. 2004;47(24):5872-93.
161. Weiser MJ, Wu TJ, Handa RJ. Estrogen receptor-beta agonist diarylpropionitrile: biological activities of R- and S-enantiomers on behavior and hormonal response to stress. Endocrinology. 2009;150(4):1817-25.
162. Brentnall M, Rodriguez-Menocal L, De Guevara RL, Cepero E, Boise LH. Caspase-9, caspase-3 and caspase-7 have distinct roles during intrinsic apoptosis. BMC Cell Biol. 2013;14:32.

163. Lubczyk V, Bachmann H, Gust R. Investigations on Estrogen Receptor Binding. The Estrogenic, Antiestrogenic, and Cytotoxic Properties of C2-Alkyl-Substituted 1,1-Bis(4-hydroxyphenyl)-2-phenylethenes. Journal of Medicinal Chemistry. 2002;45(24):5358-64.
164. Zheng N, Liu L, Liu W, Zhang P, Huang H, Zang L, et al. ERbeta up-regulation was involved in silibinin-induced growth inhibition of human breast cancer MCF-7 cells. Arch Biochem Biophys. 2016;591:141-9.
165. Amaral C, Varela C, Borges M, Tavares da Silva E, Roleira FMF, Correia-da-Silva G, et al. Steroidal aromatase inhibitors inhibit growth of hormone-dependent breast cancer cells by inducing cell cycle arrest and apoptosis. Apoptosis : an international journal on programmed cell death. 2013;18(11):1426-36.
166. Amaral C, Lopes A, Varela CL, da Silva ET, Roleira FM, Correia-da-Silva G, et al. Exemestane metabolites suppress growth of estrogen receptor-positive breast cancer cells by inducing apoptosis and autophagy: A comparative study with Exemestane. The international journal of biochemistry & cell biology. 2015;69:183-95.
167. Thiantanawat A, Long BJ, Brodie AM. Signaling pathways of apoptosis activated by aromatase inhibitors and antiestrogens. Cancer Res. 2003;63(22):8037-50.
168. DiPaola RS. To arrest or not to G(2)-M Cell-cycle arrest : commentary re: A. K. Tyagi et al., Silibinin strongly synergizes human prostate carcinoma DU145 cells to doxorubicin-induced growth inhibition, G(2)-M arrest, and apoptosis. Clin. cancer res., 8: 3512-3519, 2002. Clin Cancer Res. 2002;8(11):3311-4.
169. Kroemer G, Galluzzi L, Brenner C. Mitochondrial membrane permeabilization in cell death. Physiol Rev. 2007;87(1):99-163.
170. Elmore S. Apoptosis: a review of programmed cell death. Toxicol Pathol. 2007;35(4):495-516.
171. Broker LE, Kruyt FA, Giaccone G. Cell death independent of caspases: a review. Clin Cancer Res. 2005;11(9):3155-62.
172. Jiang S, He R, Zhu L, Liang T, Wang Z, Lu Y, et al. Endoplasmic reticulum stress-dependent ROS production mediates synovial myofibroblastic differentiation in the immobilization-induced rat knee joint contracture model. Exp Cell Res. 2018;369(2):325-34.
173. Brown GC, Borutaite V. There is no evidence that mitochondria are the main source of reactive oxygen species in mammalian cells. Mitochondrion. 2012;12(1):1-4.
174. Circu ML, Aw TY. Reactive oxygen species, cellular redox systems, and apoptosis. Free Radic Biol Med. 2010;48(6):749-62.
175. Kallio A, Zheng A, Dahllund J, Heiskanen KM, Harkonen P. Role of mitochondria in tamoxifen-induced rapid death of MCF-7 breast cancer cells. Apoptosis : an international journal on programmed cell death. 2005;10(6):1395-410.
176. Cipolletti M, Solar Fernandez V, Montalesi E, Marino M, Fiocchetti M. Beyond the Antioxidant Activity of Dietary Polyphenols in Cancer: the Modulation of Estrogen Receptors (ERs) Signaling. Int J Mol Sci. 2018;19(9).
177. Lecomte S, Demay F, Ferriere F, Pakdel F. Phytochemicals Targeting Estrogen Receptors: Beneficial Rather Than Adverse Effects? Int J Mol Sci. 2017;18(7).
178. Petrelli A, Giordano S. From single- to multi-target drugs in cancer therapy: when aspecificity becomes an advantage. Curr Med Chem. 2008;15(5):422-32.
179. Kucuksayan E, Ozben T. Hybrid Compounds as Multitarget Directed Anticancer Agents. Curr Top Med Chem. 2017;17(8):907-18.
180. Viana JdO, Félix MB, Maia MdS, Serafim VdL, Scotti L, Scotti MT. Drug discovery and computational strategies in the multitarget drugs era. Brazilian Journal of Pharmaceutical Sciences. 2018;54(spe).
181. Ma XH, Shi Z, Tan C, Jiang Y, Go ML, Low BC, et al. In-silico approaches to multi-target drug discovery : computer aided multi-target drug design, multi-target virtual screening. Pharm Res. 2010;27(5):739-49.